

**Insights into the roles of novel Epidermal Patterning Factors (EPFs) secreted peptides
in stomatal development, and MAP phosphatases MKP2 and DsPTP1 in chloroplast
development**

Pooja Kaushik

A Thesis

in

The Department

of

Biology

Presented in Partial Fulfillment of the Requirement

for the Degree of Doctor of Philosophy (Biology) at

Concordia University

Montreal, Quebec, Canada

February 2025

© Pooja Kaushik, 2025

CONCORDIA UNIVERSITY

School of Graduate Studies

This is to certify that the thesis prepared

By: **Pooja Kaushik**

Entitled: **Insights into the roles of novel Epidermal Patterning Factors (EPFs) secreted peptides in stomatal development, and MAP phosphatases MKP2 and DsPTP1 in chloroplast development**

and submitted in partial fulfillment of the requirements for the degree of

DOCTOR OF PHILOSOPHY (Biology)

complies with regulations of university and meets the accepted standards with respect to original and quality.

Signed by the final examining committee:

_____ Chair

Dr. Peter Darlington

_____ External Examiner

Dr. Tamara Western

_____ Examiner

Dr. William Zerges

_____ Examiner

Dr. Selvadurai Dayanandan

_____ Examiner

Dr. Paul Joyce

_____ Supervisor

Dr. Patrick Gulick

Approved by _____

Dr. Robert Weladji, Graduate Program Director

April 01, 2025 _____

Dr. Pascale Sicotte, Dean of Faculty of Arts and Science

Abstract

Insights into the roles of novel Epidermal Patterning Factors (EPFs) secreted peptides in stomatal development, and MAP phosphatases MKP2 and DsPTP1 in chloroplast development

Pooja Kaushik, PhD

Concordia University, 2025

As the global population grows and water scarcity becomes more pressing, improving photosynthetic efficiency and reducing crop losses due to drought stress are critical challenges for modern agriculture. This thesis addresses these challenges by investigating stomatal development, drought stress tolerance, and chloroplast biogenesis in plants. The primary objectives of the research were to identify epidermal patterning factors (EPF) signaling peptides involved in stomatal development in monocot model plant, *Brachypodium distachyon* (Brachypodium), to explore the role of *Arabidopsis thaliana* (Arabidopsis) *EPFL1*, *EPFL2*, and *EPFL3* genes in drought tolerance, and finally, to investigate the roles of Arabidopsis Mitogen Activated Protein Kinase (MAPK) phosphatases (MKP2 and DsPTP1) in chloroplast biogenesis. The findings revealed that Brachypodium EPF peptides (BdEPFL1-1, BdEPFL2-2, BdEPFL6-1, and BdEPFL6-2) play a role in stomatal patterning, with overexpression leading to reduced stomatal density, validated through complementation studies in Arabidopsis. In the drought tolerance study, overexpression of *EPFL1* significantly enhanced drought resistance in an ABA-dependent manner, whereas *EPFL2* worked in an ABA-independent manner, highlighting distinct regulatory pathways for these gene products. The final part of this research focused on the roles of MAPK phosphatases MKP2 and DsPTP1 in regulating chloroplast biogenesis. Mutant analyses showed that the absence of these phosphatases resulted in impaired chloroplast development, stunted growth, and an albino phenotype, revealing their role as negative regulators of chloroplast formation. Higher order mutants with mutant alleles for MAPKs revealed their likely downstream targets. These findings offer important insights into plant development, with implications for enhancing crop resilience and photosynthesis in response to global climate challenges.

Acknowledgments

First and foremost, I would like to thank God for his countless blessings and for guiding me through every step of this journey. His grace and strength have been a constant source of support.

To my parents, I owe everything. Their unconditional love, support, and belief in me have been my greatest motivation. I am forever grateful to my brother, Suryakant Kaushik, for always being there for me, and to my husband, Varinder Pal, for his endless love, patience, and encouragement during this journey.

I would like to thank Dr. Jin Suk Lee for providing the essential lab space, funding, resources, and valuable guidance that were instrumental in laying the groundwork for my research. I would also like to express my gratitude to my administrative supervisor, Dr. Patrick Gulick, for his consistent support and guidance during my thesis submission. His advice and help were important to the completion of this thesis, and I am deeply appreciative of his mentorship.

I extend my heartfelt thanks to my committee members, Dr. William Zerges and Dr. Selvadurai Dayanandan, for their valuable feedback, thoughtful suggestions, and constant encouragement, which have helped me refine my research.

I am immensely grateful to my lab members, especially Amarjeet, whose friendship and support have been a constant source of strength throughout this journey. His encouragement and presence have made this experience truly special. I extend another special thanks to Neha and Stacey, for their collaboration, friendship, and support. My sincere thanks also go to Xutong, Zoe, Zakaria, Kritika, Sehyuk and Janlei for making the lab environment a productive and positive space.

A special thanks to Dr. Sabrina Brunette, for her immense help in analyzing my results and guiding me through bioinformatic analysis. Her expertise and insights were invaluable throughout my research. I would also like to acknowledge Chris Law, for his support and assistance in microscopy techniques.

Thank you all for being an integral part of this accomplishment.

Table of Contents

List of Figures.....	vii
List of Tables	ix
List of Abbreviations.....	x
<i>Chapter 1. Introduction.....</i>	<i>1</i>
1.1 General Introduction	2
<i>Chapter 2. Identification of novel EPF secreted peptides specifying stomatal development and patterning in Brachypodium.....</i>	<i>4</i>
2.1 Introduction.....	5
2.1.1 Stomata development in dicots	6
2.1.2 Stomatal development in monocots.....	8
2.1.3 Role of EPF peptide signaling in stomata development.....	10
2.2 Materials and Methods.....	16
2.2.1 Plant materials and growth conditions	16
2.2.2 Plasmid construction	16
2.2.3 Agrobacterium mediated transformation and transgenic development	17
2.2.4 DNA extraction and genotyping.....	18
2.2.5 RNA extraction and cDNA synthesis	20
2.2.6 Microscopy and quantitative analysis of stomatal phenotype.....	20
2.3 Results	22
2.3.1 Identification of putative EPF peptides controlling stomal development and patterns in Brachypodium	22
2.3.2 Functional analysis of BdEPF candidates	24
2.3.3 Cross-species complementation assay of potential BdEPF homologs by using Arabidopsis Promoter	27
2.3.4 Effect of overexpression of BdEPFLs on the epidermal phenotype in Brachypodium.....	30
2.4 Discussion.....	34
<i>Chapter 3. To investigate the potential of Arabidopsis EPFL genes in drought tolerance.....</i>	<i>37</i>
3.1 Introduction.....	38
3.1.1 Drought stress	39
3.1.2 Abscisic acid and plant development	40
3.1.3 Root development	41
3.1.4 Seed germination.....	42
3.2 Materials and Methods.....	44
3.2.1 Plant material and growth conditions.....	44
3.2.2 <i>In-silico</i> expression analysis of the <i>EPFL1</i> , <i>EPFL2</i> and <i>EPFL3</i> subfamily.....	46
3.2.3 Genomic DNA preparation and PCR	46
3.2.4 Phenotypic characterization	47
3.2.5 Synthesis of cDNA and qPCR analysis	47
3.2.6 β -glucuronidase (GUS) reporter assay.....	47
3.2.7 Stomata Regulation Assay	48
3.2.8 Quantitative analysis of stomatal phenotype.....	48

3.3 Results	49
3.3.1 RNA-sequencing data analysis	49
3.3.2 Effects of Drought Stress on EPFL1/2/3 mutants	51
3.3.3 Relative water loss assay	53
3.3.4 qPCR analysis of drought stress inducible genes	55
3.3.5 GUS assay showing EPFL expression in response to ABA and drought	57
3.3.6 Mechanism of drought tolerance	59
3.3.7 Influence on stomatal density and stomata regulation	63
3.4 Discussion	65
Chapter 4: Investigating the roles of the Arabidopsis MAPK phosphatases, MKP2 and DsPTP1 in chloroplast biogenesis.	
4.1 Introduction	
4.1.1 Mitogen-activated protein kinase (MAPK) cascades	72
4.1.2 MAP kinase phosphatases	73
4.1.3 Chloroplast biogenesis and MAPK signaling	78
4.2 Materials and Methods	
4.2.1 Plant materials and plant growth conditions	81
4.2.2 Plasmid construction	81
4.2.3 Agrobacterium-mediated transformation	82
4.2.4 DNA extraction and PCR genotyping	82
4.2.5 Microscopy	83
4.2.6 Photosynthetic pigment quantification assay	84
4.2.7 Bimolecular fluorescence complementation and transient expression assays .84	
4.3 Results	
4.3.1 Identification of phosphatases that control chloroplast development and biogenesis	86
4.3.2 Photomorphogenic response in <i>mkp2 dsptp1</i> mutants and silique seed segregation assay	88
4.3.3 Effects of <i>mkp2 dsptp1</i> double mutant on chloroplast production, chloroplast volume and photosynthetic pigments in the guard cells	89
4.3.4 Analysis of chloroplast ultrastructure	93
4.4 Downstream MAPKs regulating chloroplast development	
4.4.1 Seedling phenotype and Guard Cell chloroplasts of high order mutants	93
4.4.2 Bimolecular fluorescence complementation (BiFC) assays in transient tobacco system	95
4.5 Discussion	
5. Conclusions	
6. References	

List of Figures

Figure 2.1: Stomatal development in dicot, Arabidopsis.

Figure 2.2: An illustration of comparison between dicot and monocot stomatal development.

Figure 2.3: Phylogenetic tree, sequence alignment and identity matrix of BdEPFL peptides from Arabidopsis and Brachypodium.

Figure 2.4: Expression levels of EPF homologs in Brachypodium root, leaf division zone, and mature leaf.

Figure 2.5: Ectopic expression of grass stomatal EPF homologs exhibits stomatal development defects in Arabidopsis.

Figure 2.6: Quantitative analysis of 10-day-old abaxial cotyledon epidermis for ectopic expression of grass stomatal EPF homologs exhibiting stomatal development defects in Arabidopsis.

Figure 2.7: Complementation of Arabidopsis *epf1* and *epf2* mutants by *BdEPF* homologs.

Figure 2.8: Quantitative analysis of 10-days-old abaxial cotyledon epidermis for complementation of Arabidopsis *epf1* and *epf2* mutants by *BdEPF* homologs.

Figure 2.9: Overexpression analysis of BdEPFL1-1 in Brachypodium.

Figure 2.10: Confocal images of leaf division zone of wild type and transgenic Brachypodium overexpressing *BdEPFL1-1* with the *ZmUbi::BdEPFL1-1* construct.

Figure 2.11: Phenotypic characterization of the *OE BdEPFL1-1* Brachypodium transgenic lines.

Figure 3.1: An illustration showing ABA-dependent and ABA-independent drought signaling pathways.

Figure 3.2: RNA-seq analysis of *EPFL1/2/3* genes.

Figure 3.3: Drought phenotypes of WT, loss of function, overexpressing, and high-order mutants in a drought and rewatered panel.

Figure 3.4: Relative water loss in WT, mutants, overexpression and high order mutants.

Figure 3.5: Expression profiles of ABA-responsive genes.

Figure 3.6: GUS expression patterns of *EPFL1pro:GUS*, *EPFL2pro:GUS* and *EPFL3pro:GUS*.

Figure 3.7: Seed germination assay in response to ABA.

Figure 3.8: Root inhibition assay in response to ABA.

Figure 3.9: Epidermal score representing stomatal density and non-stomatal density of WT, *epfl1*, *epfl2* and *epfl1/2* mutants.

Figure 4.1: A diagram showing a typical MAPK cascade in eukaryotes.

Figure 4.2: A model illustrating ABI4 activity modulation via transcriptional and post-translational (PTM) MPK 3/6 pathways

Figure 4.3: Identification and complementation of the *mkp2 dsptp1* mutant.

Figure 4.4: Developmental characteristics of the *mkp2 dsptp1* mutant.

Figure 4.5: Embryo greening and seed silique segregation analysis in 6-Week-Old Arabidopsis.

Figure 4.6: Effect of *mkp2 dsptp1* knockout on chloroplast production and chloroplast volume in stomata guard cells.

Figure 4.7: Photosynthetic pigment quantification assay and chloroplast ultrastructure.

Figure 4.8: Epistatic analysis of high-order mutants using chloroplast production assay.

Figure 4.9: Bimolecular fluorescence complementation (BiFC) analysis to test for physical interaction between MKP2/CIMKP2, DsPTP1/CIDsPTP1 and candidate kinases.

List of Tables

Table 2.1: Plasmid List Used in Chapter 2.

Table 2.2: Primer List Used in Chapter 2.

Table 3.1: Plasmid List Used in Chapter 3.

Table 3.2: Primer List Used in Chapter 3.

Table 3.3: Table showing statistical analysis for relative water-loss assay.

Table 4.1: Plasmid List Used in Chapter 4.

Table 4.2: Primer List Used in Chapter 4.

List of Abbreviations

ABA	Abscisic Acid
BiFC	Bimolecular fluorescence complementation assay
C	Cysteine
CaMV	Cauliflower mosaic virus
cDNA	Complementary DNA
CDS	Coding sequence
Chl	Chlorophyll
Chl <i>a</i>	Chlorophyll <i>a</i>
Chl <i>b</i>	Chlorophyll <i>b</i>
CI	Catalytically inactive
Col	Columbia Ecotype
Co-IP	Co-immunoprecipitation
DIC	Differential interference contrast microscopy
DNA	Deoxyribonucleic Acid
DPG	Days post germination
DSP	Dual-specificity phosphatase
DsPTP1	Dual-specificity Protein Tyrosine Phosphatase 1
ER	ERECTA Ecotype
ERL1	ERECTA-like 1
ERL2	ERECTA-like 2
EPF	Epidermal Patterning Factor
EPFL	Epidermal Patterning Factor-Like
EST	Estradiol
GFP	Green Fluorescent Protein
GUS	β -glucuronidase

IBR5	Indole-3-Butyric Acid Response 5
LB	Luria-Bertani medium
LHCB	Light-harvesting chlorophyll <i>a/b</i> binding
M	Mature peptide
MAPK	Mitogen-activated protein kinase
MAPKK	Mitogen-activated protein kinase kinase
MAPKKK	Mitogen-activated protein kinase kinase kinase
MKP	Mitogen-activated protein kinase phosphatase
mRNA	Messenger RNA
MS	Murashige and Skoog media
OX	Over-expression
PHS1	Propyzamide-Hypersensitive 1
PTP	Protein tyrosine phosphatase
PYR	Pyrabactin resistance
RLKs	Receptor-Like Kinases
RNA	Ribonucleic Acid
SA	Salicylic Acid
SDS	Sodium Dodecyl Sulfate
SLGC	Stomatal Lineage Guard Cell
SMC	Subsidiary Mother Cell
SRR	Sequence Read Achieve Run
T-DNA	Transfer DNA
TBO	Toluidine Blue O
YFP	Yellow florescent protein
WT	Wild Type
AtEPF1	<i>Arabidopsis thaliana</i> Epidermal Patterning Factor 1

AtEPF2	<i>Arabidopsis thaliana</i> Epidermal Patterning Factor 2
BdEPFL1-1	<i>Brachypodium distachyon</i> Epidermal Patterning Factor-like 1-1
BdEPFL1-2	<i>Brachypodium distachyon</i> Epidermal Patterning Factor-like 1-2
BdEPFL2-1	<i>Brachypodium distachyon</i> Epidermal Patterning Factor-like 2-1
BdEPFL2-2	<i>Brachypodium distachyon</i> Epidermal Patterning Factor-like 2-2
BdEPFL6-1	<i>Brachypodium distachyon</i> Epidermal Patterning Factor-like 6-1
BdEPFL6-2	<i>Brachypodium distachyon</i> Epidermal Patterning Factor-like 6-2

Chapter 1. Introduction

1.1 General Introduction

The continuous growth of the global population over the past 50 years has created immense pressure on agricultural systems to generate enough food. Characterized by elevated temperatures, altered rainfall patterns, and frequent extreme weather, climate change poses an inevitable challenge to the productivity of global agriculture. Drought stress is one of the most detrimental factors affecting crop yields, leading to reduced plant growth, and diminished photosynthetic capacity (FAO 2017, [Weblink 1](#)). Developing crops with enhanced drought resistance is vital to sustain food production in the face of these challenges. Addressing these critical issues requires a multi-disciplinary approach that integrates sustainable agricultural practices with advanced technologies, ensuring global food security. A comprehensive understanding of plant growth and development, particularly focusing on the regulation of key developmental and metabolic processes such as stomatal development and photosynthesis, respectively, is crucial for developing strategies to enhance crop productivity and stress tolerance (Hussain *et al.*, 2018). By manipulating these key physiological traits, such as stomatal density and photosynthetic efficiency of crops through breeding and transgenic approaches, we can enhance photosynthetic efficiency, improve water-use efficiency, and increase tolerance to extreme climate conditions, including drought, which can allow farmers to increase crop yields.

Plants, like all living organisms, must continuously adapt to fluctuations in their external environment for normal growth and development. This adaptation centers on their ability to detect environmental signals and activate complex signaling pathways that orchestrate the necessary physiological and genetic responses. By integrating these signals, plants can fine-tune their growth and development, optimizing processes such as photosynthesis and resource utilization while enhancing their tolerance to different stress conditions (Ashapkin *et al.*, 2020).

Stomata are the primary respiratory structures in plants. These microscopic pores are essential for enabling photosynthesis, allowing plants to absorb CO₂, and convert sunlight into carbon fixation, while simultaneously regulating transpiration to maintain water balance (Bergmann *et al.*, 2004). The establishment of cell fate is critical for generation of cellular diversity, tissue development, and organ formation, thereby influencing every aspect of organismal development. Stomatal development serves as a key structure for studying cell fate determination and patterning in plants. Although monocots play a crucial role in the global food supply, many aspects of their growth, development, and physiology including stomatal

development, are not as well understood as in dicot plants. Thus, it is crucial to understand stomatal development in depth.

Chloroplasts are photosynthetic organelles in plants that facilitate carbon dioxide fixation, produce pigments, and synthesize amino acids, with light being critical for their photosynthesis. Chloroplast development involves coordination and balance between nuclear and plastid gene expression. The mitogen-activated protein kinase (MAPK) cascade represents a fundamental and conserved signaling pathway in plants, regulating a range of cellular functions and mediating responses to environmental stressors (McCarty & Chory 2000). Mitogen-activated protein kinase (MAPK) signaling pathways are essential for coordinating various aspects of chloroplast biogenesis and function, influencing the development and differentiation of chloroplasts from proplastids, the precursor organelles (Zhou *et al.*, 2019). A comprehensive understanding of the intricate mechanisms that regulate these MAPK signaling pathways is crucial for improving plant growth, enhancing photosynthetic efficiency, and developing strategies to enhance agricultural productivity.

Keeping these points in focus, the aims of this PhD thesis are outlined below with a focus on optimizing plant productivity and developing drought resistant crops:

Aim 1: Identification of novel Epidermal Patterning Factor (EPF) secreted peptides specifying stomatal development and patterning in *Brachypodium distachyon* (Brachypodium).

Aim 2: Investigation the potential of *Arabidopsis thaliana* (Arabidopsis) Epidermal Patterning Factor -like (EPFL) genes in drought tolerance.

Aim 3: Investigation the roles of the Arabidopsis MAPK phosphatases, MKP2 and DsPTP1 in chloroplast development.

Chapter 2. Identification of novel EPF secreted peptides specifying stomatal development and patterning in *Brachypodium*.

2.1 Introduction

The determination of cell fate is key to establishing cellular diversity, promoting tissue development, and constructing organs which ultimately influence all stages of an organism's development. Within cellular development, the development of stomata has emerged as a fascinating framework for studying cell fate determination, and cell-to-cell signaling.. Stomata are specialized respiratory organs found on the surface of aerial parts in nearly all land plants which regulate carbon dioxide and water vapor exchange and thus play a fundamental role in photosynthesis and respiration (Tuzet *et al.*, 2011). Distribution and development of stomata differ between dicots and monocots. Generally, in dicots, stomata consists of two kidney shaped guard cells surrounding a pore that can control the extent of the exchange of gases by adjusting the stomatal aperture by turgor driven movement of these guard cells (Pillitteri & Torii, 2012). Usually, stomata are randomly distributed throughout the leaf epidermis in dicots. However, in grasses, stomata are dumbbell shaped which are flanked by two subsidiary cells and are organized in specific stomatal cell files (Matkowski, & Daszkowska-Golec, 2023) Figure 2.2.

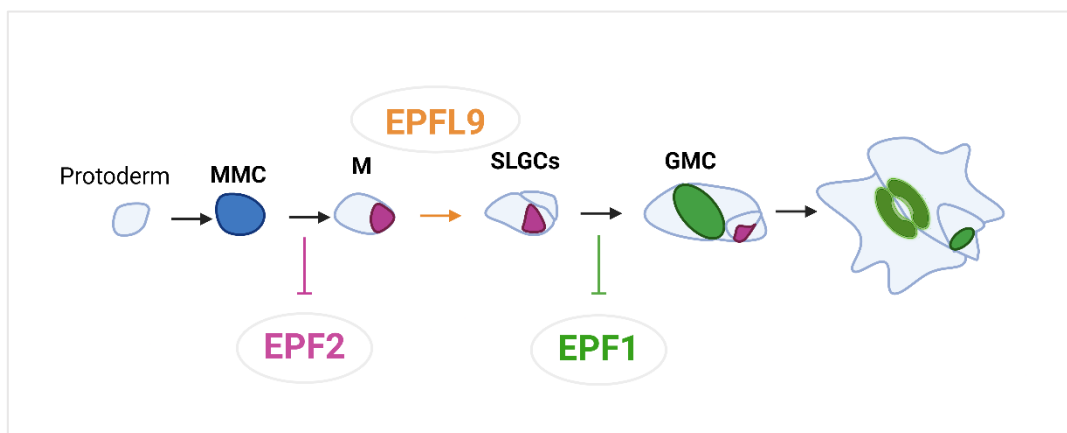


Figure 2.1: In Arabidopsis, protodermal cells (light blue) transform into Meristemoid Mother Cells (MMCs) (dark blue), which then divide asymmetrically into two cells: meristemoids (smaller; pink) and Stomatal Lineage Ground Cell (SLGC) (bigger; pale blue). Meristemoid develops into Guard Mother Cell (GMC) (green), which divides symmetrically into two guard cells (GCs). SLGC can split into pavement cells (pale blue) or satellite meristemoid (pink). Adapted from Pillitteri and Torii (2012). The diagram was generated using BioRender.

2.1.1 Stomata development in dicots

Stomata number and distribution affect the gas exchange which in turn is tied to coordinated cell growth and division. In *Arabidopsis*, the process of stomata development is highly regulated and sequential. In epidermal cells, it begins with a set of precursor cells termed “protodermal cells” that undergo asymmetric divisions and form meristemoid mother cells. These meristemoid mother cells initiate the stomatal lineage by undergoing asymmetric “entry division” that produces two new cells. The small triangular cell is called a “meristemoid” and a larger sister cell is termed as a “stomatal-lineage ground cell”. The meristemoid can either differentiate into an oval guard mother cell that later undergoes symmetric division to ultimately differentiate into mature guard cells or it may first undergo few amplifying cell divisions before producing a mature guard mother cell (Han *et al.*, 2021) (Figure 2.1). A stomatal-lineage ground cell on the other hand can either differentiate into a lobed pavement cell or it can undergo an asymmetric spacing division to create a “satellite meristemoid” which is positioned away from existing stomatal precursors. Such oriented divisions of stomatal-lineage ground cell are important to ensure stomata develop at least one-cell apart from one another through regulation by cell-cell signaling components that ensures the “one-cell spacing” rule is maintained (Herrmann and Torii, 2021).

Key changes in stomatal development in *Arabidopsis* are regulated by the stepwise expression of three closely related basic-helix-loop-helix (bHLH) transcription factors: SPEECHLESS (SPCH), MUTE, and FAMA (Gudesblat *et al.*, 2012; Bhave *et al.*, 2009; MacAlister *et al.*, 2007; Pillitteri *et al.*, 2007; Ohashi-Ito and Bergmann, 2006). The first transcription factor, SPCH, controls the entry into initial asymmetric cell divisions expressing in meristemoid mother cells. The *spch* mutation results in the epidermis composed entirely of pavement cells (MacAlister *et al.*, 2007). Differentiation of meristemoid to guard mother cell is controlled by MUTE and loss of function mutations in *mute* result in a no stomata phenotype with meristemoids undergoing multiple divisions (Pillitteri *et al.*, 2007). FAMA is essential for the final transition of cell states from guard mother cell to guard cell. FAMA null mutants result in abnormally divided guard mother cells that fail to differentiate into guard cells (Ohashi-Ito and Bergmann, 2006). Two additional redundant bHLH proteins, AtICE1 and AtSCRM2, are continuously expressed in the stomatal lineage and assist in cellular transitions during stomatal development by heterodimerizing with SPCH, MUTE, and FAMA (Kanaoka *et al.*, 2008).

Intercellular signaling that dictates tissue organization is crucial for the stomata distribution in plants. Cell spacing is orchestrated by intercellular signaling, which begins with the activation of transmembrane receptors i.e. Too Many Mouths (TMM) and the ERECTA-family receptors: ERECTA, ERECTA-like 1 (ERL1), and ERECTA-like 2 (ERL2), by their peptide ligands, Epidermal Patterning Factors (EPFs), in response to environmental or developmental conditions (Hara *et al.*, 2007, 2009; Hunt and Gray, 2009; Shpak *et al.*, 2005; Nadeau and Sack, 2002). These receptor-ligand interactions trigger the activation of a downstream MAPK cascade (Wang *et al.*, 2007; Bergmann *et al.*, 2004).

In *Arabidopsis*, the role of the MAPK cascade in stomatal differentiation was characterized by mutation in *YDA*, a Mitogen-Activated Protein Kinase Kinase Kinase (MAPKKK). The mutation results in over proliferation of stomata. In contrast, expression of a constitutively active *YDA* (CA-*YDA*) under the control of the native promoter eliminates stomata (Bergmann *et al.*, 2004). The downstream signaling pathways of *YDA* involve mitogen-activated protein kinase kinases (MKK); MKK4/MKK5, and MPK3/MPK6, two pairs of functionally redundant kinases. By controlling asymmetric cell divisions and stomatal cell differentiation, MKK4/MKK5 and MPK3/MPK6 act as negative regulators of stomatal development. Loss-of-function mutants of *mkk4* and *mkk5* or *mpk3* and *mpk6* lead to the formation of clustered stomata. On the other hand, the activation of the MKK4/5-MPK3/6 pathway suppresses asymmetric cell divisions and stomatal fate determination, preventing stomatal differentiation (Wang *et al.*, 2007).

Mutant and genetic analyses have confirmed the pivotal role of the *YDA* MAPK signaling pathway in suppressing stomatal production in *Arabidopsis* during early developmental phases (Lampard *et al.*, 2009; Lampard *et al.*, 2008). On the other hand, during later developmental phases, a positive regulation of stomatal development in guard mother cell in a cell-type specific manner has been noted, achieved by another MAPK module comprising *YDA*, MKK7/9, and MPK3/6 (Lampard *et al.*, 2014; Lampard *et al.*, 2009). Interestingly, CA-MKK7 and CA-MKK9 plants have an epidermis consisting of epidermal pavement cells and clusters of small cells that are like meristemoids. Expression of *FAM_{Pro}:CA-MKK7* or *FAM_{Pro}:CA-MKK9* results in gross overproduction of stomata and formation of guard cells that protrude from epidermis, a phenotype that resembles *FAM_{Pro}:CA-YDA* plants (Lampard *et al.*, 2009).

2.1.2 Stomatal development in monocots

Throughout history, cereals have been a staple in human diets and a key component in animal feed, playing a crucial role in sustaining humans. Research indicates that cereals account for 51% of calories and 47% of protein in the average human diet (FAO 2023).

Advances in agricultural practices and biotechnology have continued to improve the yield and resilience of these cereals, helping to meet the growing global demand for food. However, with an estimated surge in the world population to 9 billion from 8 billion by 2050, food shortages and water scarcity will become severe problems globally (UN, WPP 2019, [Weblink 2](#)). Additionally, drought conditions, lowering groundwater levels, and desertification are expected to become increasing challenges in the upcoming 4-6 decades (IPCC, 2014, [Weblink 3](#)). Other significant challenges include climate change, soil degradation, pests and diseases, resource inequality, biodiversity loss, and the need for efficient water management. Addressing these issues requires a multifaceted approach, including advancements in agricultural technology, sustainable farming practices, and policies that promote equitable resource distribution and environmental conservation. Therefore, production of drought resistant cereal crops with better health and yield characteristics is desirable.

In monocots like grasses and cereals, stomatal development is a complex process that diverges considerably from that in dicots. Understanding these differences is key to improving crop resilience and productivity, especially when facing environmental challenges. In young leaves, stomatal development occurs along a spatiotemporal gradient, beginning at the base and progressing upwards as the leaf grows (McKown, and Bergmann 2020). This developmental pathway can be divided into six stages, as illustrated in Figure 2.2. During stage I, near the leaf base, precursor cells proliferate in specific rows before stomatal-lineage cell specification. As these differentiating cells move up the leaf blade, alternate cells undergo an asymmetric 'entry' division, forming a smaller guard mother cell and a larger sister cell (stage 2). In stage 3, adjacent cells then divide asymmetrically to create subsidiary mother cells. Once the cells have grown, mature guard mother cells are flanked by two nascent subsidiary cells (stage 4). A final symmetric division of the guard mother cell produces two immature guard cells (stage 5). In final stage 6, the stomatal complex then matures and expands, forming a pair of dumbbell-shaped guard cells that separate to create the stomatal pore. Each mature grass stomatal complex thus includes a central pore, a pair of dumbbell-shaped guard cells, and two flanking subsidiary cells (Hepworth *et al.*, 2018) (Figure 2.2).

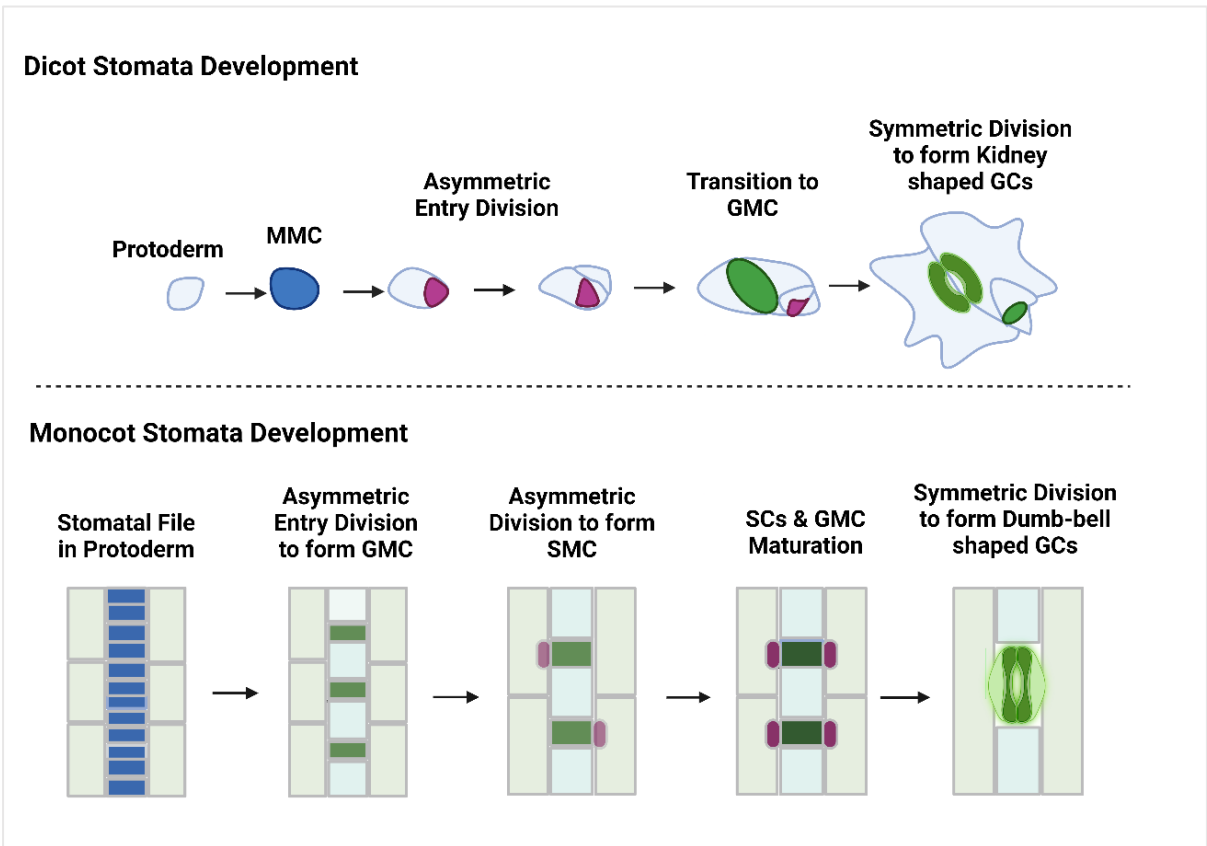


Figure 2.2: An illustration of comparison between dicot and monocot stomata development. GC (Guard cell); GMC (Guard mother cell); SC (Subsidiary cells); SMC (Subsidiary mother cell). The diagram was generated using BioRender. (illustrate)

Building on extensive research into Arabidopsis, scientists are now uncovering new insights into the genetic regulation of stomatal development in grass species. Studies using forward and reverse genetics in rice (*Oryza sativa*), and Brachypodium have revealed that the expansion of *SPCH*, *MUTE*, *FAMA*, *ICE1/SCRM*, and *SCRM2* homologs during grass evolution created an ‘alternatively wired’ genetic framework for stomatal patterning (Conklin *et al.*, 2019; Chen *et al.*, 2017; Raissig *et al.*, 2016; Liu *et al.*, 2009). Functional studies of Brachypodium’s *SPCH* paralogs (*BdSPCH1* and *BdSPCH2*) demonstrate that they have partially redundant roles in the determination of stomatal fate (Chen *et al.*, 2017; Raissig *et al.*, 2016). *BdSPCH2* alone is sufficient to induce stomatal fate and can function as guard mother cell master regulator (Raissig *et al.*, 2016). *OsSPCH2* controls the initiation of stomatal files in rice (Liu *et al.*, 2009). *BdICE1* and *BdSCRM2* have evolved to perform different functions in Brachypodium, unlike in Arabidopsis, where *ICE* and *SCRM2* are functionally redundant (Raissig *et al.*, 2016). *BdICE1* determines stomatal fate during the initial asymmetric cell divisions leading to stomatal file formation, whereas *BdSCRM2* is vital for the differentiation of the stomatal complex in guard mother cells before subsidiary mother cell formation (Raissig *et al.*, 2016). While *MUTE* in Arabidopsis is necessary solely for guard mother cell identity by preventing asymmetric divisions of the meristemoid, *BdMUTE* in Brachypodium is mobile and moves from the guard mother cell to the adjacent subsidiary mother cells. This movement helps establish subsidiary mother cell identity and promotes cell division (Conklin *et al.*, 2019; Raissig *et al.*, 2017). Nevertheless, these investigations have revealed only a tiny fraction of complex mechanisms involved in stomatal development in grasses. With advancement in technology and the increase in the availability of full genome sequences, further analysis of genes involved in stomatal development in cereals could prove to be useful in manipulating stomatal density on cereal leaves and have the potential to develop new crops with lower water consumption and better yield.

2.1.3 Role of EPF peptide signaling in stomata development

The EPIDERMAL PATTERNING FACTOR (EPF)/ EPF-Like family comprises a group of small, cysteine-rich secreted peptides that are integral to controlling stomatal development in plants. These peptides are defined by the presence of six conserved cysteine residues, which are vital for their functional activity. The N-terminal signal sequence is cleaved from a precursor protein upon the maturation of the secreted peptide and six or eight cysteine residues are responsible for intramolecular disulfide linkages (Katsir *et al.*, 2011). The functional diversity of EPF family peptides arises from the conserved cysteine residues, and the distinctive

loop structure they produce. These loops exhibit significant sequence variability, along with differences in length between the fourth and fifth conserved cysteines (Kondo *et al.* 2010). This variability enables the peptides to carry out a range of functions in stomatal development and plant patterning.

Within the EPF family, various members are involved in distinct aspects of stomatal patterning and broader plant developmental processes. The EPF family in *Arabidopsis* is relatively small consisting of 11 members (EPF1, EPF2 and EPFL1 to EPFL9/STOMAGEN) (Pillitteri and Dong, 2013). The EPFL8 peptide is placed in one subgroup, whereas EPF1, EPF2, and EPFL7 are part of another subgroup that is closely linked to a third subgroup, which includes only EPFL9. In addition, EPFL4, EPFL5, and EPFL6 (collectively termed the *CHALLAH* or *CHAL* family) form a subgroup, primarily regulating growth processes like stem elongation and pedicel development through interactions with ERECTA-family (ERf) receptors. These peptides act redundantly as ligands for ER family receptors, with *chal cll2* mutants mimicking *er* mutant growth defects. Their signaling is spatially restricted by the TMM receptor, which prevents crosstalk between growth-regulatory CHAL family signals and stomatal-patterning *EPF1/2* signals (Abrash *et al.*, 2011). The last subgroup consists of the remaining three EPFs: EPFL1, EPFL2, and EPFL3 (Bessho-Uehara *et al.*, 2016; Tameshige *et al.*, 2016). The four key members, EPF1, EPF2, EPFL9, and EPFL6/CHALLAH (CHAL), of the EPF family play crucial roles in the development of stomata (Katsir *et al.*, 2011). These peptides are responsible for controlling not only how often asymmetric divisions occur but also the way these divisions are oriented.

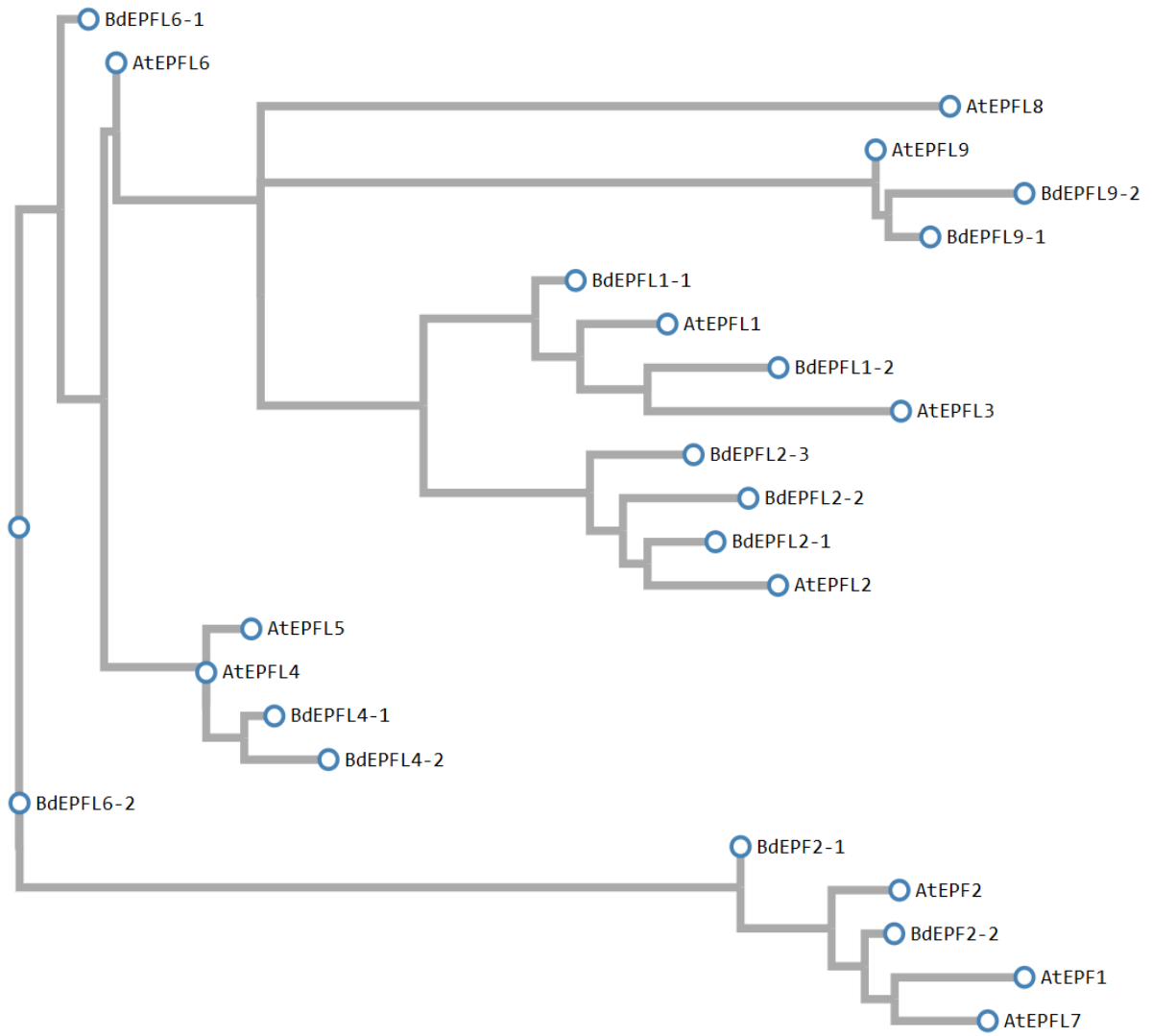
Both *EPF1* and *EPF2* negatively regulate early stages of stomatal differentiation and patterning through common receptors. Because they function at different stages of development, each has a distinct impact on the patterning of the epidermis (Richardson and Torii, 2013). *EPF2* is expressed in protodermal cells prior to their division and plays a key role in regulating early developmental decisions that influence both stomatal and ground cell proliferation. Its overexpression inhibits asymmetric divisions into the stomatal lineage and its loss increases asymmetric divisions causing the increase in production of both guard cells and neighboring stomatal-lineage guard cells (Hara *et al.*, 2009; Hunt and Gray, 2009). *EPF1* is expressed at a later stage and first appears in meristemoids. Mutation in *EPF1* results in incorrect orientation of asymmetric divisions that results in formation of pairs of physically adjacent stomata (Hara *et al.*, 2007). When *EPF1* is overexpressed, protodermal cells divide asymmetrically and the resulting meristemoids do not differentiate further (Hara *et al.*, 2009).

The double mutants *epf1 epf2* have an additive phenotype with approximately twice the density of stomata than wild type (WT) (Hunt and Gray, 2009).

EPFL9 (STOMAGEN) counteracts the functions of *EPF1* and *EPF2*, acting as a positive regulator of stomatal development. It is expressed in the leaf mesophyll layers (Kondo *et al.*, 2010; Sugano *et al.*, 2010). Overexpression or the application of a chemically synthesized EPFL9 peptide increases stomatal density and the presence of adjacent stomata (Kondo *et al.*, 2010; Sugano *et al.*, 2010). Conversely, RNA interference (RNAi) knockdown of *STOMAGEN* results in fewer stomata and guard cells (Sugano *et al.*, 2010). Apart from these three EPFs, more studies are needed to characterize the remaining *BdEPFs* for their role in stomata development. Research done previously has established that controlling stomatal density can significantly impact water use efficiency (WUE) in plants. Frank *et al.*, (2015) constitutively overexpressed *EPF2* in *Arabidopsis* and found the reduction in maximal stomatal conductance (mmol/m/s) due to reduced stomatal density leading to an increase in both instantaneous and long-term WUE without significant alteration in photosynthetic capacity. In contrast, Dunn *et al.*, (2019) reported that in bread wheat (*Triticum aestivum*) severe reduction in stomatal density has a detrimental effect on yield, but moderate reduction in stomatal density had an increase in intrinsic water use efficiency and no significant change in yield was observed. Similar findings were observed in *Brassica napus* by Jiao *et al.*, (2023), where overexpression of the homologous gene *Bna.EPF2* led to 19.02% decrease in stomatal density and size, resulting in approximately 25% lower transpiration rates and improved drought tolerance. Importantly, these modifications did not negatively impact yield traits such as CO₂ assimilation. Most recently, Nerva *et al.* (2023) discovered that intrinsic differential expression of *VvEPFL9*, *VvEPF1*, and *VvEPF2* genes among four grape varieties (*Vitis vinifera*) were associated with modifications in stomatal density, size, and number, suggesting that anatomical changes in stomatal characteristics are genotype dependent, thereby, contributing to intraspecific variability in drought stress tolerance in grapevine. By using several transgenic techniques, Lu *et al.* (2019) also showed that overexpression of *OsEPF1* or *OsEPF2* significantly decreased rice stomatal density. Conversely, *OsEPFL9* knockdown produced transgenic plants with fewer stomata in modified rice than in WT. These studies highlight that careful genetic alterations and breeding programs can enhance drought resilience without sacrificing productivity. Hence, identifying and describing stomatal development genes in monocots can provide insights into cell differentiation, leading to improved crop water efficiency and plant output. Therefore, studying genes that regulate stomatal development would be beneficial.

Previous studies from our lab identified 13 EPF homologs in *Brachypodium* (Jangra et al., 2021). The genes were named based on their sequence similarity with members of the gene family in *Arabidopsis*. Figure 2.3 illustrates the sequence similarity and identity matrix between mature EPFL peptides from *Arabidopsis* and *Brachypodium*. Of these 13 BdEPFs, 11 were expressed highly in the leaf division zone suggesting their role in stomatal development. From these 11 BdEPFs, Jangra *et al.*, (2021) documents the characterization of four BdEPFs showing an required role in stomata development. My aim was to identify new BdEPFs involved in stomata development from the remaining seven BdEPFs. In this study, I successfully identified six BdEPFs, of which four potential BdEPFs could regulate stomatal development in monocots.

A



2.2 Materials and Methods

2.2.1 Plant materials and growth conditions

I used *Arabidopsis Columbia* (Col) as WT control and previously characterized mutants and transgenic plants, including *epf1* (Hara *et al.*, 2007), *epf2* (Hara *et al.*, 2009), *proEst:EPF1 in epf1* and *proEST::EPF2 in epf2* (Lee *et al.*, 2012) *Agrobacterium*-mediated transformation was used to introduce each transgene into both the Col and mutant backgrounds.

Seeds were sterilized by immersing them in a solution containing 5% sodium hypochlorite (NaOCl) and 0.1% triton X-100 for 10 minutes on a rotary shaker. They were then washed for 4-5 times with autoclaved double distilled water. Seeds were vernalized at 4°C in the dark for 2-3 days. Seeds were subsequently plated on ½ Murashige and Skoog (MS) medium with 1% sucrose and 0.68% agar (BiShop Canada). The seedlings were screened on ½ MS medium plates with hygromycin antibiotic (250 mg/L) and cultivated in a growth chamber under regulated conditions of 22°C temperature, 100 $\mu\text{mol m}^{-2} \text{s}^{-1}$ light intensity, and a long-day cycle (18 h light/6 h dark). Selected *Brachypodium* seedlings (5-6 days old) and *Arabidopsis* seedlings (10 days old) were moved to soil (2 black earth: 1 vermiculite: 1 peat moss) and cultured at 22°C in a long-day environment (18 h light/6 h dark). Nine *Arabidopsis* seedlings were placed into each soil container to ensure constant development throughout the trial, whereas for *Brachypodium*, four seedlings were transplanted per pot.

2.2.2 Plasmid construction

Constructs for the estradiol-inducible expression of *Brachypodium EPF* genes in *Arabidopsis* were generate (Zuo *et al.*, 2000). The constructs for expression of *Brachypodium* genes under the regulation of *Arabidopsis* promoters were developed in the Gateway cloning system (Invitrogen) vector pGWB501 R4. For *Brachypodium* overexpression transgenic lines, the pIPKb002 plasmid was used. Table 2.1 provides complete information on the plasmid constructs used for this study.

Table 2.1: List of Plasmid used

Plasmid Description	Insert	Vector	Bac ^R	Plant ^R
<i>Est::BdEPFL1-1</i>	BdEPFL1-1 (pXTW13)	pER8	Spec	Hyg
<i>Est::BdEPFL1-2</i>	BdEPFL1-2 (pJSL310)	pER8	Spec	Hyg
<i>Est::BdEPFL2-1</i>	BdEPFL2-1 (pJSL297)	pER8	Spec	Hyg
<i>Est::BdEPFL2-2</i>	BdEPFL2-2 (pJSL298)	pER8	Spec	Hyg
<i>Est::BdEPFL6-1</i>	BdEPFL6-1 (pJSL311)	pER8	Spec	Hyg
<i>Est::BdEPFL6-2</i>	BdEPFL6-2 (pJSL313)	pER8	Spec	Hyg
<i>AtEPF1pro:BdEPFL1-1</i>	pAtEPF1:BdPFL1-1 (pBK1 + pXTW13)	pGWB501 R4	Spec	Hyg
<i>AtEPF1pro:BdEPFL2-2</i>	AtEPF1pro:BdEPFL2-2 (pBK1 + pJSL298)	pGWB501 R4	Spec	Hyg
<i>AtEPF1pro:BdEPFL6-1</i>	pEPF1:BdEPFL6-1 (pBK1 + pJSL311)	pGWB501 R4	Spec	Hyg
<i>AtEPF1pro:BdEPFL6-2</i>	pAtEPF1:BdEPFL6-2 (pBK1 + pJSL313)	pGWB501 R4	Spec	Hyg
<i>AtEPF2pro:BdEPFL1-1</i>	pAtEPF2:BdEPFL1-1 (pJSL146 + pXTW13)	pGWB501 R4	Spec	Hyg
<i>AtEPF2pro:BdEPFL2-2</i>	AtEPF2pro:BdEPFL2-2 (pJSL146 + pJSL298)	pGWB501 R4	Spec	Hyg
<i>AtEPF2pro:BdEPFL6-1</i>	pAtEPF2:BdEPFL6-1 pJSL146 + pJSL313)	pGWB501 R4	Spec	Hyg
<i>AtEPF2pro:BdEPFL6-2</i>	pAtEPF2:BdEPFL6-2 (pJSL146 + pJSL313)	pGWB501 R4	Spec	Hyg
<i>ZmUbi1pro:BdEPFL1-1</i>	BdEPFL1-1 (pXTW13)	pIPKb002	Spec	Hyg

2.2.3 Agrobacterium mediated transformation and transgenic development

Using 250-500 ng of plasmid DNA, competent *Agrobacterium* (GV3101 strain) cells were transformed with the cloned constructs. DNA was added to about 50 μ L of GV3101 cells which were then transferred to prechilled glass cuvettes on ice. Electroporation was carried out with a Bio-Rad MicroPulsar Electroporator, which delivered an electric shock for 2 seconds. After adding 1mL of Super Optimal broth with Catabolite repression (SOC) medium, tubes were incubated at 28 °C for 1 h at 180 rpm. Aliquots of 50 μ L of developed cells were placed on LB

medium plates (1% NaCl, 1% Tryptone, 0.5% yeast extract in ddH₂O, pH 7.0, 0.68% agar) with suitable bacterial antibiotic selection. After 2 days of incubation at 28°C, modified *Agrobacterium* colonies were used to inoculate liquid broth culture for floral dipping.

Transgenic *Arabidopsis* lines were developed in accordance with Clough and Bent (1998). Four hundred mL of LB medium was inoculated with selected antibiotics and Gentamycin, using 4-4.5 mL of primary overnight-grown GV3101 cells containing the transgene, which was then incubated for 1.5 days at 28 °C and 200 rpm. After OD 0.6, cells were centrifuged in 2000Xg for 20 minutes. The pellet was resuspended in a 400 mL dipping solution containing 5% sucrose and 0.05% Silwett L-77. Plants with about 10 cm inflorescences were inverted and the bolted area was dipped for 5 seconds twice in the dipping solution. Dipped plants were covered with a transparent tray lid and stored overnight in the dark at room temperature. The next morning, the plants were placed upright and watered in the growth chamber. After 1-2 weeks of development, plants were dried in a greenhouse before harvesting the seeds.

After harvesting, transgenic seeds were sown on ½ MS plates with hygromycin antibiotic (250 mg/L) for transgene selection. Resistant transgenic seedlings were selected, at 10dpg using 40-50 seedlings from each plate at T1 or from each line at T2. Selected transformants were confirmed by both antibiotic resistance and phenotype with green leaves and solid roots, then transferred to soil to produce next-generation seeds.

2.2.4 DNA extraction and genotyping

To validate the transgene insertion and background, DNA was collected from individual or pooled leaf samples from transgenic lines. The genomic DNA was isolated using the procedure of Edwards *et al.* (1991). To extract DNA, a 100 mg sample of *Arabidopsis* leaves were ground and placed in a 1.5 mL microcentrifuge tube with 200 µl of DNA extraction buffer (200 mM Tris-HCl, pH 7.5, 250 mM NaCl, 25 mM EDTA, 0.5% SDS in autoclaved ddH₂O water). The samples were then vortexed at 6000Xg for 5 minutes. After that, 150 µL of supernatant was collected in a new Eppendorf tube, mixed with 150 µL of isopropanol (1:1 v/v) by inverting, and incubated at room temperature for 2 minutes. After a 5-minute centrifugation at 6000Xg, supernatant was removed and 500 µL of ethanol were added. Again, after centrifugation for 2 minutes, the supernatant was removed, and the tubes were dried with a speed vacuum for 15-20 minutes or air dried overnight. The isolated DNA was resuspended in 50 µL of ddH₂O and stored at 4°C for future use. PCR was performed to detect transgene on a Bio-Rad T100™ Thermal Cycler to identify plant genotypes using

construct specific and gene specific primers and using WT primers for endogenous genes as controls. Lines showing 3:1 segregation at T2 were selected as single copy TDNA insertions and at T3 lines with 100% germination on antibiotic plates were selected as homozygous for the transgene. Table 2.2 shows the primers used to determine background and gene specificity.

Table 2.2: List of primer used

Gene name	Primer name	Primer Sequence (5' to 3')
<i>BdEPFL1-1</i>	BdEPFL1-1 1 XhoI f	CACCCTCGAGATGGCCGTGAGCTCAGCACCT
	BdEPFL1-1 453 SpeI.rc	CGGACTAGTGGGGTTGTAGAGGCGGC
<i>BdEPFL1-2</i>	BdEPFL1-2 1 XhoIf	CGCCTCGAGATGAGCTCACCAGCTGCCAT
	BdEPFL1-2 375 SpeI.rc	CGGACTAGTTCAGGGGTCGTAGAGTCGGT
<i>BdEPFL2-1</i>	BdEPFL2-1 1 XhoIf	CGCCTCGAGATGGTCCATTTCTTGCAATGCA
	BdEPFL2-1 456 SpeI.rc	CGGACTAGTTCATGGATCAAGGATGCTGCCT
<i>BdEPFL2-2</i>	BdEPFL2-2 1 XhoIf	CGCCTCGAGATGGACCATCTTTTCCTGCT
	BdEPFL2-2 393 SpeI.rc	CGGACTAGTTCATGGGCTCAATATCAAG
<i>BdEPFL6-1</i>	BdEPFL6-1 1 XhoIf	CGCCTCGAGATGGAGAGCTCCCGGGGGA
	BdEPFL6-1 411 SpeI.rc	CGGACTAGTCTATGGCATGTAGAGCCGGTT
<i>BdEPFL6-2</i>	BdEPFL6-2 1 XhoIf	CGCCTCGAGATGCCATCCTGCACGGGGA
	BdEPFL6-2 447 SpeI.rc	CGGACTAGTTTACGGCATGTAGAGGCGGT
EST promoter	pER8 f	TCATTTTCATTTGGAGAGGACACGCT
	pER8 rc	TCGAAACCGATGATACGGACG
AtEPF1	EPF1 -705f	GTTAAGCCGTTGACTTTGG
AtEPF2	EPF2 -677f	TCATCCTTGTGTACAATATGATC

2.2.5 RNA extraction and cDNA synthesis

RNA was extracted from ten-day-old Arabidopsis transgenic seedlings cultivated on ½ MS plates, with or without 30µM estradiol. The samples were promptly frozen in liquid nitrogen and stored at -80°C. The RNeasy Mini plant kit (Qiagen) was used to extract total RNA from 6-8 independent T1 or T2 lines, both with and without 30 µM Estradiol, following the manufacturer's recommendations. To prevent RNA degradation, tissues were pulverized with a prechilled plastic pestle and liquid nitrogen before adding 450 µL of RLT buffer (premixed with beta-mercaptoethanol in a 1:100 ratio). After centrifuging Eppendorf tubes for 1 minute, the lysate was transferred to a QIA shredding spin column and centrifuged at maximum speed 6000Xg for 2 minutes. The supernatant was then combined with 1 volume of 95% ethanol. The solution was immediately transferred to the RNA binding column, followed by 350µl of RW1 buffer. The tubes were centrifuged at 6000xg for 15 seconds. Next, 80 µL of DNase1 (5U/ µL) (Qiagen) was added and incubated for 15 minutes at room temperature. After incubation, 350 µL of RW1 buffer was added and the column centrifuged at 6000Xg for 15 seconds. Next, 500 µL of RPE buffer was added and the columns were centrifuged at 6000Xg for 15 seconds, followed by 2 minutes centrifugation at 6000Xg. RNA was eluted in a new 1.5 mL microcentrifuge tube using 30 µL of RNAase-free elution buffer and stored at -80°C. cDNA was synthesised using 1 ng DNA using Thermo Scientific RevertAid RT Kit (Thermo Scientific, Canada). For RT-PCR, uninduced samples for each gene were used as control for confirming the induction by estradiol in SimpliAmp Thermal Cycler (Thermo Scientific, Canada).

2.2.6 Microscopy and quantitative analysis of stomatal phenotype

The phenotypic analysis of Arabidopsis epidermal cells was investigated using a Nikon C2 laser scanning confocal microscope with a sharp objective lens (40x). A tiny portion of the leaf was cut and mounted in 5-10 µL of propidium iodide (2 mg/mL ddH₂O). A 561 nm laser was used to stimulate propidium iodide (PI) fluorescence during imaging. To view green fluorescent protein (GFP) signals, a 488 nm excitation filter was utilized. For imaging, a 1.49 refractive index immersion oil was used for the 40X lens. Bandpass filters (BP 525/50 for GFP and BP 561 for PI) were used to filter emission wavelengths. The photographs were processed with Fiji program (ImageJ) and false colored with Photoshop CS6 (Adobe).

For differential interference contrast (DIC) microscopy, leaf samples were cut into 0.5 cm pieces and put into clearing solution (9:1 ethanol:acetic acid). After clearing for 3-4 days, samples were transferred to multiwell plates submerged in 1-2 mL of 1N KOH solution for at

least 2 hrs, followed by two washes with ddH₂O. The samples were then placed in a 1.5 mL MCT containing 1mL Hoyer's medium for 1-2 days in dark (Bergmann *et al.*, 2004). For viewing, samples were mounted in Hoyer's medium and imaged using a Leica DM6000 microscope.

Stomatal phenotypes were analyzed quantitatively using Toluidine Blue O (TBO)-stained epidermal samples, as previously described (Guseman *et al.*, 2010). The cotyledons of 10-day-old *Arabidopsis* seedlings and the base of first leaves of 6- to 8-day-old *Brachypodium* seedlings were fixed in 1 mL of a 9:1 ethanol:acetic acid solution for imaging. Fixed samples were treated twice with 70%, 50%, and 20% ethanol for 20 minutes each the day before imaging, then kept in 1mL ddH₂O solution. The next day, samples were stained with 1 mL of filtered 0.5%(w/v) TBO stain in 1.5 mL tubes, followed by 3-4 minutes of incubation at room temperature (RT). After removing the TBO stain, samples were washed 4-5 times with ddH₂O. The samples were mounted in 15% glycerol and photos were acquired with a Nikon Eclipse TiE inverted epifluorescence microscope and a DsRi2 digital camera (Nikon). I counted the number of stomata and non-stomatal cells in each image and calculated the density for each cell type. Non-stomatal cells included pavement cells, meristemoids and stomatal lineage ground cells (small cells in the vicinity of stomata). Significant differences across genotypes were evaluated using Tukey's HSD test ($P < 0.05$) or Student's t-test ($P < 0.0001$).

2.3 Results

2.3.1 Identification of putative EPF peptides controlling stomal development and patterns in *Brachypodium*

To investigate the possible roles of six EPFL members of the *Brachypodium* EPF gene family in growth and development, we performed real-time quantitative PCR (qRT-PCR) on tissues roots, and division zone, and mature zone in leaves at different developmental stages, to analyze how the expression of each EPF gene varies across different organs and developmental stages in *Brachypodium*.

The expression of six BdEPFL family members, namely *BdEPFL1-1*, *BdEPFL1-2*, *BdEPFL2-1*, *BdEPFL2-2*, *BdEPFL6-1*, and *BdEPFL6-2* are predicted to encode peptides with high sequence similarity to *Arabidopsis* stomatal EPFL1, EPFL2 and EPFL6 peptides, was significantly higher in leaf division zone than in leaf mature zone or roots. The names BdEPFL1-1 and BdEPFL1-2 were assigned to reflect their close high sequence similarity to the AtEPFL1 peptide. A similar naming approach was used for other BdEPFL family members. The observed expression patterns (Figure 2.4) suggest the possible involvement of these genes in regulating stomatal development in monocots.

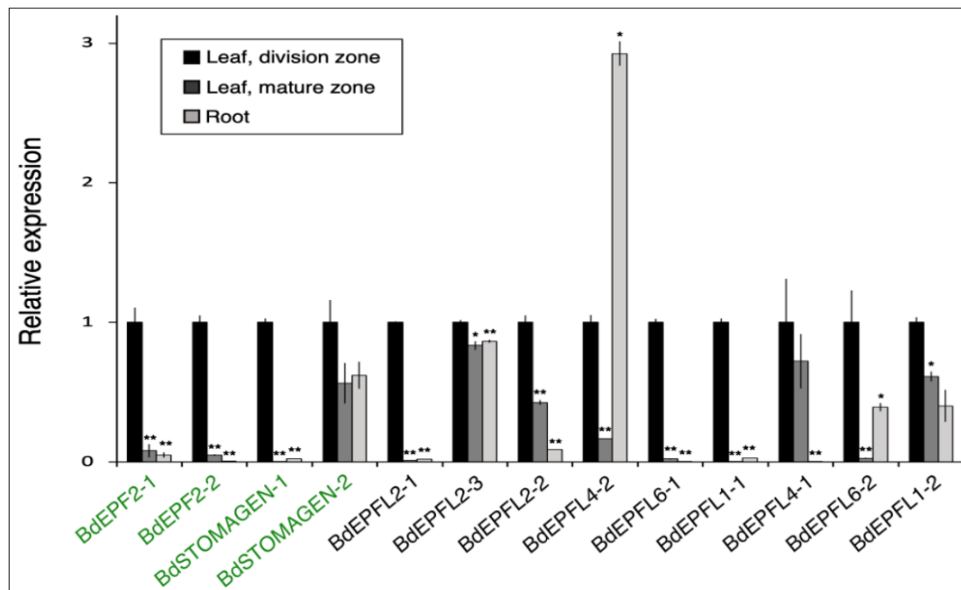


Figure 2.4: Expression levels of EPF homologs in several *Brachypodium* tissues: roots, young leaves and mature leaves. Young leaves and roots were collected from plants 5-7 days post germination (dpg). Samples of mature leaves were collected 10 weeks following germination. BdUBC18 served as an internal control, and the values for leaf division zone were set to 1. Data are mean \pm SEM (n=3). Normalization was done with respect to each gene expression level in the leaf division zone. Graph adapted from Jangra *et. al.*, (2021).

2.3.2 Functional analysis of BdEPF candidates

Stomatal EPFs are the most extensively studied members of the EPF family in Arabidopsis. To explore the functional relevance and conservation of grass EPF homologs, in-depth analysis of Brachypodium peptides with sequence similarity to Arabidopsis stomatal EPFs showed that when *EPF1/EPF2* homologs from Brachypodium are overexpressed in Arabidopsis, they inhibit the initiation of stomatal lineage, whereas *EPFL9/STOMAGEN* promotes the development of stomata (Jangra *et al.*, 2021). In this study, additional *BdEPF* gene family members, *BdEPFL1*, *BdEPFL2* and *BdEPFL6*, were overexpressed in transgenic Arabidopsis plants using an estradiol-induction system. Subsequently, transgenic Arabidopsis seeds carrying inducible *BdEPFL* genes under control of the estradiol promoter were sown on ½ MS media supplemented with or without estradiol. Seedlings, ten dpg were screened for defects in epidermal phenotypes in the presence and absence of induced estradiol.

The inducible system worked well as the induced control lines (EST:EPF1 and EST:EPF2) had an expected stomatal development phenotype of arrested divisions and pavement cells respectively, while the WT showed normal stomatal development (Figure 2.5 A-C). Estradiol induced *BdEPFL1-2*, *BdEPFL2-1* lines did not show any defect in epidermal phenotype on screening, whereas induced *BdEPFL1-1*, *BdEPFL2-2*, *BdEPFL6-1* and *BdEPFL6-2* had epidermis where multiple cells were arrested in asymmetric divisions and failed to develop normal stomata when compared to WT (Figure 2.5 A-I and Figure 2.6).

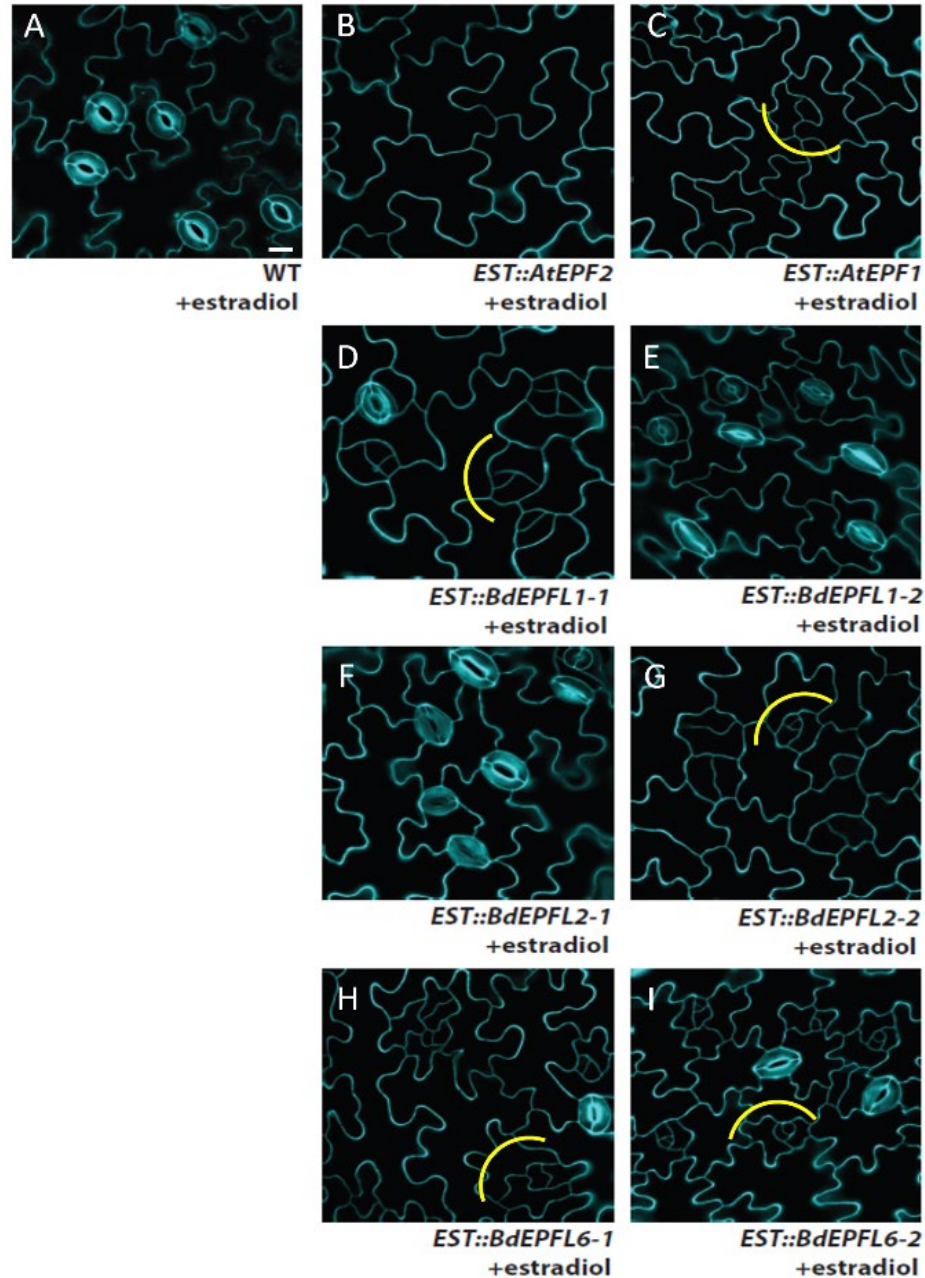


Figure 2.5: Ectopic expression of stomatal EPF homologs exhibits stomatal development defects in Arabidopsis. (A-I) Representative confocal images of the abaxial cotyledon epidermis of 10-day-old Arabidopsis transgenic seedlings carrying estradiol-induced constructs that were treated with estradiol. (A) WT, (B) *Est::AtEPF1*, (C) *Est::AtEPF2*, (D) *Est::BdEPFL1-1*, (E) *Est::BdEPFL1-2*, (F) *Est::BdEPFL2-1*, (G) *Est::BdEPFL2-2*, (H) *Est::BdEPFL6-1*, and (I) *Est::BdEPFL6-2*. Scale bar = 30 μ m. Yellow brackets depict excessive entry division.

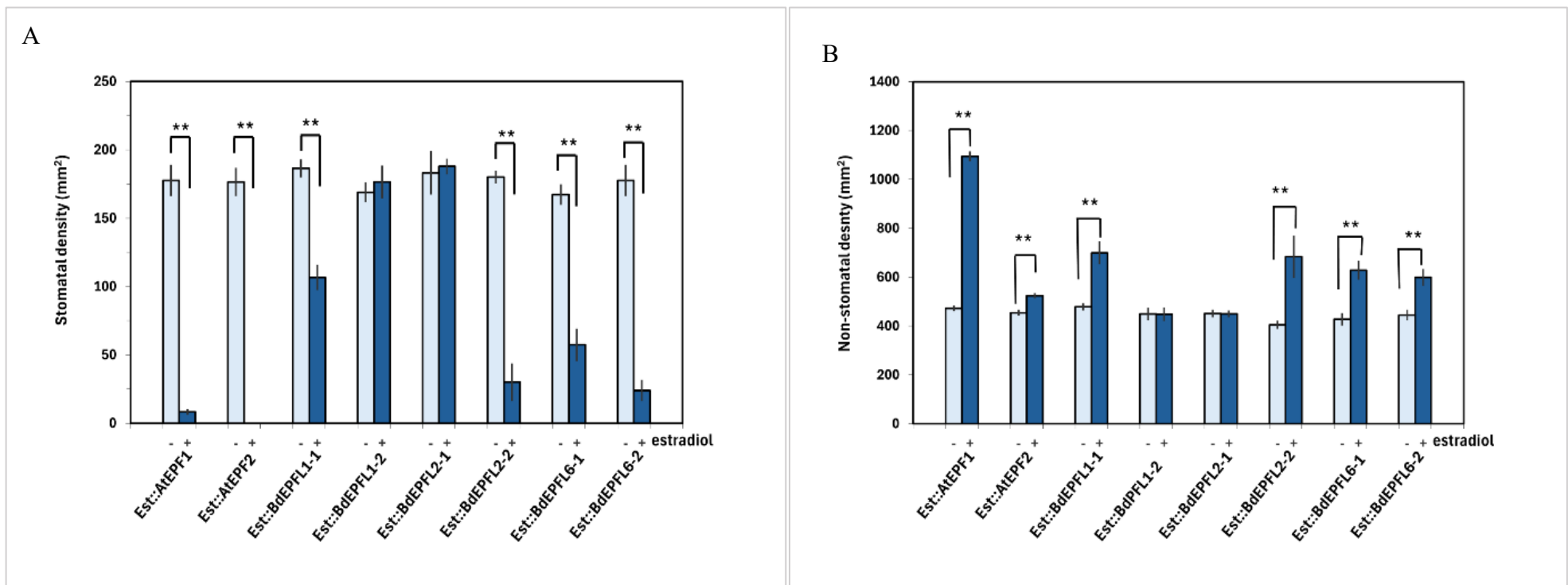


Figure 2.6: Quantitative analysis of stomatal density on the abaxial cotyledon epidermis of 10-day old seedlings for *Arabidopsis* lines with ectopic expression of *Brachypodium* stomatal EPF homologs. They exhibit stomatal development defects in *Arabidopsis*. (A) Stomatal density, (B) Non-stomatal density from *Arabidopsis* transgenic seedlings, harboring constructs of EPF homologs from *Brachypodium*. Comparison was made between plants induced and uninduced transgenic seedlings. ‘-’ indicates no estradiol and ‘+’ indicates estradiol by estradiol. Data presented means \pm standard error. ** $P < 0.0001$ (Student’s t-test); $n = 8-10$ for each genotype.

2.3.3 Cross-species complementation assay of potential BdEPF homologs by using Arabidopsis Promoter

I performed cross-species complementation analysis to further specify the function of BdEPFLs in regulation of stomatal development. To achieve this, *BdEPFL1*, *BdEPFL2*, *BdEPFL6* candidates were expressed under the native *AtEPF1* and *AtEPF2* promoters in *epfl* and *epf2* loss of function mutant lines to drive their expression with the tissue specific and developmental stage specific expression of the endogenous homolog. *AtEPF1* expression is observed in late meristemoids, guard mother cells and young guard cells and *AtEPF2* expression is reported to be in the early developmental stages *viz.* meristemoid mother cells and early meristemoids (Hara *et al.*, 2009; Hara *et al.*, 2007). Of six *BdEPFLs* analyzed in overexpression study, four (*BdEPFL1-1*, *BdEPFL2-2*, *BdEPFL6-1* and *BdEPFL6-2*) were carried forward for complementation studies. Since *BdEPFL1-2* and *BdEPFL2-1* did not show epidermal defects, these were not used for further study.

The *epfl* mutants exhibited the stomatal clustering phenotype that arises due to defects in the regulation of spacing divisions (Hara *et al.*, 2007). The construct *AtEPF1pro::BdEPFL2-2* expressed in *epfl* suppressed the stoma clustering phenotype of *epfl*, however, other lines (*AtEPF1pro::BdEPFL1-1*, *AtEPF1pro::BdEPFL6-1* and *AtEPF1pro::BdEPFL6-2*) suppressed the *epfl* mutant phenotype partially (Figure 2.7 B-F). The observed reduction in stoma clustering phenotype of *epfl* in *AtEPF1pro::BdEPFL2-2* lines was statistically significant (Figure 2.8 A). The *BdEPFL1*, *BdEPFL2*, and *BdEPFL6* genes were then screened for complementation of epidermal phenotype of *epf2* which has a phenotype of excessive entry divisions causing a significant increase in nonstomatal cell density (Hara *et al.*, 2009; Hunt and Gray, 2009). In this case, *AtEPF1pro::BdEPFL2-2* in *epf2* had no influence on epidermal phenotype (Figure 2.7 G-K). However, lines *AtEPF2pro::BdEPFL1-1*, *AtEPF2pro::BdEPFL6-1*, *AtEPF2pro::BdEPFL6-2* expressed in *epf2* appeared to partially reduce the non-stomatal cell density (Figure 2.8 B). Hence, these results are somewhat consistent with the overexpression of Brachypodium EPFL homologs in Arabidopsis. The reduced effect of the transgenic expression of these genes under the control of Arabidopsis promoter compared to the 35S promoter is likely due to the lower strength of the Arabidopsis promoters relative to the 35S promoter. In summary, these results suggest that while *BdEPFL2-2* can replace *AtEPF1*, it does not perform the same function as *AtEPF2* in Arabidopsis.

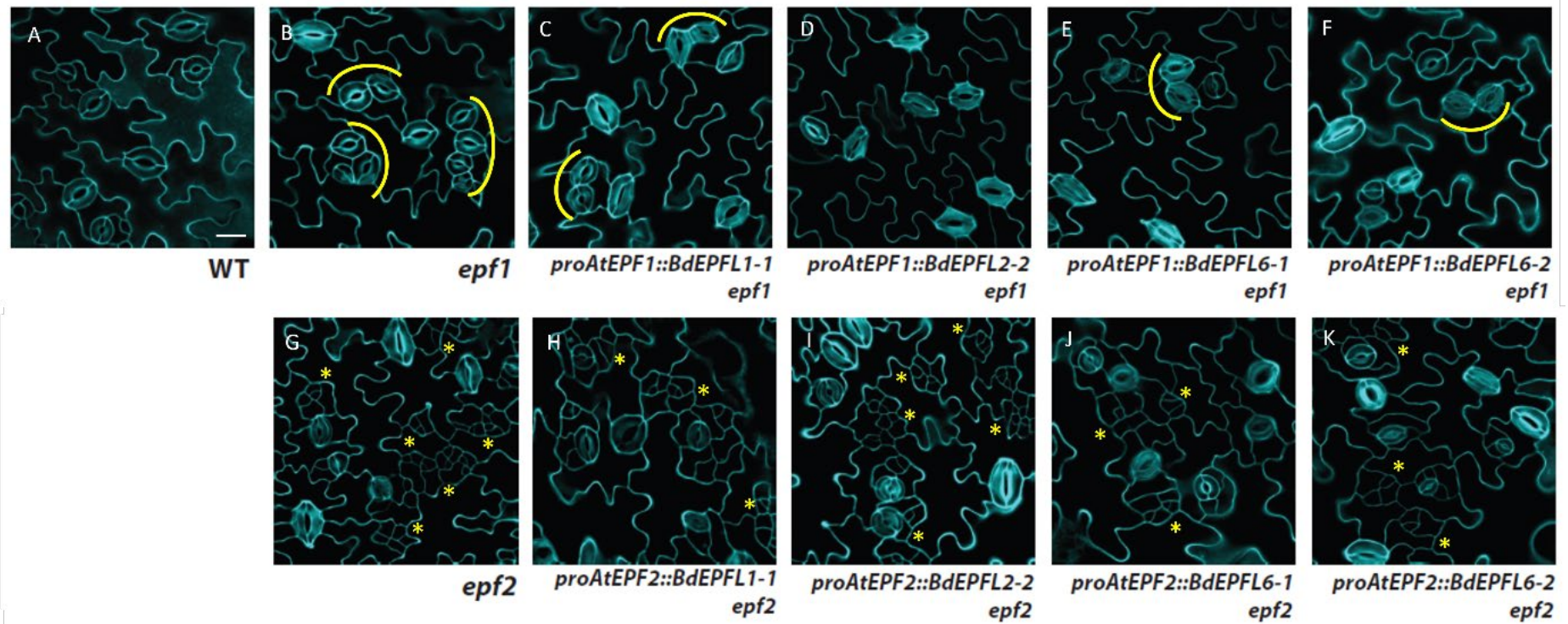


Figure 2.7: Complementation of Arabidopsis *epf1* and *epf2* mutants by *BdEPF* homologs. (A-K) Images of 10-day-old abaxial cotyledons of the (A) WT, (B) Arabidopsis *epf1* mutant, (C) *AtEPF1::BdEPFL1-1* in *epf1*, (D) *AtEPF1::BdEPFL2-2* in *epf1*, (E) *AtEPF1::BdEPFL6-1* in *epf1*, (F) *AtEPF1::BdEPFL6-2* in *epf1*, (G) Arabidopsis *epf2* mutant, (H) *AtEPF2::BdEPFL1-1* in *epf2*, (I) *AtEPF2::BdEPFL2-2* in *epf2*, (J) *AtEPF2::BdEPFL6-1* in *epf2*, (K) *AtEPF2::BdEPFL6-2* in *epf2*. Scale bar= 30 μ m. Yellow brackets depict stomatal pairing phenotype, asterisks show excessive entry division.

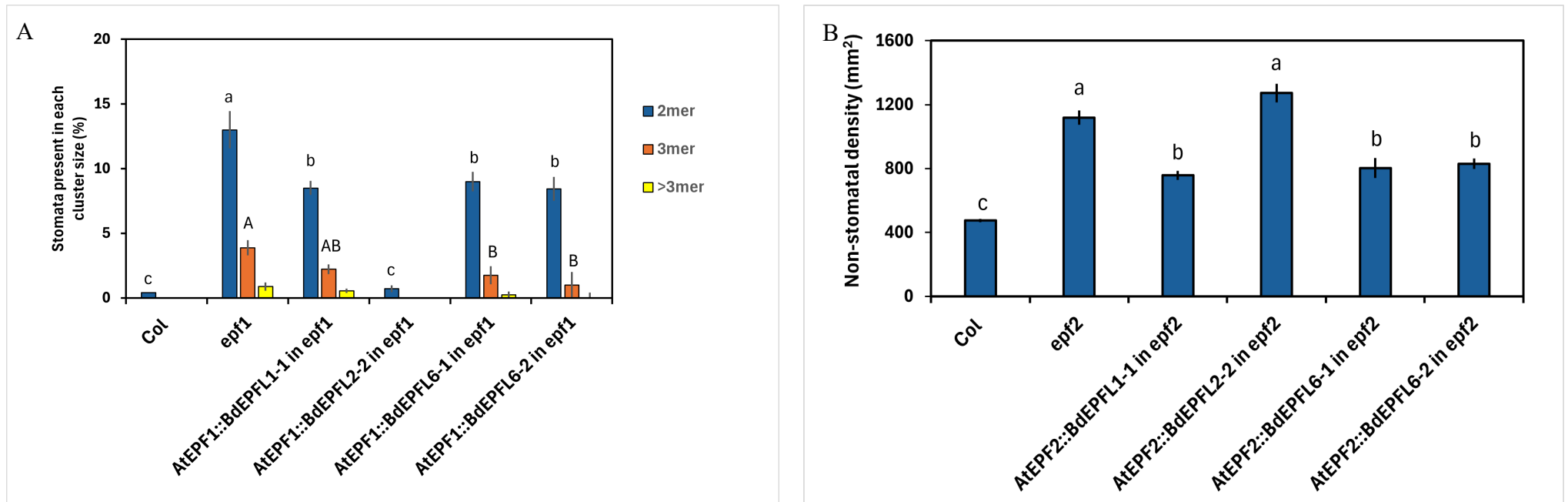


Figure 2.8: Quantitative analysis of 10-day-old abaxial cotyledon epidermis for complementation of Arabidopsis *epf1* and *epf2* mutants by *BdEPF* homologs. (A) Cluster count per stomata group in the *epf1* mutant and the *epf1* mutant expressing Brachypodium EPF genes, (B) Nonstomatal epidermal cell density of 10-day-old abaxial cotyledons of the *epf2* mutant and the *epf2* mutant expressing *AtEPF2* and Brachypodium EPF homologs. Data presented are mean \pm s.e (n=7-8). Following one-way ANOVA, Dunnett's Multiple Comparison test was performed with $P < 0.0001$. In Figure A, independent statistical analysis was performed for each stomata cluster level. The results of Dunnett's MC test for 2 mers are shown in the series a, b and those for 3 mers are shown in the series A, B.

2.3.4 Effect of overexpression of BdEPFLs on the epidermal phenotype in Brachypodium

To gain further insight into the role of BdEPFLs in regulating grass stomatal development, which is different from dicot stomatal development, I next prepared the transgenic Brachypodium lines overexpressing the BdEPFLs under the control of *Zea mays* ubiquitin promoter through embryogenic callus transformation. *BdEPFL1-1* was selected for generating overexpression transgenic lines in Brachypodium as it demonstrated partial complementation with both *Atepf1* and *Atepf2* mutants in Arabidopsis, suggesting its potential involvement in the stomatal development pathway of grasses. Validation of these transgenic lines overexpressing BdEPFL1-1 was done using qRT-PCR.

The two overexpressing lines of OxBdEPFL1-1 #1 and #2 had statistically significant reduction in stomatal density in Brachypodium, while non-stomatal density remained unchanged. Subsequently, although not significant, data suggest an increase in hair cell density for overexpression lines which further suggests that hair cell development is the default fate for the smaller cell after first asymmetric division (Figure 2.9 A-F). Detailed microscopic analysis of different stages of stomata development revealed that there was no difference between WT and Ox lines during stomatal file establishment and asymmetric division to guard mother cell. However, during guard mother cell maturation and subsidiary cell formation, OxBdEPFL1-1 is deficient in establishing subsidiary cells surrounding the guard mother cells. Additionally, the overexpression lines exhibited two adjacent stomatal files, while normally single stomatal file separated by 2-3 non-stomatal files is developed in WT. Overall, BdEPFL1-1 appears to act as a negative regulator by potentially limiting the subsidiary cell formation and preventing establishment of guard mother cell fate in small daughter cell after asymmetric division (Figure 2.10).

Moreover, phenotypic assessment of the overexpression lines revealed that these plants had stunted growth, delayed blooming, and reduced seed fertility (Figure 2.11). These results confirmed the negative regulatory role of BdEPFL1-1 in plant growth and seed fertility..

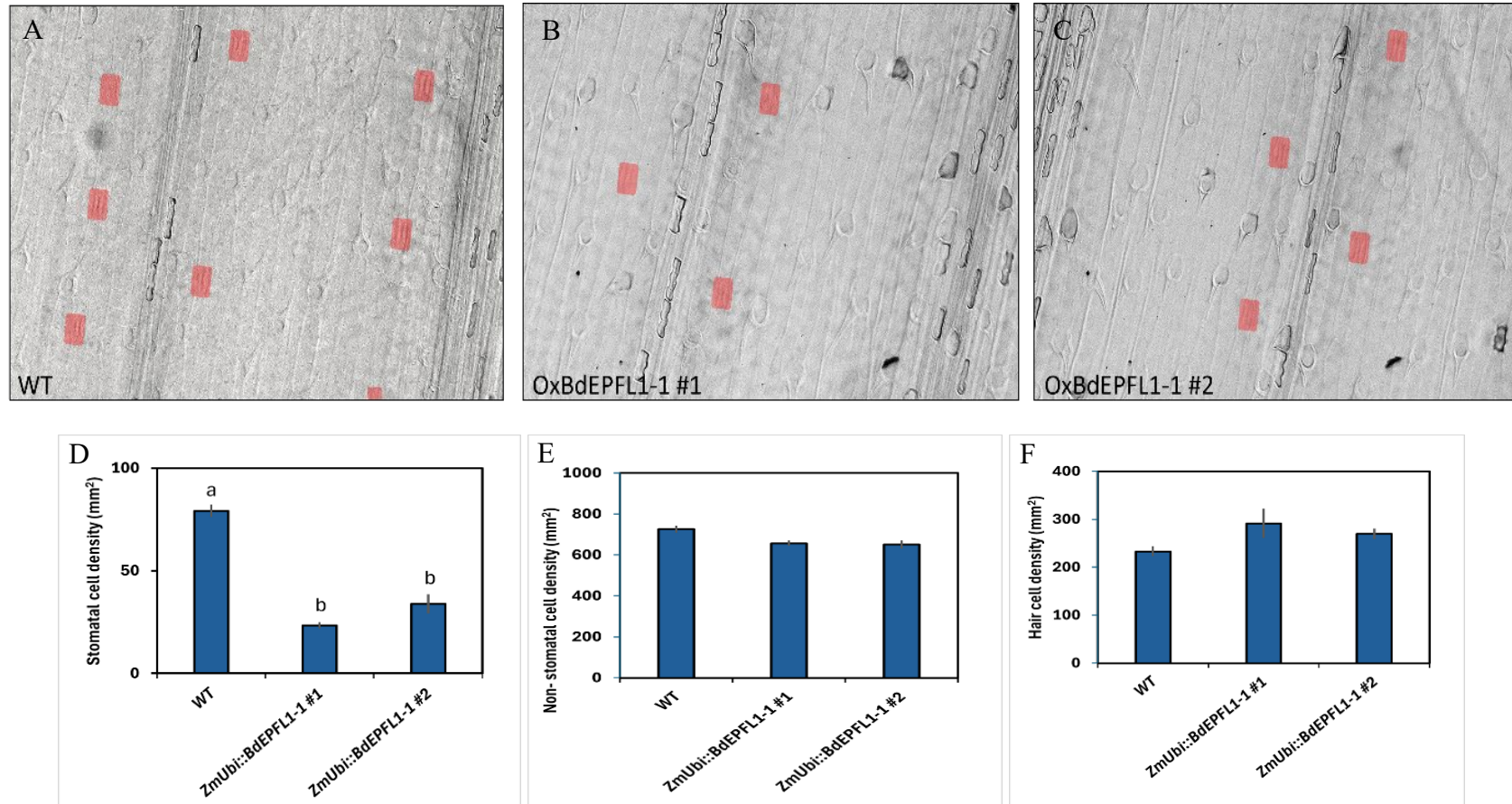


Figure 2.9: Overexpression analysis of BdEPFL1-1 in Brachypodium. (A-C) Differential interference contrast (DIC) microscopy images of stomata (red) from cleared leaf tissue in (A) WT, (B) *OxBdEPFL1-1 #1* and (C) *OxBdEPFL1-1 #2*. (D-F) Quantitative analysis of 1st leaf epidermis 1-2cm from two Ox transgenic lines: D, Stomatal density (number of stomata per mm²) from #1 and #2 transgenic Brachypodium seedling compared with WT. E, Non-Stomatal density from #1 and #2 transgenic Brachypodium seedlings compared with WT. F, Hair cell density from #1 and #2 transgenic Brachypodium seedlings compared with WT. Data represent mean \pm SE ($n = 8$). Following one-way ANOVA, Tukey's Multiple Comparison test was performed comparing means of different genotypes against WT with $P < 0.05$. Genotypes with no significant differences were assigned same letter.

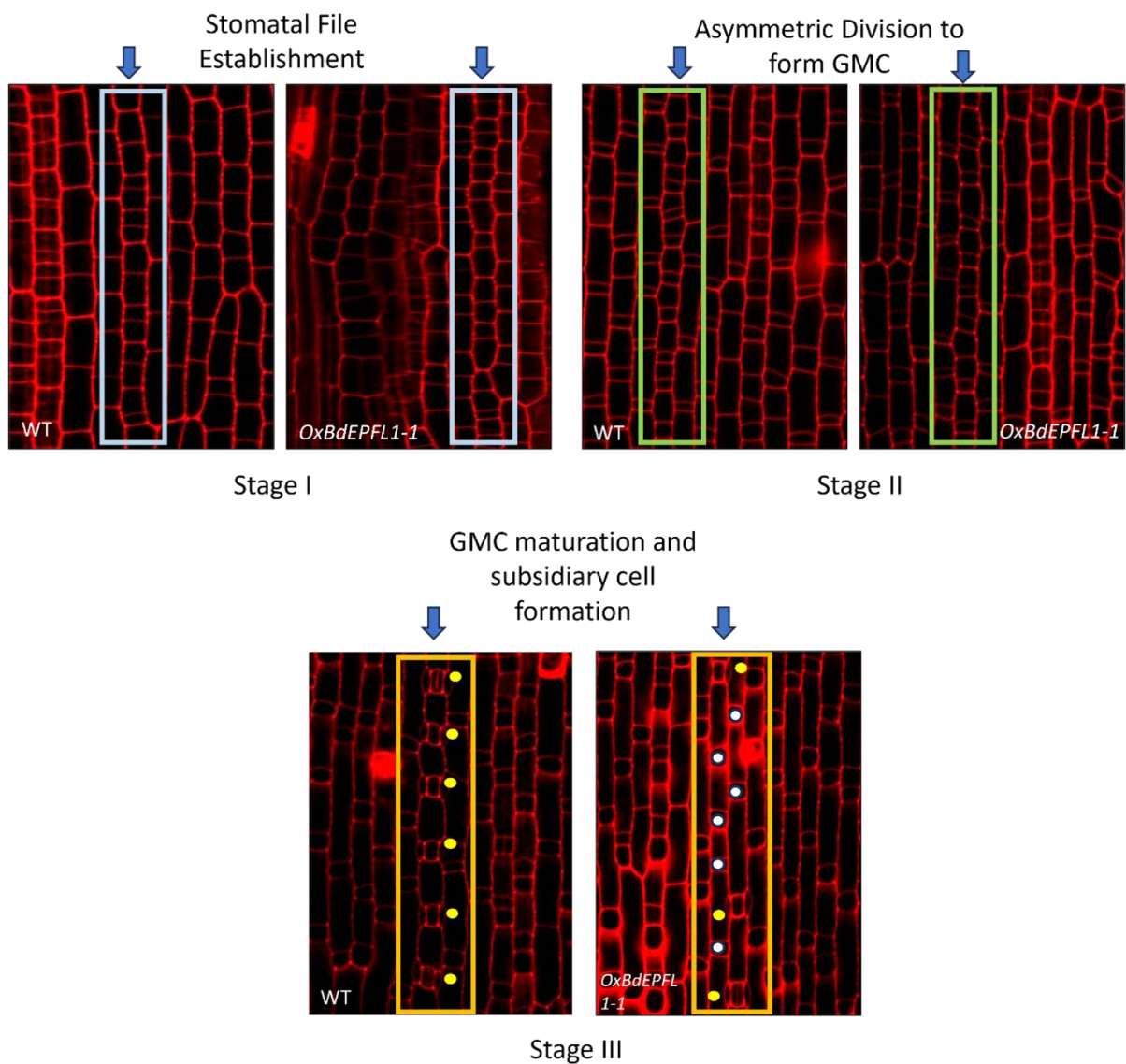


Figure 2.10: Confocal images of leaf division zone of WT and transgenic *Brachypodium* overexpressing *BdEPFL1-1* with the *ZmUbi::BdEPFL1-1* construct. Stages 1-3 as follows: A stomatal file is established (Stage I; blue), following an asymmetric division (Stage II; green), Guard mother cell (GMC) induce subsidiary cell formation from laterally adjacent cells (Stage III; orange), which divide asymmetrically to produce subsidiary cells from the smaller daughter cell. Yellow dots indicate mature guard mother cells flanked by mature subsidiary cells depicting normal stomatal complex formation. White dots indicate guard mother cells that are not flanked by subsidiary cells, an aberrant phenotype.

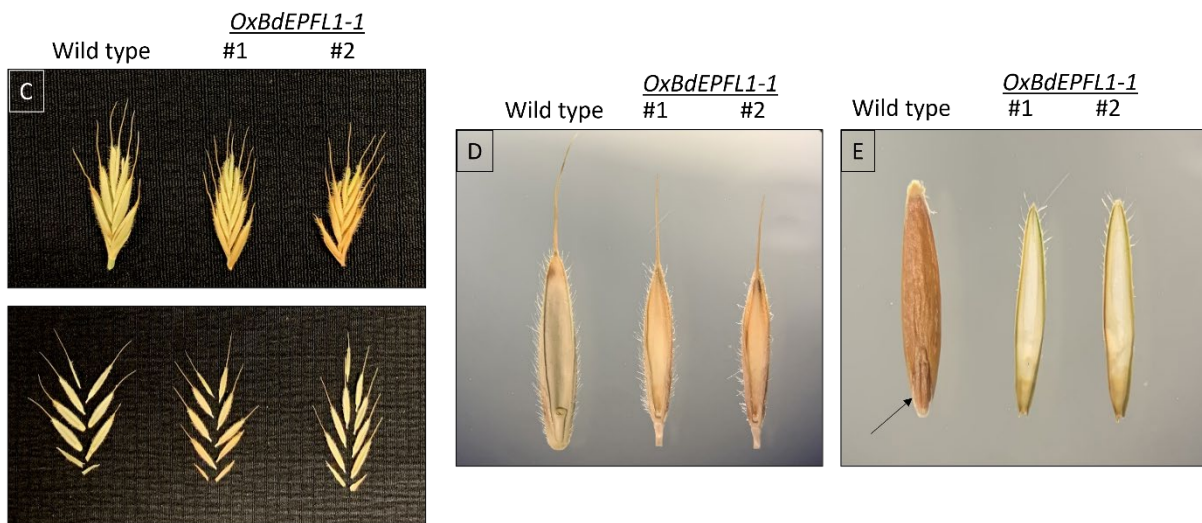


Figure 2.11: Phenotypic characterization of the *OxBdEPFL1-1* Brachypodium transgenic lines. (A-B) *OxBdEPFL1-1* has stunted growth and delayed flowering compared to the WT at (A) young stage and (B) flowering stage. (C-E) Brachypodium grain morphology. (C) Spike from WT and OE showing spikelet arrangement. (D) Ventral surface of intact grains showing smaller size of grain from Ox lines compared to WT. (E) After removal of the husk, the endosperm and embryo is visible in WT. Arrow indicates the position of the embryo. Seeds from Ox lines are sterile.

2.4 Discussion

In this study, I explored the biological functions of EPFL peptides within *Brachypodium*, a model monocot plant used to study developmental processes that differ from those of dicots. A study published from our lab (Jangra *et al.*, 2021) utilizing *in-silico* phylogenetic analysis has identified 13 EPFL homologs in *Brachypodium*. To explore the functional roles and evolutionary conservation of EPFL homologs in grasses, previous lab members conducted studies on a subset of grass EPFs, namely *Brachypodium* EPF1, EPF2, and EPFL9/STOMAGEN, that are homologous to the *Arabidopsis* stomatal EPFs. Two *Brachypodium* genes with high similarity to AtEPF2, and two genes with high similarity to AtEPFL9/STOMAGEN were identified as candidate orthologs in *Brachypodium*.

Furthermore, we found two *Brachypodium* genes with high similarity to each of the *Arabidopsis* *EPFL1*, *EPFL4* and *EPFL6* genes and three with high similarity to *Arabidopsis* *EPFL2*. The multiple genes with high similarity to a single *Arabidopsis* gene are designated by a -1, -2 or -3 following the standard gene name. Subsequently, these genes were screened for their expression in different zones in *Brachypodium* and *BdEPFL1-1*, *BdEPFL1-2*, *BdEPFL2-1*, *BdEPFL2-2*, *BdEPFL4-1*, *BdEPFL6-1* and *BdEPFL6-2* were found to have strong expressions in leaf division zone reflecting a potential role in stomata development. Subsequently, inducible overexpression analysis showed an epidermal phenotype coupled with reduction in stomatal density for these *BdEPFLs* (*BdEPFL1-1*, *BdEPFL2-2*, *BdEPFL6-1* and *BdEPFL6-2*) in transgenic *Arabidopsis*. To find similar development stage-specific functions of EPFLs and *Arabidopsis* EPFs, I performed cross-species complementation analyses of these *BdEPFLs* in *Arabidopsis*. Expression of *BdEPFLs* in *Atepf1* and *Atepf2* *Arabidopsis* mutants under their respective *Arabidopsis* promoters revealed that *BdEPFL2-2* complements *Atepf1* with significant reduction of stomata clustering, whereas *BdEPFL1-1*, *BdEPFL6-1*, and *BdEPFL6-2* partially complemented both *Atepf1* and *Atepf2* by statistically significantly decreasing the stomatal clustering when these genes were expressed under the regulation of the *AtEPF1* promoter, and reducing the nonstomatal density under the *AtEPF2* promoter. These findings expand the identification of members of the EPF gene family that are active in the regulation of stomatal development, namely *EPF1*, *EPF2* and *EPF9/Stomagen* (Jangra *et al.*, 2021).

Previous findings from our lab also indicated that functional analyses of *AtEPF1/AtEPF2*-like genes in *Triticum aestivum* (wheat) (*TaEPF1*, *TaEPF2*) and

Brachypodium (*BdEPF2-1* and *BdEPF2-2*) show their crucial role in controlling early steps of stomatal initiation, and the establishment of stomatal cell files, rather than in differentiation or progression (Jangra *et al.*, 2021). Expression of several monocot grass EPF1/EPF2 homologs driven by the endogenous *AtEPF2* promoter (*AtEPF2pro::BdEPF2-1*, *AtEPF2pro::BdEPF2-2*, *AtEPF2pro::TaEPF1* and *AtEPF2pro::TaEPF2*) significantly rescued the epidermal phenotype of *epf2* in Arabidopsis, which is characterized by excessive entry divisions. However, these were not able to complement *epf1* in Arabidopsis. These findings suggest that these genes in wheat and Brachypodium function similarly to the Arabidopsis *EPF2* gene and have maintained a degree of conservation. *BdEPFL9* also regulates several stages of stomatal development and patterning in grasses. The functional similarity of *TaEPF1*, *TaEPF2* and *BdEPF2s* to *AtEPF2* highlights important aspects of monocot stomata development during guard mother cell formation by first asymmetric division, which could be similar to meristemoid formation in Arabidopsis where *EPF2* is specifically active in dicots. Monocots undergo two asymmetric divisions which lead to formation of a guard mother cell and subsidiary mother cell while Arabidopsis meristemoids undergo one asymmetric division to form meristemoid cells (Figure 2.3) (Hepworth *et al.*, 2018; Sena 2009; Stebbins and Jain, 1960).

Overexpression of *BdEPFL1-1* in Brachypodium expanded the identification of *BdEPFLs* in Brachypodium that affects stomata development. A significant decrease in stomatal density in both overexpression lines confirmed the inhibitory role of *BdEPFL1-1* in stomata development. Next, I performed stage-specific analysis of monocot stomata development in WT and *BdEPFL1-1* overexpression lines. The *OxBdEPFL1-1* line inhibited the establishment of subsidiary mother cells and guard mother cell fate in small daughter cells after asymmetric division. Additionally, *OxBdEPFL1-1* lines showed frequent arrested asymmetric division hinting towards a role in late stomata development in dicots. However, cross-species complementation shows that *BdEPFL1-1* resulted in a phenotype intermediate between those of the *Atepf1* and *Atepf2* mutants with partial reduction in stomatal clustering phenotype and nonstomatal density, therefore, pointing at potential specificity for monocot stomata development. However, specificity of these effects needs to be further explored since *BdEPFL1-1* was ectopically overexpressed which could lead to downstream effects that are not necessarily associated with its gene expression in its endogenous context. Surprisingly, sequence alignment data revealed that *BdEPFL1-1* shares 30% and 31.91% sequence identity with *AtEPF1* and *AtEPF2*, respectively (Figure 2.3 A-C). These relatively low similarity

percentages suggest that the observed intermediate phenotype may arise from functional similarities rather than high sequence conservation. In Arabidopsis, EPF peptides interact primarily with ERECTA family receptors which play crucial roles in stomatal patterning and spacing. On the other hand, monocots like Brachypodium and rice have a more limited number of known EPF receptors. The specific receptor interactions in monocots can also differ; for example, OsEPFL2 in rice has been implicated in regulating traits such as awn development rather than direct stomatal regulation (Xiong *et al.*, 2022). Moreover, recently Sakai *et al.*, (2021) showed that BdEPFL1, a putative ligand for BdERECTA, is more abundant in parenchyma tissue of shoot apex than in developing vascular bundle and implicated BdERECTA's pleiotropic role in vasculature anastomosis and vascular tissue organization. Consequently, ERECTA may utilize distinct molecular mechanisms for its functions in stomatal regulation and the elongation of above-ground plant organs (Kosentka *et al.*, 2019). This indicates that although the core function of stomatal regulation is preserved, the precise molecular components and their interactions have evolved uniquely in these plant lineages. Future structural and biochemical studies will be essential to understand these differences to investigate the regulation of important agronomic traits by these EPF secreted peptides.

Additionally, the phenotypic evaluation of the Brachypodium overexpression lines revealed distinct developmental abnormalities, including stunted growth, delayed flowering, and reduced seed fertility (Figure 2.11). In a recent report (not peer-reviewed) by Ferguson *et al.*, 2024, constitutive overexpression of SbEPF1 in sorghum (*Sorghum bicolor*) led to improved water use efficiency and reduced stomatal density, however, negative pleiotropic effects on reproductive development were also reported with impaired panicle and flower development. The impaired growth and reproductive traits observed in this study also confirm that the role of BdEPFL1-1 is not restricted to normal stomatal development but potentially affects broader physiological and developmental processes including grain yield and fertility further underscoring the importance of EPFLs in crop yield management.

3. To investigate the potential of Arabidopsis EPFL genes in drought tolerance.

3.1 Introduction

Multicellular organisms rely on communication between cells to regulate development and adapt to environmental changes across a variety of cell types. Because plant development is largely postembryonic and characterized by continuous organ formation, intercellular signaling is crucial throughout the life of the plant (Lee *et al.*, 2012). Small organic molecules and peptides serve as primary messengers in plant cells. Plasma membrane receptor-like kinases detect these signals and trigger the appropriate developmental responses. The ability of receptors to interact with multiple signals and the broad range of reactions a single signal can initiate underscores the sophisticated and flexible nature of plant developmental pathways (Kostenska *et al.*, 2019).

Arabidopsis development highlights the importance of intercellular signaling, with secreted peptides known as EPFs playing crucial roles in this signal transduction. These peptides are essential for regulating the development of stomata, inflorescences and tissue morphogenesis (Abrash *et al.*, 2011). As part of the larger class of cysteine-rich secreted peptides, EPF/EPFL are small proteins rich in cysteine. They interact with key receptors of stomata development, ERECTA family and TMM (Lee *et al.*, 2012)

The ERECTA-EPFL signaling module plays a critical role in orchestrating diverse developmental processes in Arabidopsis, including inflorescence architecture, pedicel length, and stomatal patterning. Very few functional studies have demonstrated the versatility of EPFL peptides in mediating physiological processes. For instance, *EPFL2* influences leaf margin morphogenesis by modulating auxin distribution (Tameshige *et al.*, 2016), while *EPFL2* and *EPFL9* coordinate ovule order and spacing (Kawamoto *et al.*, 2020). Moreover, Huang *et al.*, (2014) showed that *BnEPFL6* is required for filament elongation in *Brassica napus*. Importantly, Li *et al.* (2022) revealed that the perception of EPFL1, EPFL2, EPFL3, EPFL4, EPFL5 and EPFL6 by the ERF-SERK complex is crucial for proper integument development in Arabidopsis. Furthermore, EPFL1, EPFL2, EPFL3, EPFL4 and EPFL6 function redundantly to restrict shoot apical meristem size and promote leaf initiation, underscoring the multifaceted roles of these signaling peptides in plant development (Kosentka *et al.*, 2019). Furthermore, Mohamed *et al.*, (2023) showed that ABA can promote the expression of *EPFL1* and *EPFL2* and it can partially rescue the *epfl1* and *epfl2* stomata defects by downregulating the expression of MUTE and SPCH in Arabidopsis.

3.1.1 Drought stress

Drought is a major abiotic stress characterized by a combination of low soil moisture, low atmospheric humidity, and high ambient temperatures. Drought or water deficits can be long-lasting in regions where water is scarce and unpredictable in areas affected by varying weather patterns during the plant growth period. In the last four decades, the area of the earth impacted by drought has more than doubled, and drought have affected more people than any other natural hazard during this period (FAO 2017 [Weblink 1](#)). As climate change intensifies water scarcity, the impacts of drought are anticipated to become more severe. With rising water demands driven by growing populations, the urgency for sustainable water use is increasingly being emphasized (Hussain *et al.*, 2018). Consequently, it is essential to understand the effects of drought stress on plant growth and water utilization to support the development of sustainable agricultural practices.

Drought stress significantly impacts plant growth and development, against which plants have evolved sophisticated strategies that effectively mitigate these detrimental effects, allowing them to acclimate and adapt. These strategies can be classified as two major groups: (1) drought escape and (2) drought resistance (Levitt, 1980). In drought escape, plants begin to accelerate their growth and finish their life cycle prior to the onset of severe drought as soon as they notice a slight decrease in the soil water content. Common adaptations to this strategy include early flowering and the redistribution of photo-assimilates to seeds (Fang and Xiong 2015). In drought resistance, plants experience drought conditions throughout their life and develop strategies to minimize the damage. Drought resistance is further classified into drought avoidance and drought tolerance (Osmolovskaya *et al.*, 2018). Drought avoidance involves maintaining high tissue water potential despite soil water deficit. Plants employ mechanisms like improved water uptake under stress and enhanced ability of plant cells to retain water, thereby reducing water loss. Key phenotypic strategies for drought avoidance include improved root traits and a reduction in water loss through decreased epidermal conductance (lower stomatal density, smaller stomatal apertures), reduced light absorption, and smaller evaporative surface (e.g., smaller leaf area) (Fang and Xiong, 2015; Price *et al.*, 2002). These adaptations enhance water retention and minimize water loss, allowing the plants to maintain higher tissue water content, even in dry soil conditions. Drought tolerance, in contrast, involves both phenotypic and metabolic changes that help plants withstand severe drought conditions, where they are unable to maintain high tissue water content. This strategy primarily relies on the production of antioxidants and osmo-protectants, as well as alterations in phytohormone levels

e.g. abscisic acid (ABA) level. Phenotypic adaptations may involve delay in senescence (Shinozaki and Yamaguchi-Shinozaki 2007).

3.1.2 Abscisic acid and plant development

ABA is a plant hormone that plays a role in regulating various aspects of plant growth and development, particularly in response to stress conditions. In *Arabidopsis*, ABA plays a significant role in seed germination, seedling growth, stomatal closure, and the overall adaptation to abiotic stresses (Wu *et al.*, 2016; Finkelstein, 2013). Drought stress also triggers the accumulation of ABA and activates its downstream signaling pathway, which is essential for regulating various drought-responsive modifications by regulating stomatal closure and stress-responsive gene expression (Chen *et al.*, 2020; Cutler *et al.*, 2010). Though plant drought-stress response is also regulated by ABA-independent regulatory systems as well (Takahashi *et al.*, 2020). ABA-independent gene expression is primarily regulated through the dehydration-responsive element (DRE) and C-repeat (CRT) cis-acting elements, in combination with transcription factors like DREB (dehydration-responsive element-binding) and CBF (C-repeat-binding factor) (Sakuma *et al.*, 2006; Tran *et al.*, 2004; Shinozaki, 2000). Other transcription factors, such as MYB/MYC and WRKY, are also involved in the ABA-independent regulation of drought stress responses (Figure 3.1) (Abe *et al.*, 1997).

The central components of ABA signaling are the ABA receptors PYR (pyrabactin resistance)/ PYL (PYR1-like)/ RCAR (regulatory component of ABA receptor), and the downstream signal transducing proteins PP2Cs (protein phosphatase 2Cs) and SnRK2s (sucrose non-fermenting-1-related protein kinase 2s), which together regulate the plant's response to drought stress. The PP2C phosphatases act as inhibitors in the ABA signaling pathway by deactivating SnRK2 kinases through dephosphorylation. When ABA binds to its receptor complex, it deactivates PP2Cs, leading to the activation of SnRK2s. These activated SnRK2s, in turn, activate transcription factors like abscisic acid insensitive (ABI) 4, ABI5, and ABA-responsive element (ABRE)-binding factors (ABFs), which help regulate ABA-responsive genes (Mukherjee *et al.*, 2023; Chen *et al.*, 2020).

A recent study showed that ABA regulates SPCH through SnRK2 kinases. Elevated ABA levels activate SnRKs (SnRK2.2/2.3/2.6), which directly phosphorylate SPCH at serine residues S240 and S271, leading to its degradation and the suppression of stomatal development. This reduces the number of stomata present per unit area of a leaf, indicating that drought conditions can alter guard cell development by triggering the ABA signaling pathway (Yang *et al.* 2022; Tanaka *et al.* 2013).

Drought-induced ABA production can also affect stomatal opening by influencing the ion channels that regulate the osmotic pressure within guard cells, by modulating the genes that control the opening and closing of stomata or both. Light promotes stomatal opening by activating transporters that facilitate K^+ uptake by guard cells, with H^+ -ATPase AHA2 playing a key role in this process by allowing both K^+ and water uptake (Inoue and Kinoshita, 2017). On the other hand, ABA inhibits this light-driven activation of H^+ -ATPase by dephosphorylating the C-terminal threonine residue and engaging secondary messengers like H_2O_2 , phosphatidic acid, NO, H_2S , and Ca^{2+} . A recent study indicates that ABA not only inhibits H^+ -ATPase but also activates it through a different mechanism. ABA induces BAK1 (BR11-associated receptor kinase 1) to phosphorylate and hyperactivate H^+ -ATPase AHA2. This activation results in an accelerated efflux of H^+ , leading to cytoplasmic alkalization, generation of reactive oxygen species (ROS), and ultimately the closure of stomata (Pei *et al.*, 2022).

3.1.3 Root development

The root system of a plant plays a crucial role in its survival by anchoring it to the ground and enabling the absorption of essential minerals and moisture necessary for growth and development. To optimize water uptake, plants can adapt their root architecture by modulating primary, lateral, and adventitious root growth, as well as root hair length and distribution. Under drought stress, plants often prioritize primary root elongation to access deeper water sources while reducing lateral root development. This strategic adaptation ensures the plant's survival and resilience in challenging environmental conditions (Freschet *et al.*, 2021).

ABA plays a significant role in developmental regulation of roots. Leung *et al.*, 1997 showed that root growth of WT Arabidopsis seedlings is reduced to 20% when roots are placed in 10 μ M ABA for 4 days. ABA signaling mutants *aba insensitive 1-1 (abi1-1)* and *abi2-1* showed reduced ABA sensitivity for primary root growth (Rodriguez *et al.*, 1998; Leung *et al.*, 1997). Similarly, ABA signaling-deficient triple mutants *highly aba-induced 1/2/3 (hai1hai2hai3)* are very sensitive to ABA effects with enhanced inhibition of root elongation (Bhaskara *et al.*, 2012). ABA is also involved in modulating the formation of lateral roots. Genetic studies on ABA-deficient mutants, such as *aba2-1* and *aba3-1*, demonstrate a greater frequency of lateral root emergence compared to the WT under control and stress conditions (Deak and Malamy, 2005). Under drought stress, ABA levels rise rapidly in roots modulating the distribution of auxin to control root system architecture (Xu *et al.*, 2013). Antagonistic action of exogenous ABA on auxin concentrations in the root tip has been reported previously

where ABA promotes the expression of *ABI4* encoding an AP2/ERF domain-containing transcription factor inhibiting PIN1 transporter, resulting in reduced polar auxin transport (Rowe *et al.*, 2016).

3.1.4 Seed germination

Seed germination is a critical process in the life of plant and begins with seeds absorbing water and concludes when the radicle emerges by breaking the seed's protective coat. It is influenced by environmental and developmental cues that involve ABA degradation upon imbibition which precedes the activation of germination by gibberellin, another hormone (Carrera-Castano *et al.*, 2020).

During seed maturation, ABA induces primary dormancy by repressing germination through the regulation of key genes such as *ABI3*, ensuring seeds remain dormant until conditions are favorable (Liu *et al.*, 2013). This process prevents vivipary and allows seeds to synchronize germination with optimal environmental cues (Rodríguez-Gacio *et al.*, 2009). In vegetative tissues, ABA mediates drought resistance by triggering stomatal closure to minimize water loss and activating stress-responsive genes that enhance drought tolerance (Wang *et al.*, 2024). Both processes rely on ABA biosynthesis, degradation, and signaling pathways, highlighting their dual role in developmental regulation and environmental stress adaptation. ABA catabolism is a crucial step to initiate seed germination. Its degradation occurs through sequential hydroxylation and conjugation steps. First, ABA is converted to phaseic acid (PA) then dihydrophaseic acid (DPA) and DPA-4-O-β-D-glucoside (DPAG), eventually resulting in the ABA degradation. Studies have reported decreased levels of ABA and higher levels of PA and DPA during imbibition of Arabidopsis and barley seeds emphasizing the inhibitory role of ABA in germination (Millar *et al.*, 2006; Jacobson *et al.*, 2002). Moreover, many studies demonstrated that ABA signaling through the ABI3,4,5-mediated cascades is a key factor in ABA-mediated regulation of seed dormancy and development (Barros-Galvão *et al.*, 2020; Dekkers *et al.*, 2016; Lee *et al.*, 2015; Carles *et al.*, 2002).

Thus, understanding the role of specific genes involved in drought stress tolerance can help in developing and breeding more tolerant crops better suited for dry regions across the globe. Therefore, in this thesis work, I attempted to understand the novel role of the *EPFL1*, *EPFL2* and *EPFL3* subfamily in drought stress response.

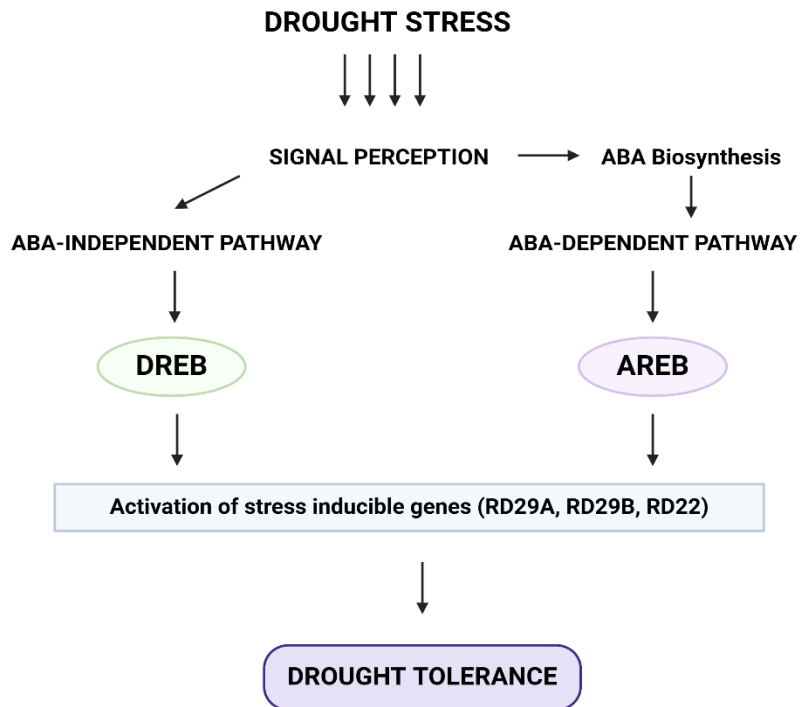


Figure 3.1: An illustration showing ABA-dependent and ABA-independent drought signaling pathway. Inspired by Anami *et al.*, 2009.

3.2 Materials and Methods

3.2.1 Plant material and growth conditions

For all assays, the *Arabidopsis* Col accession was used as the WT. Seeds were sown on MS medium and stratified at 4°C for 3 days, and then transferred to a growth chamber and grown under a long or short-day cycle, as required, with a light intensity of 100 $\mu\text{mol m}^{-2} \text{s}^{-1}$ at 22°C. For the root-inhibition assays, 3-day-old seedlings were transferred to MS medium containing ABA (95% ethanol was used as solvent, stock concentration 100mM) and grown for an additional 7 days. For the germination assays, 30 seeds were plated on MS medium with different ABA concentrations at 4°C. The plates were shifted to illumination under white light at 100 $\mu\text{mol m}^{-2} \text{s}^{-1}$ and 22°C for 8 days to assess germination rates after 72 hours. For physiological experiments, seedlings were transplanted at 7-8 dpg in pots containing a 1:1 mixture of black earth and vermiculite under a 12-hour light/12-hour dark cycle in a growth chamber for 3-4 weeks.

The *epfl1-1* (CS104435) transposon insertion mutant in the Columbia background was acquired from the *Arabidopsis* Biological Resource Center. The *epfl2-1* transposon-insertion mutant, designated as CSHL ET5721, was obtained from Cold Spring Harbor Laboratory. The *epfl3-2* was obtained from the Elena Spark group. Furthermore, previous lab members had crossed the mutants to generate high order mutants *epfl-1 epfl2-1* and *epfl-1 epfl2-1 epfl3-2* in the Columbia genetic background. Homozygous plants were identified using PCR and used for analysis. The other mutants used in this study included *pp2ca1* (SALK0128132) and pentamutant line *pyr/pyl12458*. The primers used to examine these mutants are listed in Table 3.1.

The transgenic lines which overexpress the EPF genes used in the study included *35S::EPFL1*, *35S::EPFL2*, *35S::EPFL3* in vector pGWB2, and promoter::*GUS* reporter lines used in the study include *pEPFL1::GUS*, *pEPFL2::GUS* and *pEPFL3::GUS* in vector pGWB3. Transgenes were introduced to Col using *Agrobacterium*-mediated transformation except for *pEPFL2::GUS* which was obtained from collaborators. Table 3.2 describes the plasmid constructs used in this study.

Table 3.1: Primers used in the study

Gene name	Primer name	Primer Sequence (5' to 3')
<i>epfl1-1</i>	EPFL1 74 f Spm3_v2 (SM line)	ATCCTTTCTTCAACCTATCCAACCTCCT TACGAATAAGAGCGTCCATTTTAGAGTGA
<i>epfl2-1</i>	EPFL2 1f GUS 43 rc	ATGGTGTGGAGCAGCAACATGTCAAGC GTTTTTTGATTTACGGG
<i>epfl3-2</i>	epfl3-2 1f LB GABI	ATGGAATACATGTTCTTATTAATGT TAATAACGCTGCGGACATCTACATT
<i>EPFL1-1</i>	EPFL1 74 f EPFL1 436 rc	ATCCTTTCTTCAACCTATCCAACCTCCT TTAAGGATTATAAAAAGTGGCCATTGCA
<i>EPFL2-1</i>	EPFL2 1f EPFL2 540rc	ATGGTGTGGAGCAGCAACATGTCAAGC TCAAGGGTTGTAGATAGAGTTACCA
<i>EPFL3-2</i>	epfl3-2 1f epfl3-2 300 rc	ATGGAATACATGTTCTTATTAATGT TTAAGGAGGAGGACAATGGCATCT
<i>pyr1-1</i>	pyr1-1 R LBa1	TTATTCATCATCATGCATAGGTG TGGTTCACGTAGTGGGCCATCG
<i>pyl1-1</i>	pyl1-1 RP LBa1	AACCATGCCTTCCGATTTAAC TGGTTCACGTAGTGGGCCATCG
<i>pyl2-1</i>	pyl2-1 F LBa1	ACCATGGGCTCATCCCCGGCCGTGA TGGTTCACGTAGTGGGCCATCG
<i>pyl4-1</i>	pyl4-1 RP LBa1	TAAGACTCGACAACGACGGTC TGGTTCACGTAGTGGGCCATCG
<i>pyl5</i>	pyl5 R Spm3 (SM line)	TTATTGCCGTTGGTACTTCGA ACCGTCGACTACCTTTTTTCTTGTAGTG
<i>pyl8</i>	pyl8 RP Sail_Lba1	TTCTTCTTCTTCCTTCATGCG GCCTTTTCAGAAATGGATAAATAGCCTTGCTTCC
<i>pp2ca</i>	pp2ca1 RP LBa1	TTTGGTTGATTTTAGGTTGCG TGGTTCACGTAGTGGGCCATCG
<i>EIF4A</i>	EIF4Af_qPCR EIF4Arc_qPCR	GGCAGTCTCTTCGTGCTGAC TCATAGATCTGGTCCTTGA AACC
<i>RD29A</i>	RD29a-RS RD29a-RA	ATCAA ACTCAAGTGGCGGGA TATCTTCCCCTCGTTGCTCC

DREB	DREB-RS	AGAGAAACAGAAGGAGCAAGGGAT
	DREB-RA	GTCGCCATTTAGGTCACGTAGAAG

Table 3.2: Plasmids used in the study

Plasmid Description	Insert	Vector	Bac ^R	Plant ^R
<i>35S::EPFL1</i>	EPFL1 (pRJ29)	pGWB2	Kan/Hyg	Kan/Hyg
<i>35S::EPFL2</i>	EPFL2 (pJSL307)	pGWB2	Kan/Hyg	Kan/Hyg
<i>35S::EPFL3</i>	EPFL3 (pRJ31)	pGWB2	Kan/Hyg	Kan/Hyg
<i>pEPFL1::GUS</i>	EPFL1 promoter (pJSL134)	pGWB3	Kan/Hyg	Kan/Hyg
<i>pEPFL2::GUS</i>	EPFL1 promoter (pJSL134)	pGWB3	Kan/Hyg	Kan/Hyg
<i>pEPFL3::GUS</i>	EPFL3 promoter (pJSL135)	pGWB3	Kan/Hyg	Kan/Hyg

3.2.2 *In-silico* expression analysis of the *EPFL1*, *EPFL2* and *EPFL3* subfamily

The public depository of Arabidopsis gene expression based on data from RNA-seq libraries (<https://plantradb.com/athrdb/>) was used to retrieve data for tissue-specific expression and expression during drought and ABA treatment of *EPFL1* (AT5G10310), *EPFL2* (AT4G37810) and *EPFL3* (AT3G13898) genes. To ensure proper interpretation, gene/sequence lengths and library size were normalized to FPKM (Fragments Per Kilobase Per Million).

3.2.3 Genomic DNA preparation and PCR

To validate the transgene insertion and background, DNA was collected for individual/master genotyping of transgenic lines. To extract DNA, 500mg of Arabidopsis leaves were ground and placed in 1.5 mL microcentrifuge tubes containing 200 microliters of DNA extraction buffer (200 mM Tris-HCl, (pH 7.5), 250 mM NaCl, 25 mM EDTA, 0.5% 20% SDS in autoclaved ddH₂O water). The samples were then vortexed at 6000Xg for 5 minutes. Aliquots of 150 µL of supernatant were collected in a new MCT, mixed with 150 µL of isopropanol (1:1v/v), and incubated at room temperature for 2 minutes. Samples were centrifuged for 5 minutes at 6000Xg, the supernatant was removed and mixed with 500 µL of ethanol. Samples were centrifuged, the supernatant was removed, and the tubes were dried with a speed vacuum for 15-20 minutes or air dried overnight. The isolated DNA was resuspended in 50 µL of ddH₂O and stored at 4°C for future use. Genotyping was done as described in Chapter 1. Table 2 shows the primers used to determine background and gene specificity.

3.2.4 Phenotypic characterization

For germination assay, 30 sterilized seeds from each genotype were sown on MS plates using different concentrations of ABA including mock, 0.5 μM , 0.8 μM , and 1 μM . After stratification in the dark at 4°C for three days, plates were moved to a growth chamber at 22°C with a 16-h/8-h photoperiod. At 3 dpg, radicle emergence was counted for each genotype at all concentrations. After 8 days, representative images of the plates were captured.

For root growth assays, seedlings were grown vertically on 1/2 MS medium. Five seedlings of each genotype, subsequently were transferred to MS plates at 3 dpg on ABA plates (mock and 20 μM). Photographs were taken, and primary root length was measured at 10 dpg and used for statistical analysis.

To measure water loss, the entire rosette of plants of similar size and developmental stage from 4-week-old plants growing under 12-hour light/12-hour dark cycle were excised from their roots, placed in open dishes, and kept on the lab bench for the indicated time, fresh weight was measured initially and every 10 mins weight loss is recorded. Water loss was measured as a percentage of weight loss compared to the initial fresh weight.

For the drought treatment experiment, 7-day-old plants were transplanted from MS medium to water-saturated soil and grown under 12-hour light/12-hour dark cycle until they were 3 weeks old. Subsequently, watering was stopped until substantial damage was seen in WT plants. The survival rate was measured 3 days following rehydration.

3.2.5 Synthesis of cDNA and qPCR analysis

To analyze ABA-responsive genes using RT-qPCR, seedlings grown under long-day conditions were transferred to liquid MS medium with or without 50 μM ABA for 3 hours. Total RNA extraction, cDNA synthesis, and RT-qPCR were performed. SYBR Green PCR Master Mix was used for PCR analysis in the CFX96 Optical Reaction Module, which was converted from a C1000 Touch Thermal Cycler. Three experiments were conducted independently, each with three technical replicates and eIF4A was used as an internal control to normalize transcript levels. Analysis by qPCR was performed using the $\Delta\Delta\text{Ct}$ method (Wu et. Al. 2016).

3.2.6 β -glucuronidase (GUS) reporter assay

Arabidopsis transgenic plants expressing EPFLpro::GUS were grown on 1/2 MS medium under 16 hour/8 hour light/dark conditions at ~22°C. X-Gluc (1 mg/mL) solutions were prepared with X-Gluc stock (10 mg/mL) , 0.5 M sodium phosphate buffer (pH 7.0), 10% Triton, 100 mM

potassium ferricyanide, 100 mM potassium ferrocyanide, and ddH₂O. Collected tissue was stored in 90% cold acetone. The volume was adjusted depending on the seedling's developmental stage: 1 mL for 3 dpv and 2 mL for more than 10 dpv. All seedlings were covered with ice and incubated for 20 minutes (3 dpv) or 30 minutes (10 dpv). The acetone was then replaced with cool ddH₂O for at least 5 minutes. Following that, the cold ddH₂O was replaced with staining solution, dividing it evenly across three wells using 2 mL buffer in each and incubated for 10-20 mins. The staining buffer was replaced with staining buffer containing X-gluc, which was left to incubate at 37°C overnight before gene expression was evaluated the next morning. Chlorophyll was removed through a series of incubations in ethanol from 20% to 90% ethanol. Final storage at 4 degrees was done in 95% ethanol.

3.2.7 Stomata Regulation Assay

To perform the stomatal regulation assay, similar sized rosette leaves were excised from 4-week-old plants. To examine ABA-mediated stomatal closure, leaves were incubated in MES buffer (10 mM MES-KOH, (pH 6.15), 10 mM KCl, and 50 mM CaCl₂) in the light for 2 hours at 22°C to open the stoma. Images were taken using a Nikon-Ti microscope after adding 20 mM ABA to the buffer and incubating the leaves for an additional 2 hours in light at 22°C. To study ABA-mediated inhibition of stomatal opening in the light, four-week-old plants were incubated in a dark chamber for 24 hours to close the stomata. Leaves from the plants were then incubated in MES buffer with or without 20 μM ABA in the light at 22°C for 2 h, after which the samples were imaged under the microscope (Nikon Ti). The stomatal aperture were measured using at 20X magnification ImageJ software.

3.2.8 Quantitative analysis of stomatal phenotype

Stomatal phenotypes were analyzed quantitatively using Toluidine Blue O (TBO)-stained epidermal samples. The abaxial side of cotyledons of 10-day-old Arabidopsis seedlings were fixed in 1 mL of a 9:1 ethanol: acetic acid solution for imaging. Fixed samples were treated twice with 70%, 50%, and 20% ethanol for 20 minutes each the day before imaging, then kept in 1mL ddH₂O solution. The next day, samples were stained with 1 mL of filtered 0.5% (w/v) TBO stain in 1.5 mL tubes, followed by 3-4 minutes of incubation at room temperature. Further analysis was done as described in Chapter 1.

3.3 Results

3.3.1 RNA-sequencing data analysis

To investigate the potential role of *EPFL1*, *EPFL2*, and *EPFL3* in drought stress regulation, publicly available RNA-sequencing data were accessed from the public Arabidopsis RNA-seq library (<https://plantnadb.com/athrdb/>). For this analysis, only WT sample data were used, with no inclusion of mutant or transgenic lines unless otherwise stated. The data presented in Figure 3.2A show expression of *EPFL1*, *EPFL2*, and *EPFL3* in different organs of Arabidopsis. All three *EPFL* genes exhibited maximal expression in the seed coat, suggesting their role in seed development. Among the three *EPFLs*, *EPFL1* shows the highest expression in the seed coat further implying its role in early plant development. In comparison, the expression of these *EPFLs* was negligible in embryo and moderate in seedlings evidencing their important role in specific tissue and stage of early stages of plant development, being more pronounced in seed coat. Additionally, *EPFL1* and *EPFL2* were moderately expressed in meristem, shoot, leaf and root with *EPFL2* expression being elevated sharply in roots. Expression of *EPFL3* was low or undetected in different tissues of Arabidopsis that were included in the study.

In the next step of investigating the potential novel roles of these EPFLs in drought stress, retrieved RNA-seq data were analyzed to assess their expression under drought and ABA treatments.

To understand the difference in expression levels of EPFLs in drought with respect to mock conditions, RNA-seq data for *EPFL1*, *EPFL2* and *EPFL3* were compiled. The expression of *EPFL2* was upregulated in drought conditions whereas expression for both the *EPFL1* and *EPFL3* genes was reduced in drought conditions in comparison with mock conditions. *EPFL3* expression was significantly lower than *EPFL1* (Figure 3.2 B-D).

One of the objectives of the RNA-seq data analysis was to determine if ABA can influence the expression of *EPFLs*. As shown in Figure 3.2 E and F, the expression of both *EPFL2* and *EPFL3* is increased significantly under ABA treatment when compared to mock, indicating ABA's role in influencing the expression levels of *EPFLs* positively and leading us to hypothesize that these *EPFLs* might exert their effects via an ABA dependent pathway. Different drought related assays were performed to confirm the preliminary findings of RNA-seq data.

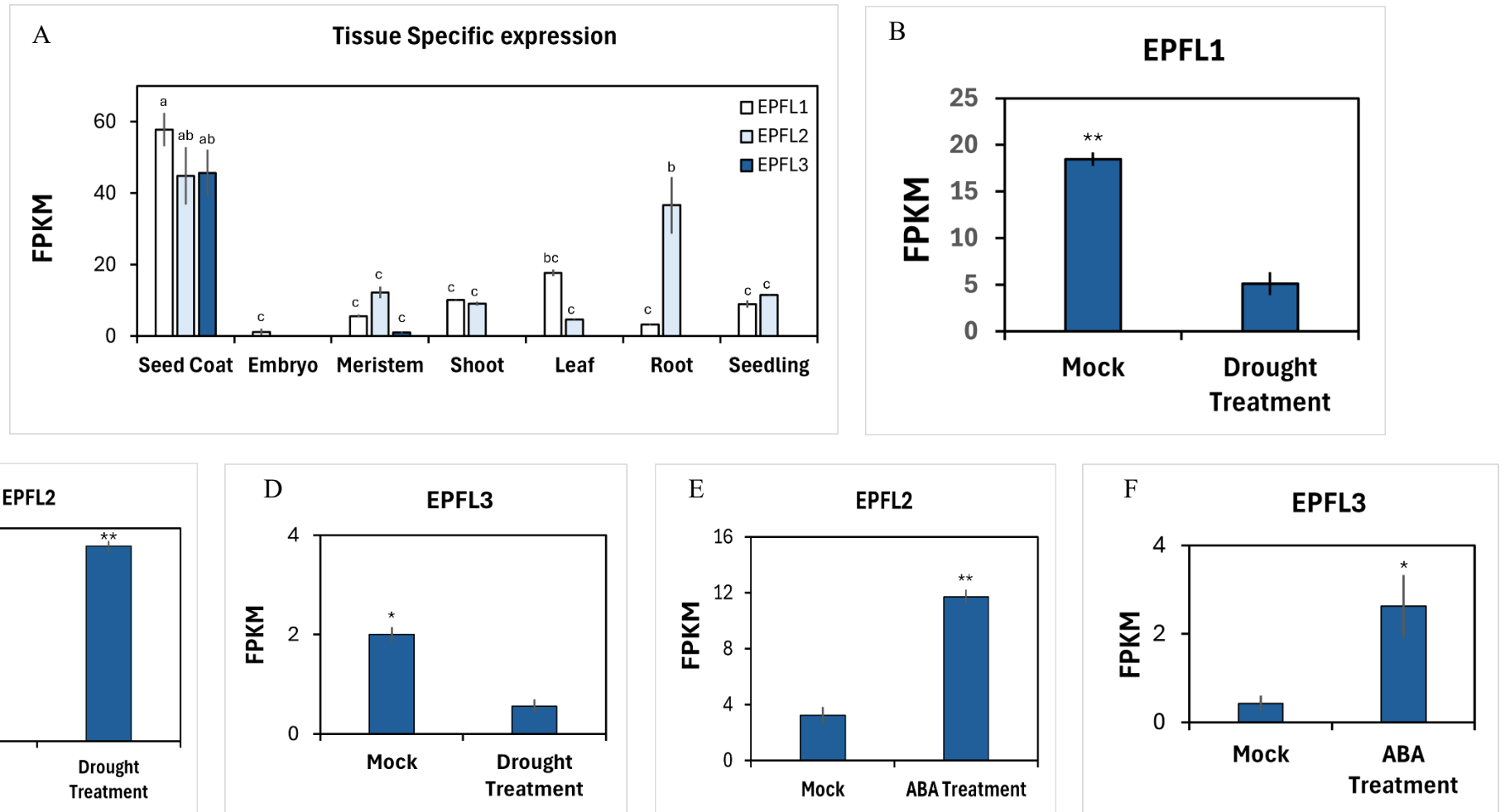


Figure 3.2: RNA-seq analysis of *EPFL1*, *EPFL2* and *EPFL3* during following stages: A. Tissue-specific expression, B-D. Expression of *EPFL1*, *EPFL2* and *EPFL3* comparing mock and drought-treated seedling, E-F. Expression of *EPFL2* and *EPFL3* comparing mock to ABA treatment. FPKM: Fragment per KB per Million. Source: Public RNA-seq Library (<https://plantnadb.com/athrdb/>). The data are the means \pm SE. Data in graph A was analyzed by one-way ANOVA, followed by Tukey's Multiple Comparison test. Significant differences between data are shown by different letters, $p < 0.05$. For graphs B, C, D, E and F Student's t-test was performed: * $p < 0.05$; ** $p < 0.001$).

3.3.2 Effects of Drought Stress on EPFL1/2/3 mutants

To understand the role of *EPFL1*, *EPFL2* and *EPFL3* in drought stress tolerance, mutants as well as overexpression lines were developed. In the ABA signaling pathway, ABA binds to PYR/PYL/RCAR receptors, forming a complex that inhibits PP2C activity. This inhibition releases SnRK2s from repression, allowing their activation via phosphorylation. Therefore, for positive and negative controls, *pp2ca* and *pyr/pyl12458* were used, the former being ABA-hypersensitive and the *pyr/pyl* quintuple mutant being ABA-insensitive. (Brandt *et al.*, 2015; Lee *et al.*, 2009)

Figure 3.3 shows that the *pyr/pyl12458* plants were severely stressed by the drought treatment as indicated by having dried leaves and reduced leaf blade area, and *pp2ca* appeared turgid with expanded leaves. In contrast and compared to both the positive and negative controls, WT plants showed moderately reduced leaf area. For *EPFL1*, the mutant *epfl1* showed a stressed phenotype, in contrast, overexpression lines of *EPFL1* behaved like positive control *pp2ca* where leaves maintain turgor with no sign of dryness indicating a positive role of *EPFL1* in enhancing drought stress response. Similarly, the physiological response of *EPFL2* to drought stress was like that of *epfl1* with *epfl2* showing signs of desiccation and overexpression lines showing no sign of desiccation when subjected to drought stress. The *EPFL3* response to drought stress was different than the *EPFL1* and *EPFL2* response. Both mutant and overexpression lines of *EPFL3* showed signs of moderate desiccation, like *WT*.

Interestingly, transgenic plants carrying double mutant *epfl1/2* and triple mutant *epfl1/2/3* showed signs of moderate desiccation like *WT*. Thus, even double and triple mutations do not have a lethal phenotype. This suggests that other EPFL peptides or unrelated signaling pathways possibly compensate for the loss of *EPFL1* and *EPFL2*.

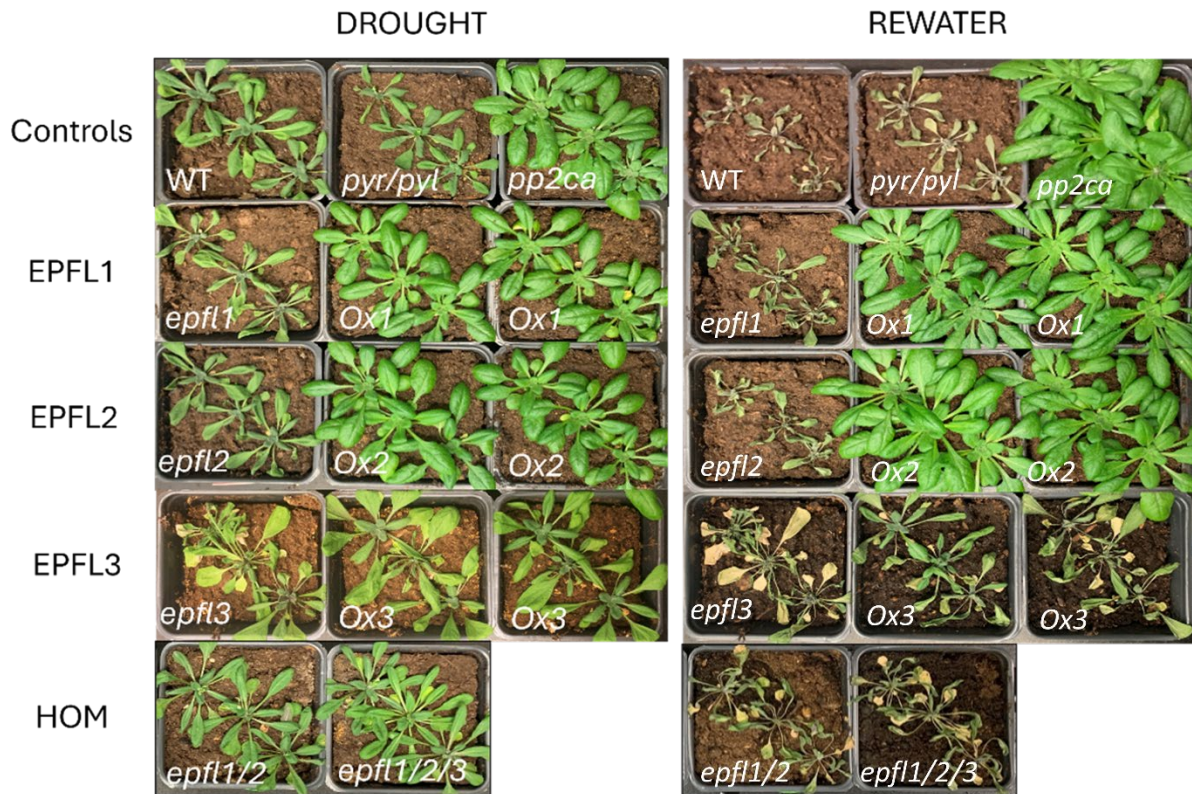


Figure 3.3: Drought phenotypes of WT, mutants, overexpression, and high order mutants (HOMs) in a drought and rewatered panel. The *pyr/pyl* line is *pyr/pyl12458*. Drought stress was administered to 21-day-old seedlings by withholding water for 14 days. The plant images for drought were captured after 10-11 days of withholding watering and revival images were taken after 3 days of rewatering.

3.3.3 Relative water loss assay

To further quantify the loss of water from leaves during drought stress water loss assay was performed using entire rosettes from 4-week-old plants. The data from that relative water loss assay mostly corroborated the phenotypic data described above (Figure 3.3). There was a clear distinction in water loss capacity between mutant lines and OX lines of *EPFL1* and *EPFL2*. Water loss analysis in rosette of *pyr/pyl12458* showed most water loss (45.54 %) with *pp2ca* showing least (20.39 %) within one hour, followed by *epfl2* (40.23 %), *epfl1/2* (36.17 %), *epfl1/2/3* (34.14 %), *epfl3* (33.64 %), *epfl1* (33.36 %) and WT (31.76 %). *OxEPFL1* and *OxEPFL2* lines had a relatively smaller water loss rate (23-26 %) as compared with *OxEPFL3* (~32.68 %). The water loss rates for *epfl3* and *OxEPFL3* were similar ~33% (Figure 3.4 A-D).

	Water loss with respect to WT	10 min	20 min	30 min	40 min	50 min	60 min
<i>pyr/pyl12458</i>	more	**	**	**	**	**	**
<i>pp2ca</i>	less	**	**	**	**	**	**
<i>epfl1-1</i>	more	ns	ns	ns	*	ns	ns
<i>epfl2-1</i>	more	**	*	**	**	**	**
<i>epfl3-2</i>	equal	ns	ns	ns	ns	ns	ns
<i>epfl1/2</i>	more	*	ns	*	**	**	*
<i>epfl1/2/3</i>	more	ns	ns	ns	*	ns	ns
<i>EPFL1 Ox1</i>	less	**	**	**	**	**	**
<i>EPFL1 Ox2</i>	less	**	**	**	**	**	**
<i>EPFL2 Ox1</i>	less	**	**	**	**	**	**
<i>EPFL2 Ox2</i>	less	**	**	**	**	**	**
<i>EPFL3 Ox1</i>	equal	ns	ns	ns	ns	ns	ns
<i>EPFL3 Ox2</i>	equal	ns	ns	ns	ns	ns	ns

Table 3.3: Table showing statistical analysis for relative water-loss assay. The *pyr* line is *pyr/pyl12458*. The data compared the means of five replicates to those of the wild type. Following one-way ANOVA, Dunnett's Multiple Comparison test was performed comparing means of relative water loss against WT (*p < 0.05, **p < 0.001 versus WT).

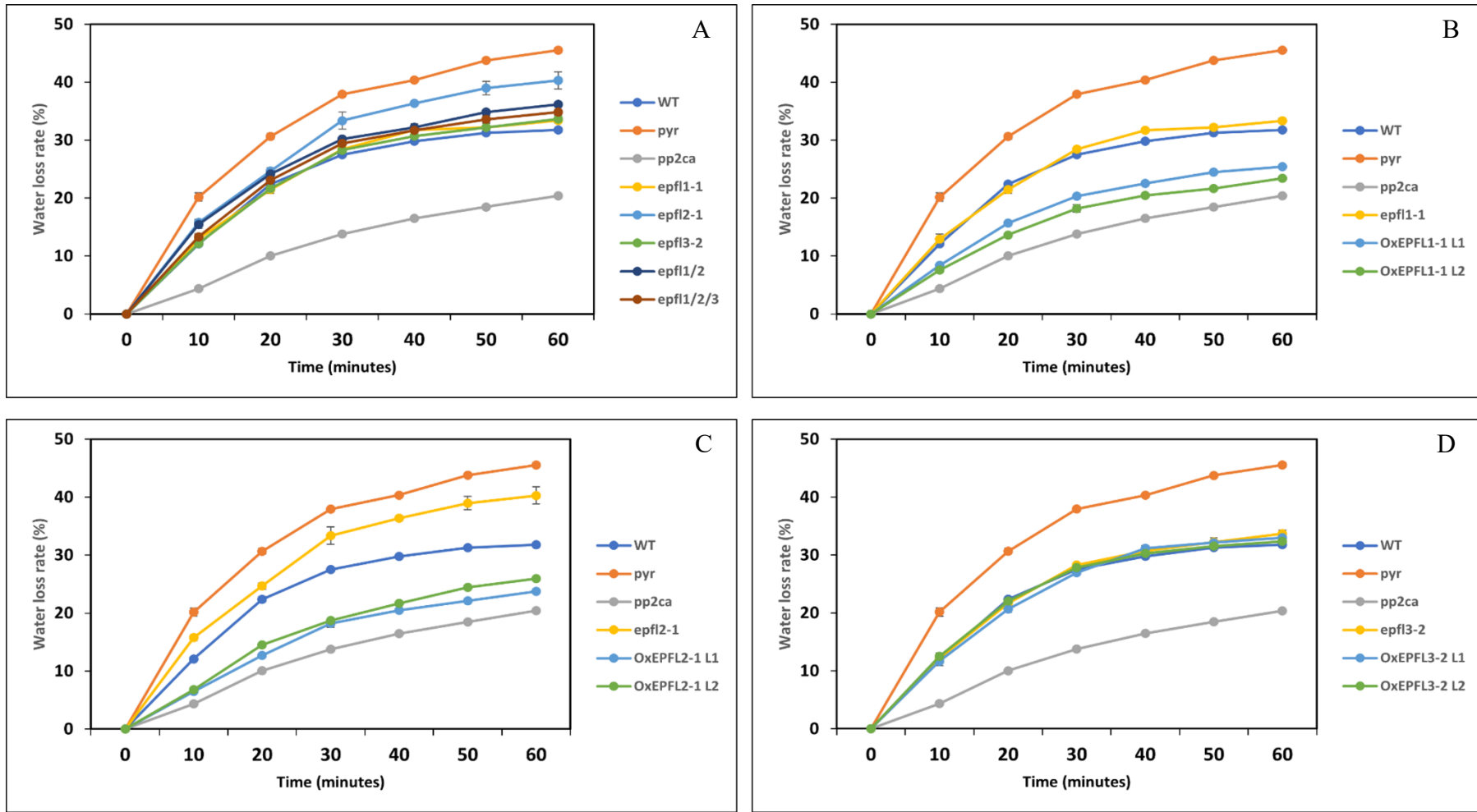


Figure 3.4: Relative water loss in: A. WT, *pyr*, *pp2ca*, *epfl1-1*, *epfl2-1*, *epfl3-2*, *epfl1/2* and *epfl1/2/3*. B. WT, *pyr*, *pp2ca*, *epfl1-1*, *OxEPFL1-1* #1 and *OxEPFL1-1* #2. C. WT, *pyr*, *pp2ca*, *epfl2-1*, *OxEPFL2-1* #1 and *OxEPFL2-1* #2. D. WT, *pyr*, *pp2ca*, *epfl3-2*, *OxEPFL3-2* #1 and *OxEPFL3-2* #2. Four-week-old plants were used to quantify water loss in detached rosettes. The *pyr* line is *pyr/pyl12458*. The data are the means \pm SE of measurement on five biological replicates.

3.3.4 qPCR analysis of drought stress inducible genes

The initial findings from the drought and water loss assay confirmed the role of *EPFL1* and *EPFL2* trending to confer drought resistance in Arabidopsis. Next, I aimed to identify whether these *EPFLs* affect the expression of drought responsive genes. For this, qRT-PCR analysis of drought stress marker genes *viz.* *RD29A* (*Response to Desiccation 29A*) and *DREB* (*Dehydration Responsive Element Binding*) was done for all the mutants and overexpression lines using 7 dpg seedlings in the presence and absence of ABA in accordance with Wu *et. al.*, (2016) (Figure 3.5). It is important to note that the regulation of *RD29A* as well as *DREB* expression includes both ABA-dependent and ABA-independent pathways. In presence of externally supplied ABA (50 μ M) the expression of both genes was more strongly upregulated in *OxEPFL1* and *OxEPFL2* than in WT. Interestingly, the expression of *RD29A* and *DREB* was reported to be higher in *OxEPFL2* lines than *OxEPFL1*. Both *EPFL1* and *EPFL2* appear to have a role in mediating ABA signal transduction.

For *EPFL3*, both mutant and Ox lines failed to show a response to the exogenously supplied ABA for the expression of *RD20* and *DREB* that differed from that of WT, which agrees with the drought and water loss data which failed to show any resistance or sensitivity to drought stress further highlighting a lack of involvement in drought tolerance and ABA mediated signal transduction. Furthermore, *epfl1*, *epfl2*, *epfl1/2* and *epfl1/2/3* mutants did not show any downregulation in *RD29A* and *DREB* expression as compared to WT, which appears to contradict the fact that overexpression of *EPFL1* and *EPFL2* results in upregulation of these genes. This shows a more complicated link between *EPFL1*, *EPFL2* and abiotic stress response genes, which might involve redundancy or compensating mechanisms in the mutants. In summary, overexpression of *EPFL1* and *EPFL2* might play a role in the activation of ABA dependent stress signaling pathways.

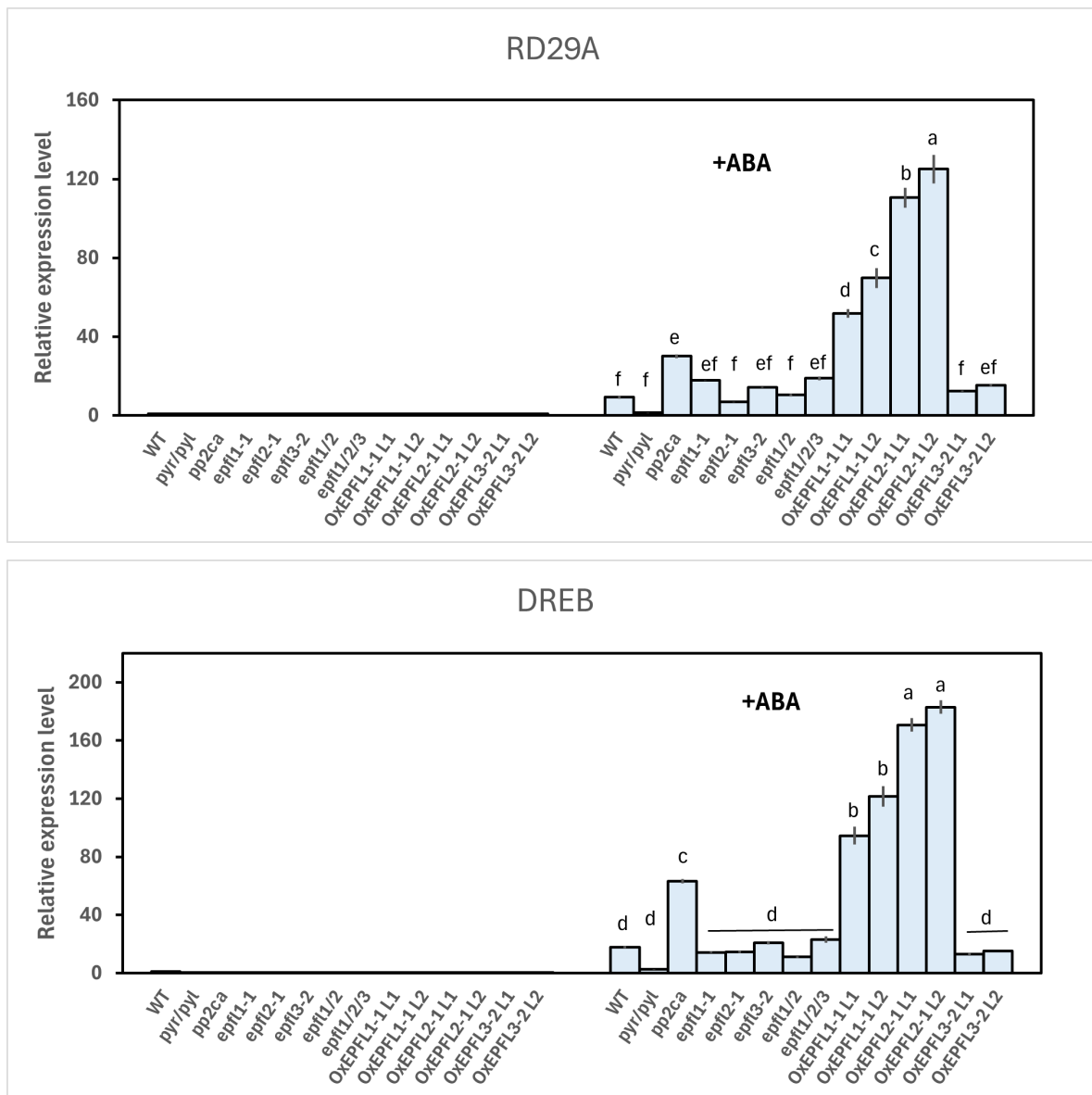


Figure 3.5: Expression profiles of ABA-responsive genes in WT, *pyr/pyl12458*, *pp2ca*, *epfl1-1*, *epfl2-1*, *epfl3-2*, *epfl1/2*, *epfl1/2/3*, *OxEPFL1-1#1*, *OxEPFL1-1#2*, *OxEPFL2-1#1*, *OxEPFL2-1#2*, *OxEPFL3-2#1* or *OxEPFL3-2#2*. Seven-day-old Arabidopsis seedlings were moved to liquid MS medium with 50 μ M ABA and sampled at 3 hours. Quantitative real-time PCR was used to evaluate gene expression. The internal control was *eIFA4*, and expression levels were normalized to those observed at time zero. Data represent the mean \pm SE of three biological replicates. Following one-way ANOVA, Tukey's Multiple Comparison test was performed. Significant differences between data are shown by different letters, $p < 0.05$.

3.3.5 GUS assay showing EPFL expression in response to ABA and drought

After expression analysis of drought stress marker genes in the presence of ABA, next I aimed to localize the expression of *EPFL1*, *EPFL2*, and *EPFL3* by GUS histochemical staining of transgenic seedlings carrying transgene GUS under the control of the *EPFL1*, *EPFL2* and *EPFL3* promoter in the presence of ABA (0.5 μ M ABA) as well as osmotic stress (5% PEG). As shown in Figure 3.6, 3 dpg seedlings show a strong uniform signal for *EPFL1* expression in the entire seedling shoot regardless of type of treatment. However, it is important to note that the intensity of histochemical stain is increased in both treatments for *EPFL1* with pronounced staining in cotyledonary leaves; possibly altering the epidermal phenotype of leaves including stomata. Surprisingly, *EPFL3* did not show any traces of expression at 3 dpg even in the presence of ABA as well as drought stress (Figure 3.6 A).

Seedlings were further analyzed for expression patterns at 14 dpg (Figure 3.6 B). At 14 dpg, under control conditions, none of the EPFLs showed expression which is in contrast with the expression pattern of *EPFL1pro:GUS* at 3 dpg showing *EPFL1*'s involvement in early stages of plant development. However, ABA treatment induced expression of *EPFL2* specifically in true leaves with expression limited at the basal ends of leaves. Treatment with 5% PEG induced the expression of both *EPFL1* and *EPFL2* with expression of *EPFL1* being localized in cotyledonary leaves whereas *EPFL2* expression was observed in true leaves towards the basal end similar to its expression pattern in presence of ABA. In addition, the *EPFL2* promoter drove GUS expression in the shoot apical meristem visible in all treatments. *EPFL3* failed to show any signs of expression under any of the treatments, including control conditions, further evidencing its non-involvement in ABA induced signaling and drought stress response.

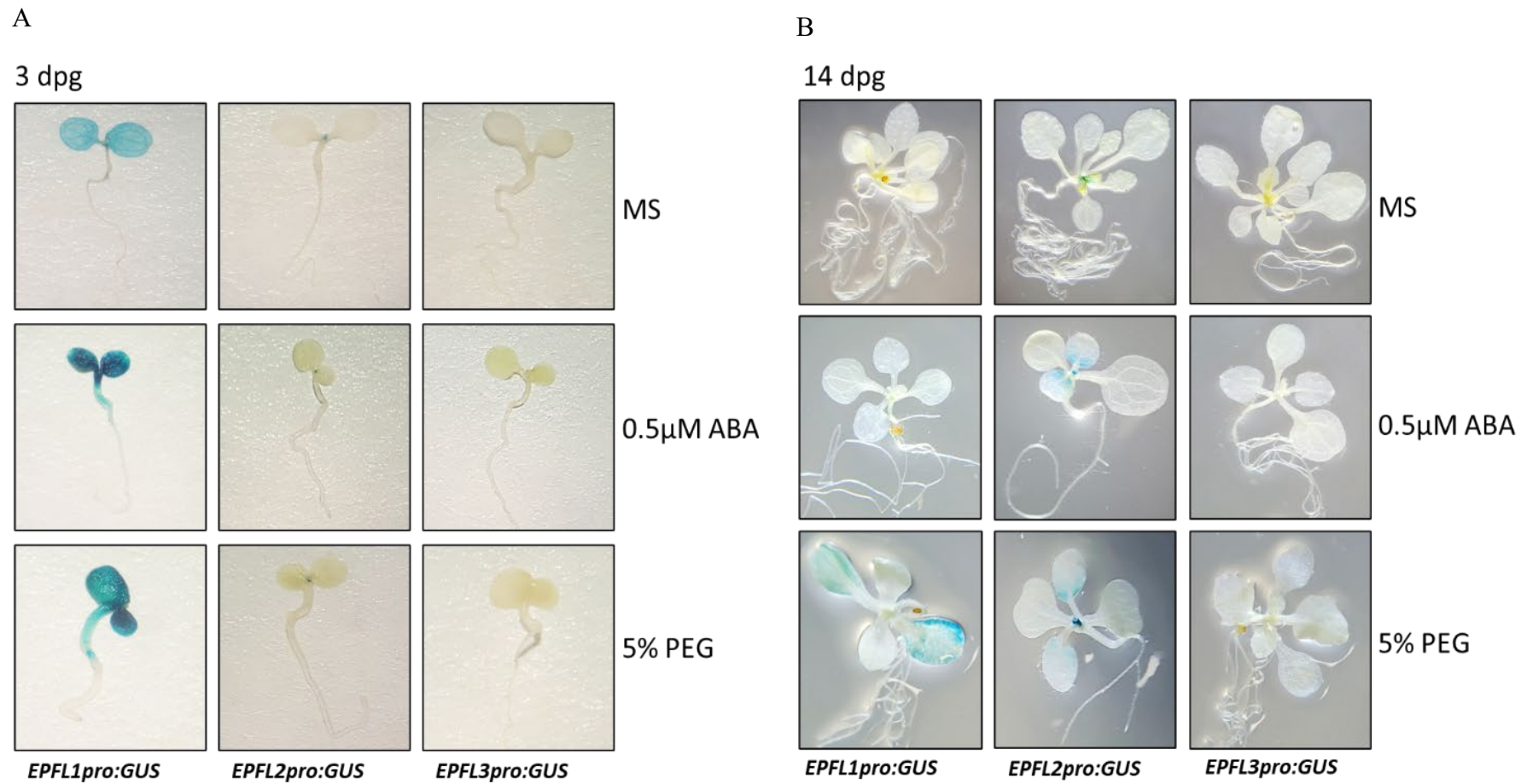


Figure 3.6: GUS expression patterns of *EPFL1pro:GUS*, *EPFL2pro:GUS* and *EPFL3pro:GUS* in: A. 3 dpg seedling, B. 14 dpg seedling from MS media, 0.5 μ M ABA and 5% PEG plates visualized using dissecting microscope.

3.3.6 Mechanism of drought tolerance

The results discussed above show that both *EPFL1* and *EPFL2* may have potential roles in drought stress responses whereas *EPFL3* did not show any significant response upon ABA treatment or osmotic stress and therefore, was not included in subsequent studies. To investigate the mechanisms of tolerance to drought stress used by *EPFL1* and *EPFL2*, the effects of ABA on different physiological parameters *viz.* seed germination and root length were recorded.

To check if ABA can influence the germination of *epfl* mutants as well as Ox lines, surface sterilized seeds were grown under control conditions as well as with 0.5, 0.8 and 1 μ M ABA supplemented medium and scored 3 days after imbibed seeds were moved to 22°C. Overall, the highest concentration of ABA (1 μ M) reduced the seed germination percentage regardless of the seed genotype. Interestingly, the presence of ABA did not influence the seed germination percentage for mutants as well as Ox lines for both *EPFL1* and *EPFL2* as it was not significantly different from WT. Thus, providing direct evidence that *EPFL1* and *EPFL2* lack ABA-induced phenotype in regulating inhibition of seed germination (Figure 3.7 A-B).

Root length of seedlings grown in presence of 20 μ M ABA was observed. ABA application indeed reduced the overall root length of seedlings regardless of lines tested. Root length of *epfl1* and *OxEPFL1* seedlings did not differ significantly from WT in control as well as ABA treatment indicating it might not be involved in root development and ABA-mediated root responses. In contrast, under control conditions, root length of *epfl2* seedlings was significantly longer than WT and *OxEPFL2* seedling's root length was significantly reduced indicating the negative role of *EPFL2* in root elongation. A similar trend on root length was seen in the presence of ABA for *EPFL2* lines with less reduction in root length in response to ABA treatment for *epfl2* than the WT and greater reduction in the *OxEPFL2* lines, but these differences were not statistically significant, likely due to large variance among the replicates. The observed trend indicates a possible role of *EPFL2* in root elongation, however, further validation by additional experiments with larger sample size is required. Furthermore, the interaction effect of genotype and ABA by 2-way ANOVA followed by Sidak's multiple comparisons test ($P < 0.05$) found no significant interaction effect which indicates that the response to the ABA treatment was not significantly different between *epfl1* and the WT, nor between *epfl2* and the WT. Besides, *epfl1/2* seedlings root length did not differ significantly from WT under control conditions, although ABA treatment caused significant decrease in root

length of these seedlings, but this was not different from the *epfl2* single mutant. (Figure 3.8 A-B).

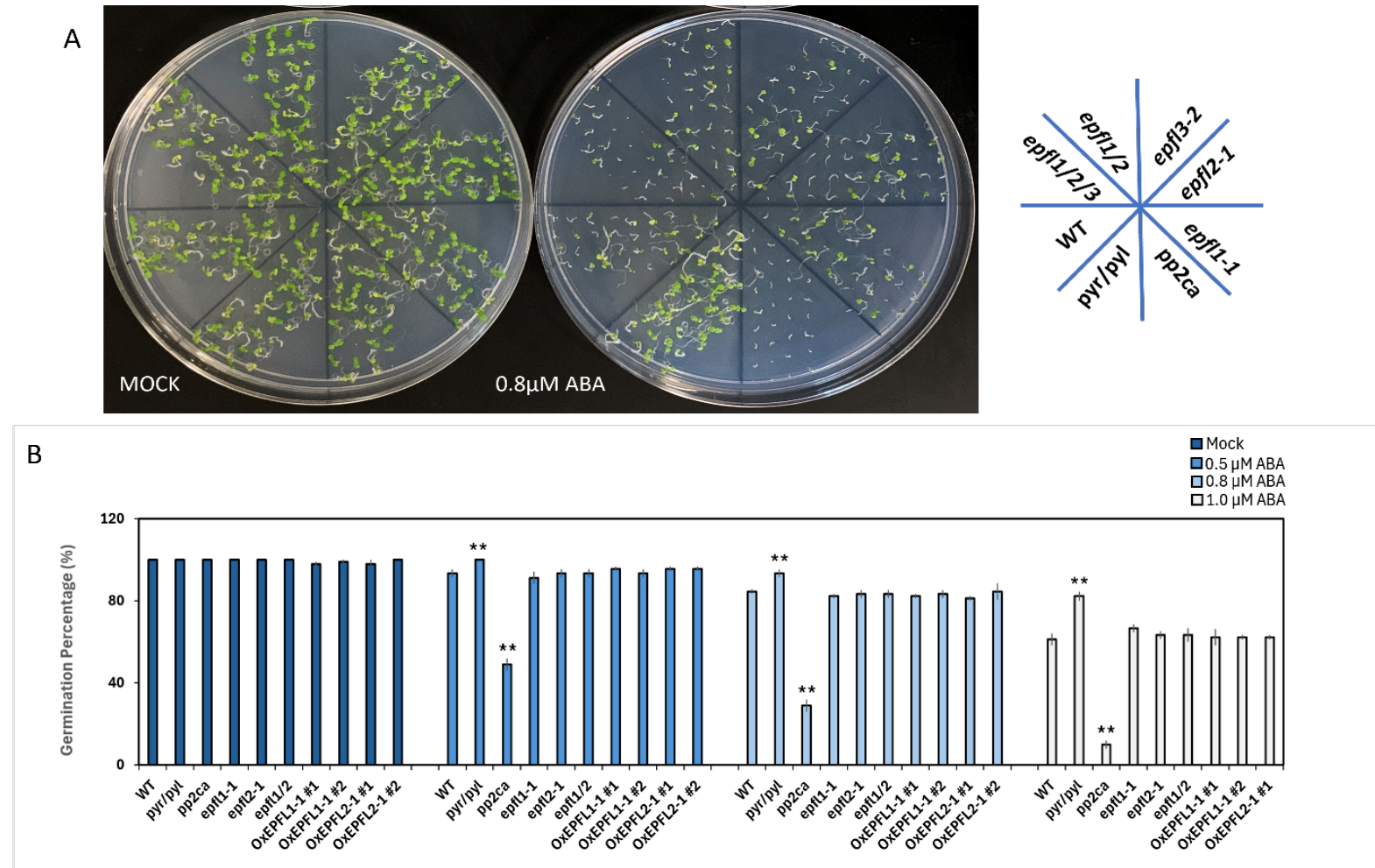


Figure 3.7: Seed germination of WT, *pyr/pyl12458*, *pp2ca*, *epfl1-1*, *epfl2-1*, *epfl1/2*, *OxEPFL1-1#1*, *OxEPFL1-1#2*, *OxEPFL2-1#1* and *OxEPFL2-1#2*, A. a representative image of mock and 0.8 μ M ABA plate at 8 dpv, B. Radicle emergence was scored after 72-h growth at 22°C on MS plates containing the indicated concentrations of ABA. Bars are mean \pm SE of three biological replications. Following one-way ANOVA, Dunnett's Multiple Comparison test was performed comparing means of seed germination percentage with respect to WT (**P < 0.001).

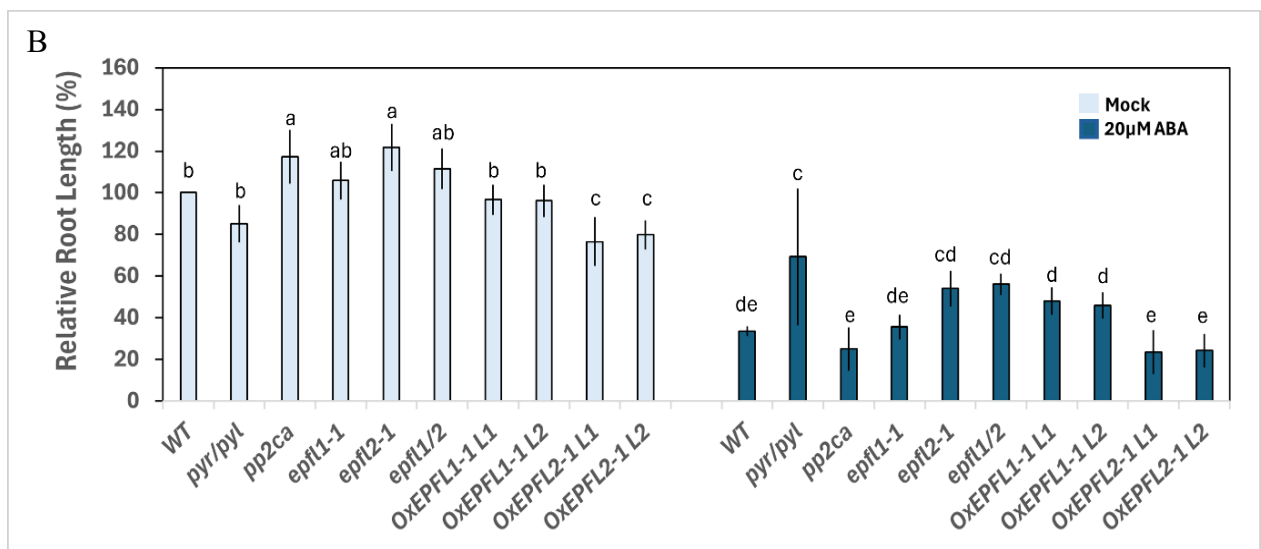
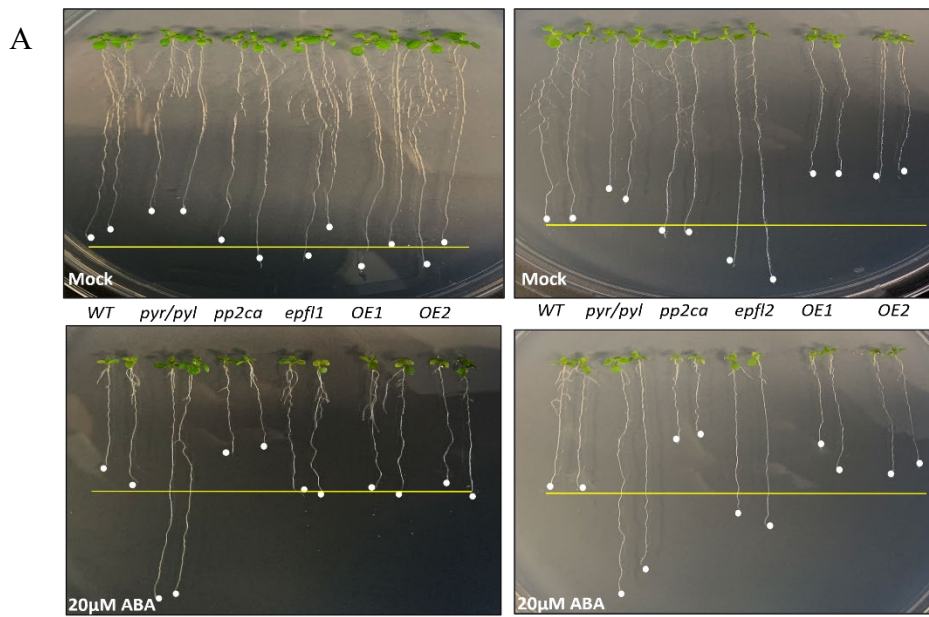


Figure 3.8: ABA-mediated inhibition of root growth in WT, *pyr/pyl12458*, *pp2ca*, *epfl1-1*, *epfl2-1*, *epfl1/2*, *OxEPFL1#1*, *OxEPFL1#2*, *OxEPFL2#1* and *OxEPFL2#2*. (A) Representative images were taken 7 days after transferring 3-d-old seedlings to MS plates supplemented without or with the indicated concentrations of ABA. (B) Quantification of primary root lengths in the indicated genetic backgrounds after ABA treatment. Bars indicate mean \pm SD of 6 replicate seedlings from a single experiment. Three biological replicates were performed with similar results. Following one-way ANOVA, Tukey's Multiple Comparison test was performed comparing means of relative root length. Significant differences between data are shown by different letters, $p < 0.05$.

3.3.7 Influence on stomatal density and stomata regulation

In the next step of investigation, I explored whether *EPFL1* and *EPFL2* could influence stomatal density. Additionally, I sought to assess if ABA impacts stomatal regulation in *EPFL1* and *EPFL2* mutants.

Epidermal scoring revealed that *epfl1* plant's stomatal density as well as non-stomatal density did not differ significantly from WT. However, both *epfl2* and the *epfl1 epfl2* double mutant plants exhibited a significant increase in stomatal density and non-stomatal density compared to WT (Figure 3.9 A-B). However, other abnormalities such as stomatal clustering and meristemoid formation were not detected in any mutant, *epfl1*, *epfl2* and *epfl1/2*.

To check whether *EPFL1* or *EPFL2* can affect stomata opening and closing, I performed a stomatal regulation assay in the presence or absence of ABA. As shown in Figure 3.9 B under normal circumstances, the *epfl1* stomata aperture did not differ significantly from WT. However, *epfl2* plants showed a significant increase in stomata aperture indicating *epfl2* might be involved in a signaling mechanism promoting stomata closure or opening in response to environmental cues. To further investigate this, the same set of assays was performed in the presence of 50 μ M ABA (Figure 3.9 C). Notably, *epfl1* plants exhibited a significant increase in stomatal aperture length, suggesting that *EPFL1* may function as part of an ABA-dependent signaling pathway that influences stomatal regulation. Moreover, the interaction effect of 2-way ANOVA followed by Sidak's multiple comparisons test ($P < 0.05$) showed a significant genotype by treatment interaction which confirmed that *epfl1* had a significantly different response to ABA treatment than WT. In contrast, *epfl2* plants appeared unaffected by ABA, as stomatal aperture width was similarly increased both in the presence and absence of ABA, indicating that *EPFL2* does not seem to be involved in ABA-mediated regulation of stomatal aperture. Moreover, the interaction effect of 2-way ANOVA followed by Sidak's multiple comparisons test ($P < 0.05$) showed a no-significant genotype by treatment interaction which confirmed that between *epfl2* had non-significant different responses to ABA treatment than WT.

I also investigated the effect of ABA on inhibiting light promoted stomatal opening. Following a 24 h period of darkness, exposure to light resulted in the greatest stomatal opening in the *epfl1*, while *epfl2* and *epfl1/2* mutants did not show statistically significant differences as compared to the WT (Figure 3.9 D).

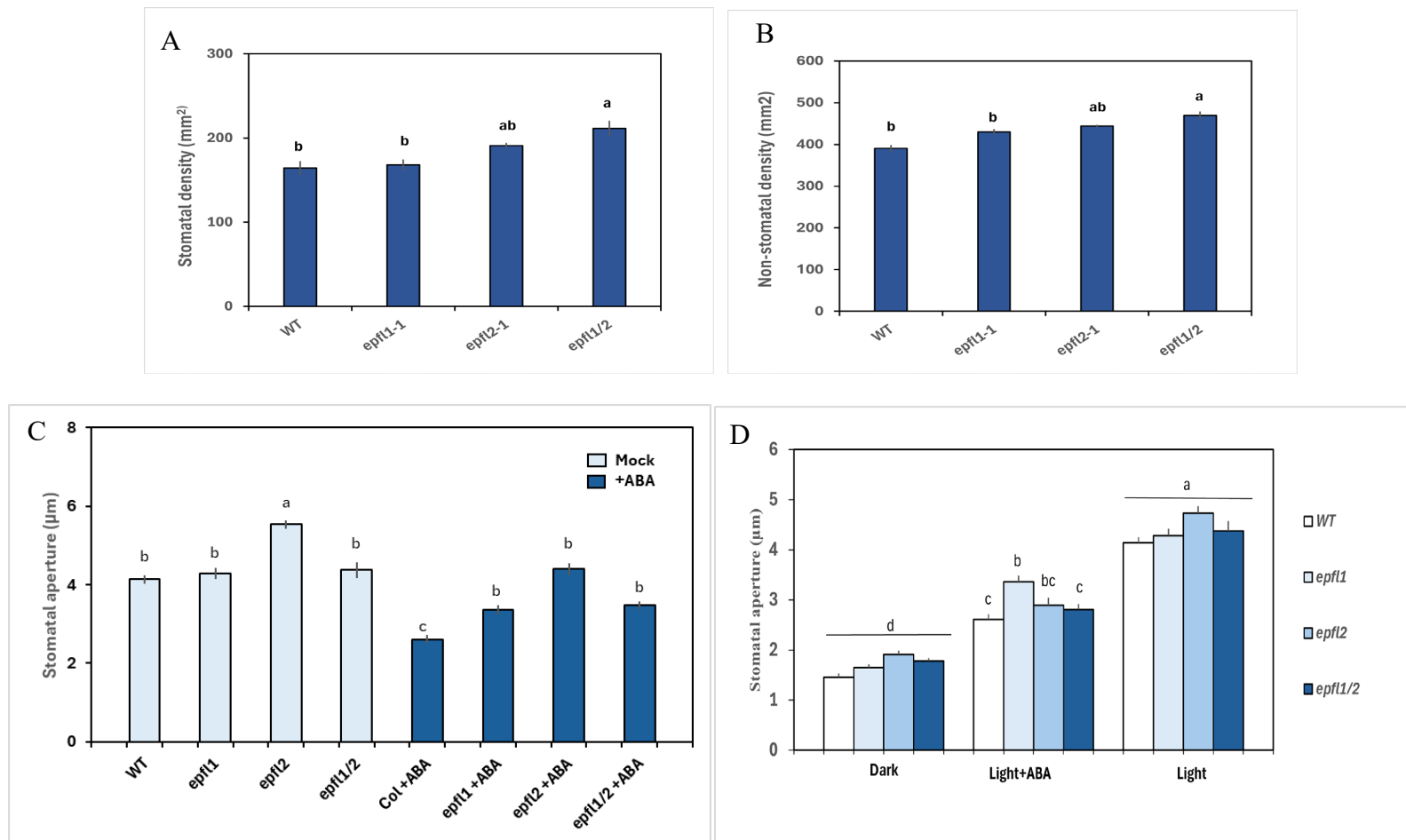


Figure 3.9: (A) Epidermal score representing stomatal density and (B) Non-stomatal density of WT, *epfl1*, *epfl2* and *epfl1/2*. (C) ABA-mediated stomatal closure in the WT, *epfl1*, *epfl2* and *epfl1/2* phenotype. Rosette leaves with fully open stomata were treated with or without 20 μM ABA for 2 h before being photographed. (D) ABA-inhibited stomatal opening in the WT, *epfl1*, *epfl2* and *epfl1/2* phenotype. Four-week-old plants were grown in a dark room for 24 h to close their stomata, and rosette leaves from the plants were treated with or without 20 μM ABA in the light for 2 h before being photographed. Bars are means ± SE of three biological replicates (20 stomata from one seedling per replicate). Following one-way ANOVA, Tukey's Multiple Comparison test was performed comparing means of stomatal aperture against respective WT (*P < 0.05; **P < 0.001). Significant differences among data are shown by different letters (P < 0.001).

3.4 Discussion

Drought-induced stress significantly disrupts normal plant physiology and metabolism, leading to inhibited growth and development, reduced crop yields, and, in severe cases, plant death. Extreme drought conditions can result in the inhibition of cell division, suppression of photosynthesis, and the closure of stomata (Taiz and Zeiger, 2002). Various environmental cues, including drought, trigger specific signal transduction cascades that regulate key aspects of stomatal development and closure. The immediate response of plants to drought stress is to close stomata, thereby reducing water loss through transpiration (Schroeder *et al.*, 2001). In contrast, long-term adaptations, changes in stomatal density, index, and size may take weeks or years to develop (Carvalho *et al.*, 2016). Additionally, root system architecture is also an important aspect of plant adaptation to drought stress, consisting of various structural features such as the number and length of main and lateral roots, branching, angle, density and length of root hairs. Plants can adjust the root system architecture in response to drought conditions (Germon *et al.*, 2020). Although water uptake is initiated by the shoot, it is the root system architecture that determines a plant's water access, thus improving root trait morphology as well as stomata development and movement is a matter of interest among geneticists and breeders to make drought resistant crop varieties (Comas *et al.*, 2013; Nardini *et al.*, 2002). In this study, RNA-seq data analysis of the *EPFL1*, *EPFL2*, and *EPFL3* genes revealed maximal expression in seed coat correlating with enhanced protective mechanisms possibly involved in the synthesis of structural components that contribute to seed coat strengthening. However, the specific stage of seed coat differentiation must be clarified, as these genes may also play roles earlier in ovule integument development or later in the differentiation of inner/outer seed coat layers. Additionally, previous work suggests that some *EPF/EPFL* family members, such as *EPFL2*, are involved in ovule patterning and fruit growth coordination (Kawamoto *et al.*, 2020) and could have extended roles in seed coat formation. This role may overlap with regulatory cascades involving epidermal patterning genes like *TTG1* and *GL2*, which are known to influence aspects of seed coat differentiation (Haughn & Chaudhury, 2005). The data also revealed the importance of this peptide sub-family during abiotic stress, especially under drought conditions with *EPFL2* levels being highest among *EPFL1*, *EPFL2* and *EPFL3*. A recent study, Xia *et al.*, (2024) reported that expression levels of *ZmEPFL2-2* and *ZmEPFL9-3* were up-regulated at 12 h and down-regulated at 24 h of the onset of drought stress. Conversely, the expression levels of *ZmEPFL3* gradually decreased with stress time with authors suggesting that patterns of expression of *EPF/EPFL* gene family are variable under drought conditions. In addition, Xia *et al.*, 2024 did not find any evidence of direct

interactions of *ZmEPF/EPFL* with proteins related to ABA signaling, however, *ZmEPFL4-1*, *ZmEPFL2-1* and *ZmEPFL4-2* were shown to interact indirectly with proteins related to phosphorylation and authors speculated that these gene products might possess ABA-like ability to regulate stomata opening and closing via phosphorylation/dephosphorylation reactions.

Liu *et al.* (2024) subjected Poplar (*Populus trichocarpa*) plants to drought stress and ABA treatment and observed that the expression patterns of *PtEPF/EPFL* genes differed under these conditions. Within three days, the expression levels of *PtEPF1-2*, *PtEPFL1-1*, and *PtEPFL3-2* were highest. From nine days of drought stress, *PtEPF2* and *PtEPFL2* exhibited the highest expression levels, while *PtEPF1-1*, *PtEPFL1-2*, *PtEPFL5-1*, *PtEPFL5-2*, and *PtEPFL6* showed peak expression at 12 days of drought treatment. In comparison, upon ABA (250 μ M) spraying, the expression levels of *PtEPF1-1*, *PtEPF1-2*, *PtEPF2*, *PtEPFL7* and *PtEPFL8* were upregulated quickly. *PtEPFL1-1*, *PtEPFL1-2*, *PtEPFL5-2* and *PtEPFL6* levels were downregulated significantly while other genes did not respond significantly to ABA treatment. This is in contrast with RNA-seq data for Arabidopsis where ABA treatment resulted in increased expression of *EPFL2* and *EPFL3*. The study by Zhiling *et al.* (2024) revealed significant expressions of *ScEPFL1* and *ScEPFL10* in rye (*Secale cereale* L.) seeds. The identification of cis-regulatory elements within *ScEPFL1* and *ScEPFL9* genes provides strong evidence for their involvement in regulating seed-specific processes. Their results also indicate that drought stress differentially regulates the expression of *EPFL* genes in rye. While *ScEPFL2*, *ScEPFL3*, and *ScEPFL10* were upregulated after 3 h in response to PEG6000 treatment, suggesting their potential role in drought tolerance, the expression of *ScEPFL4*, *ScEPFL5*, and *ScEPFL9* were downregulated. Collectively, these results underscore the critical roles of the *EPF/EPFL* family in seed development and in involvement in the drought stress response.

The mutant and Ox lines for *EPFL1*, *EPFL2*, and *EPFL3* used in this study have provided valuable insights into the role of these peptides encoded by these genes in modulating plant drought stress tolerance. The *epfl1* and *epfl2* mutants did not show significant differences in drought stress sensitivity compared to the control, suggesting that these genes may not play a prominent role in drought tolerance under native conditions. However, overexpression lines driven under the 35S promoter (*OxEPFL1* and *OxEPFL2*) exhibited significantly higher expression of both drought-responsive genes, *RD29* and *DREB*, indicating enhanced transcriptional activity related to drought stress. While these findings suggest

that *EPFL1* and *EPFL2* may contribute to drought response pathways, it is important to consider that the observed phenotypes in overexpression lines could result from ectopic expression. Specifically, the enhanced expression of downstream genes may not accurately reflect the native roles of *EPFL1* and *EPFL2*, as these genes may not normally be expressed at the developmental stages, and tissue types analyzed in this study, or in response to drought stress. Furthermore, the observed effects could be indirect, arising from downstream interactions rather than direct regulation by these genes. Despite these limitations, this study highlights the potential of *EPF/EPFL* family genes as promising targets for engineering or breeding strategies aimed at improving drought tolerance in crops. Future research employing native promoters and tissue-specific expression analyses will be essential to elucidate the precise roles of these genes in drought stress responses.

GUS histochemical staining of transcriptional reporter lines revealed *EPFL1* expression throughout seedlings at three dpv and its expression gets stronger upon osmotic stress as well as ABA treatment further supporting the findings of drought and water loss assay. Surprisingly, the expression levels declined completely in control 14 dpv old seedlings with *EPFL1* reporter lines being unresponsive to externally supplied ABA at 14 dpv which is in contrast with 3 dpv data where expression is limited to cotyledonary leaves at 14 dpv showing the spatio-temporal dynamic of expression pattern for *EPFL1*. Even though *EPFL2* expression was non-existent in 3 dpv seedlings but at 14 dpv, the histochemical staining appeared to localize to stomatal lineage cells in young true leaves at 14 dpv highlighting the importance of *EPFL2* at later stages of development potentially coinciding with stomata development. *EPFL3* transcriptional reporter lines on the other hand showed no signs of expression under any observed circumstances supporting the water loss and drought assay as well as qRT-PCR data implying it is not involved in mediating stress response in *Arabidopsis* under observed conditions. The studies by previous lab member, Seyhuk Park, also confirmed that *EPFL3* displays no expression in three distinct developmental stages including 3 dpv, 18 dpv and 39 dpv plants.

To determine whether EPFL's mode of action involves an ABA-dependent pathway, various physiological parameters were analyzed. For instance, seed germination was unaffected by ABA application in both *epfl1* and *epfl2* as well as *Ox* lines, indicating that EPFLs do not participate in the signaling mechanisms associated with ABA-mediated seed germination inhibition. Another parameter, root length, exhibited notable differences between *EPFL1* and *EPFL2*. However, *epfl1* showed no difference in mock conditions as well as

response to exogenous ABA application. In contrast, *epfl2* exhibited greater root length, while seedlings of *OxEPFL2* #1 and *OxEPFL2* #2 displayed shorter root lengths compared to respective WT. These findings were in line with RNA seq data showing significantly high expression of *EPFL2* in roots, suggest that *EPFL2* plays a role in root development that might operate independently of ABA mediated signal transduction, as the application of ABA did not alter the observed trends in root length development. Stronger and longer roots enable plants to access deeper water sources in the soil, enhancing their resistance to dry conditions (Comas *et al.*, 2013). Consequently, *EPFL2* could be targeted to potentially develop crops with improved root adaptation on drought onset.

The EPF/EPFL family can provide resistance against drought stress by controlling stomata development and the regulation of stomatal aperture. Studies concerning EPFs in Arabidopsis and monocots such as wheat and Brachypodium have given substantial evidence of these EPF/EPFL family members' role in stomata development and movement. It is possible that the actions of *EPFL1* and *EPFL2* in modulating stomatal development and stomatal aperture may be influenced by ABA signaling pathways. Therefore, for this project, I aimed to discover if *EPFL1* and *EPFL2* can influence stomata development and movement. The epidermal scoring of *epfl2* and *epfl1/2* demonstrated the increase in stomata density indicating the negative regulation of stomata development by *EPFL2* which is in line with earlier observation where other members of *EPF/EPFL* family, i.e. *EPF1* and *EPF2*, act as negative regulators of stomata development. This is in contrast with *EPFL9* that acts as positive regulator of stomata development competing with *EPF1* and *EPF2* for receptor binding sites (Lee *et al* 2012). Despite the intriguing potential of ABA signaling in relation to EPF/EPFLs, there is very little direct evidence in the literature connecting the two. In this regard, Liu *et al.*, (2016) first reported that Arabidopsis transgenic plants overexpressing *PdEPF2* isolated from *Populus* had decreased sensitivity to exogeneous applied ABA during seed germination and development. On the other hand, *epf2* plants showed pronounced sensitivity to ABA. Moreover, *PdEPF2* positively regulated the expression of *ABI1* and *ABI2* further indicating that *EPF2* might be involved in regulating the ABA signaling pathway.

In addition to their role in stomatal development, EPFLs also modulate stomatal aperture in response to external stimuli. Preliminary findings from this project indicate that *epfl1* did not have significant differences from WT, whereas *epfl2* displayed significantly more opened stomatal aperture compared to WT under control conditions. They both showed less stomatal closure than the WT in response to ABA treatment. However, two-way ANOVA with Sidak's

test ($P < 0.05$) showed a strong interaction between *epfl1* and ABA treatment while that of between *epfl2* and ABA is not significant indicating that, a decrease in stomatal aperture of *epfl1* plants might be influenced by ABA. Thus, the findings of this study provide the groundwork for a more comprehensive investigation of how these EPFLs influence stomata development and movement. Thus, further studies involving use of stomatal lineage reporter line (*TMMpro::GUS-GFP*) expressed in *epfl1*, *epfl2*, *epfl3*, and *epfl1/2* backgrounds will be crucial in understanding the specific role of these peptides in stomata development. Moreover, subsequent studies should focus on finding the corresponding receptors for these peptides by first screening the potential candidate receptors (e.g. ERECTA, ERL1, and ERL2) by similar methods of generating knock out and Ox lines. Next, high order mutants comprised of potential receptors and EPFL combinations will provide valuable insights into the signaling mechanisms involving these EPFLs-receptors in stomata development. *In vitro* techniques (e.g. yeast-two-hybrid; co-immunoprecipitation) as well as *in vivo* techniques (e.g., BiFC) will be crucial in confirming these ligand-receptor interactions.

In conclusion, this study on *EPFL1* and *EPFL2* enhances our understanding of how plants cope with drought stress. These peptides are potential candidates for mediating stress responses and interacting with pathways involved in drought adaptation. By further investigating the function of these peptides, we may optimize new strategies to improve water use efficiency and promote better growth in dry climates.

Chapter 4: Investigating the roles of the Arabidopsis MAPK phosphatases, MKP2 and DsPTP1 in chloroplast biogenesis.

Note: Some of the experiments presented in this chapter were performed independently by both myself and Zakaria Brahim. Zakaria included his own set of results from these identical experiments in his master's thesis. While we both conducted similar work, the results presented here are solely my own, derived from my independent analysis and finalization of the experiments. Below is the list of experiments performed by both me and Zakaria Brahim:

1. Complementation of the *mkp2 dsptp1* mutant: transgenic *mkp2 dsptp1* expressing a full-length clone of *DsPTP1* driven by its native promoter (*proDsPTP1::DsPTP1*).
2. Seed segregation analysis in siliques.
3. Photosynthetic pigment quantification assay.
4. BiFC analysis to test the physical interaction between MKP2/CIMKP2, DsPTP1/CIDsPTP1 and candidate kinases.

4.1 Introduction

4.1.1 Mitogen-activated protein kinase (MAPK) cascades

Plants establish signaling pathways to sense external signals and modify their physiological activities, helping them mitigate environmental impacts and ensure proper development, function, and growth (McCarty & Chory, 2000). One of the key components of signal transduction in plants and other eukaryotes is the MAPK cascade, which regulates biological behaviors such as proliferation, apoptosis, cellular survival, and gene expression. As shown in Figure 4.1, it consists of three key layers: MAP kinase kinase kinases (MAPKKKs), MAP kinase kinases (MAPKKs), and MAP kinases (MAPKs) (Zhou *et al.*, 2017). This cascade receives environmental and internal signals, delivering them to substrates and activating biological activities like cellular proliferation, differentiation, and hormonal responses. Activated by environmental cues through plasma membrane receptors, MAPKKKs phosphorylate MAPKKs at serine or threonine residues in a conserved activation loop motif (S/T–X3–S/T, where X represents any amino acid), triggering a conformational change that enhances catalysis (Rodriguez *et al.*, 2010). MAPKKs then phosphorylate downstream MAPKs at threonine or tyrosine residues in a T–X–Y motif, leading to the activation of various effector proteins such as transcription factors and enzymes, which mediate diverse cellular responses. Together, these mechanisms enable plants to adapt effectively to their environment (Bigear and Hirt, 2018).

In *Arabidopsis*, extensive research has identified 80 MAPKKKs, 10 MAPKKs, and 20 MAPKs, which together form a sophisticated signaling network crucial for regulating physiological activities (Colcombet & Hirt, 2008; Umezawa *et al.*, 2011). These MAPKs are classified into four groups based on phylogenetic analysis: Group A (MPK3, MPK6, MPK10), Group B (MPK4, MPK5, MPK11-13), Group C (MPK1, MPK2, MPK7, MPK14), and Group D (MPK8, MPK9, MPK15-20). Groups A, B, and C feature a conserved T–E–Y motif at their phosphorylation sites, while Group D is distinguished by a T–D–Y motif (Jagodzik *et al.*, 2018; Bigear & Hirt, 2018). MPK3 and MPK6, key members of Group A MAPKs, are extensively studied for their roles in regulating stomatal development and patterning, primarily through the MKK4/5-MPK3/6 module downstream of the MAPKKK YODA (Bergmann *et al.*, 2004; Wang *et al.*, 2007).

Group B MAPKs, such as MPK4, play significant roles in plant cytokinesis during meiosis and mitosis and in Pathogen-associated molecular patterns (PAMP)-triggered immunity. The *mpk4* mutation results in higher salicylic acid levels and enhanced pathogen resistance, indicating MPK4's role as a negative regulator of systemic acquired resistance. Its high expression in guard cells is crucial for regulating stomatal openings. The kinase's activity in guard cells aids in modulating responses to both biotic stresses, like pathogen attack, and abiotic stresses such as drought (Lin and Chen 2018; Töldsepp *et al.*, 2018). Group C MAPKs, including MPK1, MPK2, MPK7, and MPK14, are crucial for plant development and stress responses. These MAPKs are activated by abscisic acid (ABA), a key phytohormone involved in various stress responses and developmental processes. Their activation is regulated by upstream kinases such as MAPKKK17/18 and MKK3 (Colcombet *et al.*, 2016 Wang *et al.*, 2015; Dóczy *et al.*, 2007). MPK1 and MPK2 are particularly noted for their roles in responses to wounding, as well as in the signaling pathways of jasmonic acid (JA) and hydrogen peroxide (H₂O₂), highlighting their involvement in both biotic and abiotic stress responses (Shi *et al.*, 2010). MPK7 participates in pathogen signaling and is activated by MKK3 (Takahashi *et al.*, 2007). Group D MAPKs, such as MPK8 and MPK15, are less well-characterized than other MAPK groups. MPK15 is essential for PAMP-triggered immunity, contributing to resistance against powdery mildew through its phosphorylation. The receptor BSK1 is involved in the signaling pathway that activates MPK15 (Shi, *et al.*, 2022). MPK8 is particularly important for seed germination, functioning in conjunction with TCP14, a transcription factor associated with this process (Zhang, 2019). Overall, MAPKs exhibit diverse regulatory functions across multiple plant processes, including cell proliferation, differentiation, immunity, and stress responses, and act as crucial components in the MAPK signaling cascades.

4.1.2 MAP kinase phosphatases

MAPKs are activated by upstream phosphorylation from MAPKKs and negatively regulated by MAPK phosphatases (Keyse, 2008). The mechanism of negative regulation, in other words, dephosphorylation/deactivation of the kinases, relies on the inhibitory action of MAPK phosphatases (MKPs), which remove added phosphate groups from activated MAPKs to deactivate them. The ser/thr phosphatase cleaves phosphate from phosphoserine or phosphothreonine residues, while tyr phosphatase removes phosphate from phosphotyrosine residues in the protein.

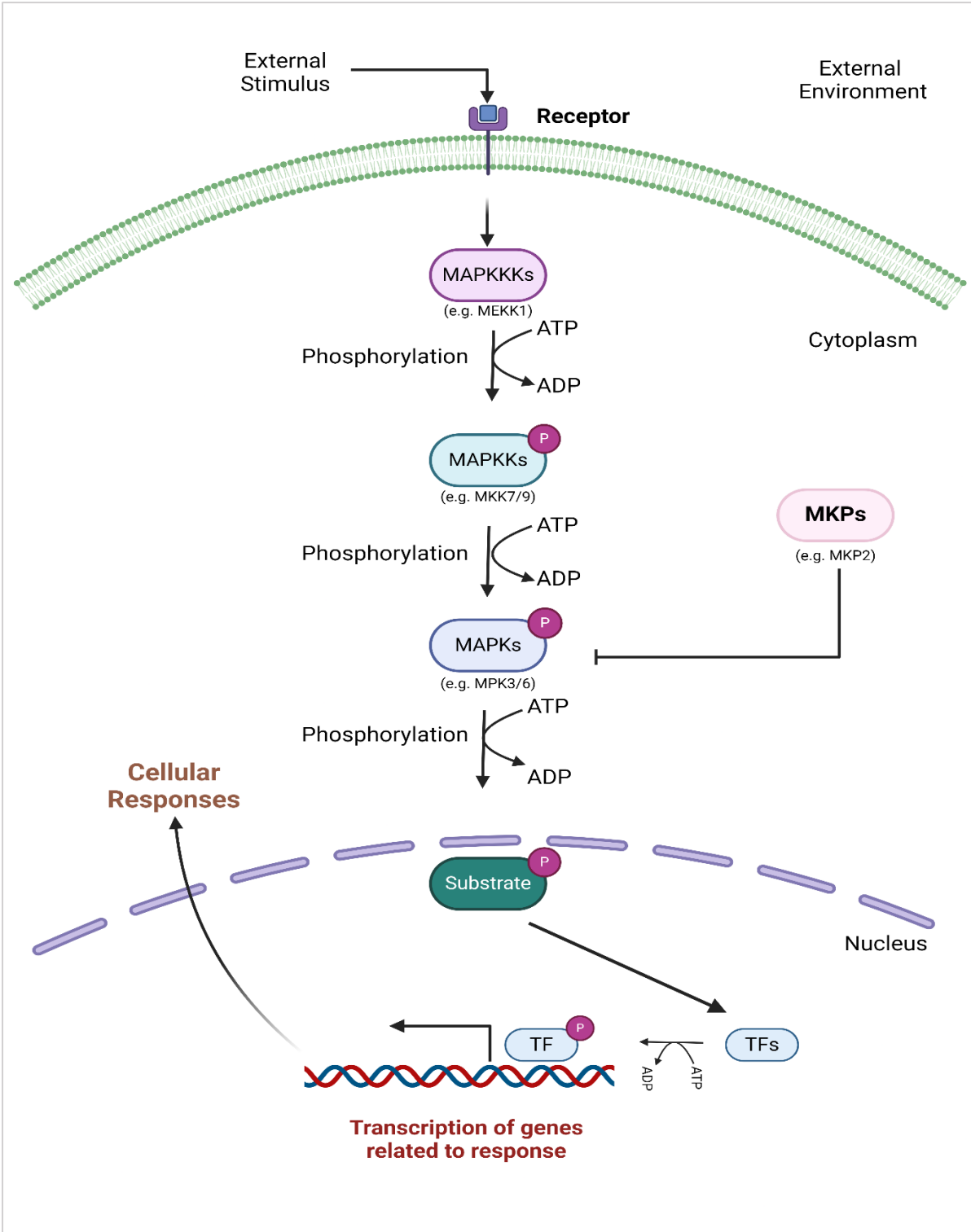


Figure 4.1 A diagram showing a typical MAPK cascade in eukaryotes. MAPK cascades consist of regulatory kinase modules that operate sequentially on a downstream target. MKPs dephosphorylate MAPKs, which negatively regulates the cascade. The diagram was generated using BioRender.

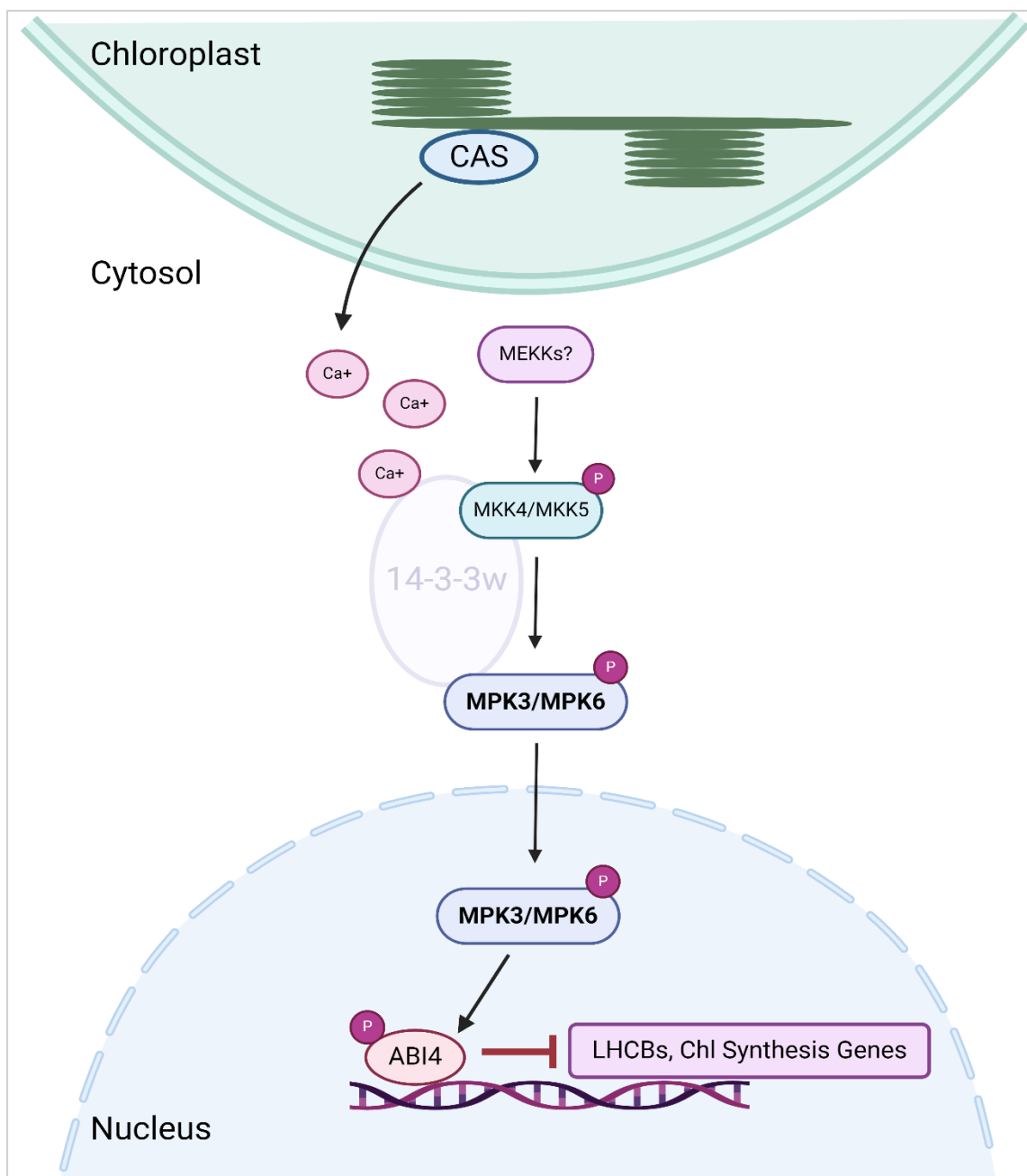


Figure 4.2: A model illustrating ABI4 activity modulation via Post-transcriptional modification (PTM) and post-translational (MPK 3/6) pathways (Guo *et al.*, 2016).

Dual-specificity phosphatase (DSPs), a subgroup of tyr phosphatases, dephosphorylates specifically on activated tyr and ser/thr residues in the substrate. The balance between the phosphorylating/activating effect of upstream MAPKKs and the dephosphorylating/deactivating effect of MKPs allows for the fine-tuning of the cell's physiological responses to environmental stimuli (Bheri *et al.*, 2021).

MKPs play significant roles in oxidative stress regulation, the innate immune response, osmotic stress regulation, and ABA signaling among other responses. It is hypothesized that MKPs might also have novel roles in plant development beyond a response to stress and could influence a broader range of physiological processes due to their association with MAPKs. MKPs have two main domains: the non-catalytic N-terminal domain, which binds to MAPKs and determines substrate specificity, and the C-terminal domain, which performs catalysis by interacting with phosphotyrosine or phosphothreonine residues. The N-terminal MAPK-binding domain shows high specificity due to docking interactions between negatively charged amino acid residues in the MAPK and positively charged residues in the MKP (Kalapos *et al.*, 2019). In the dual-specificity domain, each MKP has a unique conserved amino acid sequence. A highly conserved consensus phosphatase sequence, DX26(V/L)X(V/I)HCXAG(I/V)SRSXT(I/V)XXAY(L/I)M (X can be any amino acid), is present in their catalytic domains (Aoyama *et al.*, 2001). When MAPK binds, it induces a conformational change in the dual-specificity domain, enhancing dephosphorylation efficiency. In the Arabidopsis genome, 23 DSPs have been identified, computational analysis indicated that only five are functional MKPs because of their unique AY[L/I]M motif, which allows for dual-specific interaction with MAPKs (Kerk *et al.*, 2008). These five MKPs are Mitogen-Activated Protein Kinase Phosphatase 1 (MKP1), Mitogen-Activated Protein Kinase Phosphatase 2 (MKP2), Dual-specificity Protein Tyrosine Phosphatase 1 (DsPTP1), Indole-3-Butyric Acid Response 5 (IBR5), and Propyzamide-Hypersensitive 1 (PHS1).

DsPTP1 was the first MAPK phosphatase identified to dephosphorylate and inactivate the downstream MAPK, MPK4, *in vitro* (Gupta *et al.*, 1998). As a dual-specificity phosphatase, it specifically catalyzes the hydrolysis of phosphate groups on phosphotyrosine and phosphoserine/phosphothreonine residues. It functions as a negative regulator of osmotic stress signaling during seed germination; mutations in the *dsptp1* gene resulted in higher seed germination rates under osmotic stress conditions compared to WT plants. Conversely, overexpression of DsPTP1 suppresses seed germination under osmotic stress conditions (Liu *et al.*, 2015). Additionally, DsPTP1 contains two calcium-dependent calmodulin (CaM)

binding domains with one in the N-terminal region and the other in the C-terminal region. CaM enhances or reduces the dephosphorylation activity of DsPTP1 depending upon the substrate indicating that a CaM-mediated Ca^{2+} signaling pathway regulates its dephosphorylation activity (Yoo *et al.*, 2004). Notably, DsPTP1 also acts as a positive regulator of ABA accumulation under osmotic stress (Liu *et al.*, 2015).

MKP2 is a dual-specificity MAPK phosphatase in Arabidopsis that plays a crucial role in regulating responses to oxidative and pathogen-related stresses. Plants with reduced MKP2 expression show prolonged MPK3 and MPK6 phosphorylation in response to ozone treatment, suggesting that these MAPKs are MKP2 substrates and are a component of an oxidatively linked module (Lee & Ellis, 2007). Since loss-of-function mutations in *mkp2* strengthen immune responses to necrotrophic pathogens while lowering responses to biotrophic infections, *mkp2* is crucial for plant immunity. This implies that a MAPK network composed of MPK3/6 and MKP2 governs responses to fungal elicitors (Lumbreras *et al.*, 2010). Furthermore, by dephosphorylating and inactivating MPK3 and MPK6, MKP2 positively regulates the oxidative stress response.

MKP1 is a stress- and stimulus-inducible phosphatase that plays a crucial role in MAPK signaling by interacting with and dephosphorylating its substrates (Toulouse & Nolan, 2015). The *mkp1* null mutant in Columbia (Col) exhibits developmental issues such as early senescence, stomatal defects, and dwarfism, which are attributed to increased salicylic acid accumulation. This null mutant also demonstrates enhanced tolerance to salt stress (Bartels *et al.*, 2009). Recently, MKP1 has been identified as playing a novel role in stomatal development by influencing early stages of cell fate transitions, primarily through its inhibitory effects on MPK3 and MPK6 (Tamnanloo *et al.*, 2018).

PHS1 plays a crucial role in ABA signaling and microtubule polymerization, physically interacting with MPK18 and MPK12. The *phs1-1* mutant shows reduced root length and twisted left-hand roots, while the *phs1-3* mutant exhibits hypersensitivity to ABA and suppressed seed germination when exposed to exogenous ABA (Tang *et al.*, 2016; Quettier *et al.*, 2006). PHS1's interaction with MPK18, confirmed through yeast two-hybrid and BiFC assays, indicates that MPK18 is a substrate of PHS1, forming a signaling module that regulates microtubule functions (Walia *et al.*, 2009). IBR5 is another phosphatase that regulates auxin and abscisic acid (ABA) signaling pathways, interacting with MPK12 both *in vitro* and *in vivo* (Lee *et al.*, 2009; Monroe-Augustus *et al.*, 2003). Arabidopsis plants with the *ibr5* mutation

exhibit attenuated responses to ABA and auxin, showing less severe inhibition of root elongation and germination compared to wild-type controls (Lee *et al.*, 2009) The loss-of-function mutation in *ibr5* also results in reduced sensitivity to exogenous ABA and auxin (Monroe-Augustus *et al.*, 2003).

The dynamic nature of MKP-MAPK interactions suggests that these phosphatases might play critical roles in integrating various signals, allowing plants to adapt to changing environmental conditions. Understanding the full extent of MKP functions in plants could reveal new insights into plant development and adaptability, potentially offering strategies for improving crop stress tolerance in agricultural practices.

4.1.3 Chloroplast biogenesis and MAPK signaling

Chloroplasts are semi-autonomous organelles found in plant cells and algae, primarily responsible for photosynthesis- converting light energy into chemical energy stored in glucose (Roston *et al.*, 2018). Structurally, chloroplasts are characterized by a double-membrane envelope, which consists of an outer and inner membrane, and an internal system of thylakoid membranes arranged in stacks known as grana. These thylakoids contain chlorophyll and other pigments that capture light energy, facilitating the light-dependent reactions of photosynthesis. The stroma, the fluid-filled space surrounding the thylakoids, is where the Calvin cycle occurs, utilizing ATP and NADPH produced during the light-dependent reactions to fix carbon dioxide into organic molecules (Zhang *et al.*, 2019; Alberts *et al.*, 2002). Chloroplasts are essential for a number of metabolic functions besides photosynthesis, such as the production of plant hormones, fatty acids, and amino acids, as well as the storage of starch for energy. By generating antioxidants, they also support the plant's defense mechanisms against oxidative stress. Chloroplast development in dicots involves various stages, beginning with proplastids as the initial precursors. In Arabidopsis, proplastids develop into etioplasts containing a prolamellar body (PLB), where prothylakoids start differentiating into thylakoids, eventually leading to mature chloroplasts capable of photosynthesis (Gao *et al.*, 2023).

Albinism in plants is characterized by reduced chlorophyll levels, and often results from genetic mutations that disrupt the proper differentiation of proplastids into chloroplasts, affecting overall plant development (Silva *et al.*, 2020). Light is essential for chloroplast development, promoting growth in cotyledons and chloroplasts while suppressing hypocotyl elongation (Rosa *et al.*, 2020). As the shoot apical meristem activates leaf production, genes related to protein translation and chloroplast biogenesis are expressed. During chloroplast development, proplastids expand significantly, and their inner membranes invaginate to form

stroma, where thylakoids appear and stack through amplification. Proteins from the cytosol support thylakoid growth, entering proplastids via protein import and being delivered to thylakoids by vesicles from the inner membrane (Gutiérrez-Nava *et al.*, 2004). Thylakoids are the sites of photosynthesis originating from prothylakoids, whereas enzymes for carotenoid and chlorophyll synthesis are localized on the outer membrane of proplastids. Pigments synthesized are bound by light-harvesting chlorophyll-binding (LHCB) proteins and subsequently transported to developing thylakoids (Liu *et al.*, 2013; Hobe *et al.*, 2000). The TOC/TIC (transposon of outer/inner membrane) complex facilitates the import of proteins from the cytosol into proplastids, with light activating these complexes to enhance specificity for photosynthetic proteins (Andrès *et al.*, 2010). Additionally, the regulation of chloroplast division involves a complex interplay between nuclear and plastid genomes. Early in chloroplast development, its division occurs via binary fission, driven by a protein ring encoded by the *FtsZ1* and *FtsZ2* genes. Nuclear-encoded ribosomal proteins are expressed to establish the chloroplast's protein synthesis machinery. As the chloroplast matures, retrograde signaling from the chloroplast to the nucleus regulates the expression of photosynthetic genes. This signaling ensures that the chloroplast's development is coordinated with the overall cellular environment and metabolic needs (Stokes *et al.*, 2000).

While MAPK cascades are recognized for their roles in plant stress responses and immunity, their specific functions in chloroplast development are poorly understood. MKKK22 interacts with downstream MKK4, playing a role in this signaling pathway. In *Arabidopsis*, MAPKs MPK3 and MPK6 are involved in retrograde signaling during chloroplast biogenesis, where they are activated by upstream MAPKKs MKK4 and MKK5 to phosphorylate ABI4, a transcription factor that represses the expression of photosynthetic genes, including those in the LHCB gene family as illustrated in Figure 4.2 (Guo *et al.*, 2016). According to Guo *et al.*, (2016), the MKK4/5–MPK3/6 module also binds to 14-3-3 ω , a Ca²⁺-dependent scaffolding protein that facilitates the transport of MPK3/6 to the nucleus to activate ABI4. This interaction is regulated by CAS (Calcium Sensor Protein) CAS-mediated Ca²⁺ signaling, which ensures that this process occurs only when sufficient Ca²⁺ levels are present in the cytosol. Under photo stimulation, calcium released from chloroplasts increases cytosolic Ca²⁺ levels, which enhances the efficiency of the MAPK cascade and leads to the phosphorylation of ABI4, ultimately repressing LHCB gene expression (Zhang *et al.*, 2018; Nomura and Shiina, 2014). Additionally, it is known that at least one MAPKKK is essential for chloroplast development; for instance, the absence of OsCSL1, which encodes

MAPKKK12 in rice, leads to seedling-lethal phenotypes and chloroplast-related defects, such as yellowing leaves and death at the trefoil stage, though these phenotypes can be rescued through functional complementation (Liang *et al.*, 2022).

Based on preliminary findings of an albino lethal chloroplast biogenesis-related phenotype in *mkp2 dsptp1* double mutants, our research group aimed to understand the functions of MKP2 and DsPTP1 in plant development, as well as its potential MAPK targets. Therefore, the study's primary objectives are the following: to gain insight into the function of two MKPs, MKP2 and DsPTP1, and their involvement in plant development, and, to identify potential MAPK substrates associated with each of the two phosphatases.

4.2 Materials and Methods

4.2.1 Plant materials and plant growth conditions

All the Arabidopsis lines used for this study are from the Columbia-0 (Col-0) ecotype. Crossing the mutants produced the *mkp2/+ dsptp1* and *mkp2 dsptp1/+* higher-order mutant seeds, which were propagated in heterozygosity due to the seedling-lethal impact of the homozygous double mutant. WT and *mkp2/+ dsptp1* and *mkp2 dsptp1/+* seeds were used for developing transgenic plants in the WT and double-mutant backgrounds, respectively.

To sterilize Arabidopsis seeds, they were first placed into microcentrifuge tubes in a sterilization solution (5% bleach, 0.1% Triton X-100, ddH₂O) and shaken for 9-10 minutes. The seeds were then rinsed five times with sterile ddH₂O to remove any residual bleach. Sowing and transplanting were performed as described in Chapter 2.

4.2.2 Plasmid construction

Our research group utilized the Gateway cloning system (Invitrogen) to generate the plasmids used in this study. A detailed description of the plasmids can be found in Table 1.

Table 4.1: List of Plasmids used

Description	Insert	Vector	Bac ^R	Plant ^R
<i>MKP2pro::MKP2</i>	<i>proMKP2</i> + <i>MKP2</i> cDNA (no stop)	pR4 501	Spec	Hyg
<i>DsPTP1pro::DsPTP1</i>	<i>proDsPTP1</i> + <i>DsPTP1</i> cDNA (no stop)	pR4 501	Spec	Hyg
<i>pro35S::GFP</i>	-	pGWB5	Kan/Hyg	Kan/Hyg
<i>pro35S::MKP2-GFP</i>	<i>MKP2</i> cDNA (no stop)	pGWB5	Kan/Hyg	Kan/Hyg
<i>pro35S::DsPTP1-GFP</i>	<i>DsPTP1</i> cDNA (no stop)	pGWB5	Kan/Hyg	Kan/Hyg
<i>pro35S::DsPTP1-4xMyc</i>	<i>DsPTP1</i> cDNA (no stop)	pGWB17	Kan/Hyg	Kan/Hyg
<i>pBaTL-nYFP</i> (without ccdB)	-	pBaTL-nYFP	Spec	Basta
<i>MKP2-nYFP</i>	<i>MKP2</i> cDNA (no stop)	pBaTL-nYFP	Spec	Basta
<i>CIMKP2-nYFP</i>	<i>CIMKP2</i> cDNA (no stop)	pBaTL-nYFP	Spec	Basta

<i>DsPTP1-nYFP</i>	<i>DsPTP1</i> cDNA (no stop)	pBaTL-nYFP	Spec	Basta
<i>CID_sPTP1-nYFP</i>	<i>CID_sPTP1</i> cDNA (no stop)	pBaTL-nYFP	Spec	Basta
<i>pBaTL-cYFP</i> (without ccdB)	-	pBaTL-cYFP	Spec	Basta
<i>DsPTP1-cYFP</i>	<i>DsPTP1</i> cDNA (no stop)	pBaTL-cYFP	Spec	Basta
<i>MPK3-cYFP</i>	<i>MPK3</i> cDNA (no stop)	pBaTL-cYFP	Spec	Basta
<i>MPK4-cYFP</i>	<i>MPK4</i> cDNA (no stop)	pBaTL-cYFP	Spec	Basta
<i>MPK6-cYFP</i>	<i>MPK6</i> cDNA (no stop)	pBaTL-cYFP	Spec	Basta
<i>MPK8-cYFP</i>	<i>MPK8</i> cDNA (no stop)	pBaTL-cYFP	Spec	Basta
<i>MPK15-cYFP</i>	<i>MPK15</i> cDNA (no stop)	pBaTL-cYFP	Spec	Basta

4.2.3 Agrobacterium-mediated transformation

Agrobacterium (strain GV3101) was transformed with required clones and floral dipping was performed as in Chapter 2.

4.2.4 DNA extraction and PCR genotyping

For DNA extraction, the protocol of Edward et. al. (1991) was followed, and genotyping was performed using primers listed in Table 2. For the detailed protocol, refer to Chapter 2.

Table 4.2: List of Primers used to detect insertional mutation

Gene Names	Primer Names	DNA Sequence (from 5' to 3')
DsPTP1	dsptp1-1 (SALK092811).f	TCCCTTCCCTTATTGAACAGG
	dsptp1-1 (SALK092811).rc	AAACAATGACAGCCCATGAAC
	DsPTP1 827f	GTGTTCTTGTTTCATTGCTTTGTTGG
MKP2	mkp2-2 (SALK045800) LP	TGTCTTAACCGTTGCTGTGG
	mkp2-2 (SALK045800) RP	CTGGTTTGGGTATGGGATTG
MPK8	mpk8-1 (SALK139288)f	GTGTTGTTGAGAAGACCAGCC
	mpk8-1(SALK139288).rc	CTTCAAGATGAGCAAATTGCC
MPK15	mpk15-2 (SALK061149)f	GGCTTCCAACCTTCAGGTAAGC
	mpk15-2 (SALK061149).rc	TCCAGCATCCAAGAATGAAAC
MPK3	mpk3-1 (SALK151594)f	CTTCTGTTGAACGCGAATTGCG

	mpk3-1 (SALK151594).rc	TCCGTTGATGCAAGTTGAGCC
MPK4	mpk4 (SALK056245)f	TTGCTCTGAATACACAGCAGC
	mpk4 (SALK056245).rc	GTCTTAGAGATCAGCGGGGAC
MPK6	mpk6-2 (SALK073907)f	GATCTTTTCCATCTGCGTCAAG
	mpk6-2 (SALK073907)_v2.rc	CACTGTCGGGAACTTATCAGTGA
GFP	GFP.rc (GW)	TGCAGATGAACTTCAGGGTCAGCT
T-DNA	LBa1	TGGTTCACGTAGTGGGCCATCG
	LBb1.3	ATTTTGCCGATTTTCGGAAC

4.2.5 Microscopy

For confocal microscopy, C2-TERF was used as described in Chapter 2.

Transgenic and wild-type *Arabidopsis* plants that were 3-4 weeks old were examined under a stereo microscope for the seed segregation analysis. Using a scalpel, the siliques were first cut from the plant and then cut along their length. The pedicel is supported by fine forceps (Dumont-Inox #4) while the silique is being sliced open. Using incidental illumination and a Leica stereo microscope with a camera attachment, the open siliques were observed at a total magnification of 20X. The scale was determined using a ruler.

For Transmission Electron Microscopy (TEM), leaves of each sample were cut into small pieces (1.5 mm X 2 mm) and fixed in 2.5% (w/v) glutaraldehyde in 0.1 M sodium cacodylate buffer (pH 7.4) for a minimum of 24 h at 4°C. Afterwards, the samples were rinsed three times for 10 min each with washing buffer at RT. Samples were then postfixed in 1% (w/v) osmium tetroxide with 1.5% (w/v) potassium ferrocyanide in sodium cacodylate buffer for 2 h at 4°C. After 2 h samples were rinsed in washing buffer at RT for three times (15 min each) and stained with 1% (w/v) tannic acid for 1 h at 4°C. After 1 h of incubation at 4°C, the samples were rinsed in water three times (10 min each). Following the washing, samples were dehydrated in a graded acetone series (30%, 50%, 70%, 80%, 90%, and 100%) for 20 min at each step at RT. The 100% acetone rinse was repeated two more times for 20 min each. The samples were then gradually infiltrated with increasing concentrations of Epon 812 resin (50%, 66%, 75%, and 100%) mixed with acetone for a minimum of 8 h at each step. A 25-p.s.i. vacuum is applied, when the samples were in 100% Epon 812 resin. Finally, samples were embedded in pure, fresh Epon 812 resin and polymerized at 60°C for 48 h. After polymerization,

the 100-nm ultrathin sections were obtained and stained with 4% (w/v) uranyl acetate for 8 min and Reynolds lead citrate for 5 min. For imaging, individual sections were viewed under TEM-microscope. The imaging was performed in collaboration with Johanne Ouellette at McGill University and Dr. Nooshin Movahed at Concordia University.

4.2.6 Photosynthetic pigment quantification assay

Using pestles and liquid nitrogen, 100 milligrams of 5dpg seedlings were ground on ice. The powdered tissues were suspended in 400 μ L of 80% (v/v) acetone and centrifuged for 10 minutes at 6000Xg and 4°C. The supernatant was removed, and the sample was reextracted with successive aliquots of 200 μ L 80% acetone until each pellet turned white, signifying that the chlorophyll had been completely removed from the sample. The aliquots from single samples were combined. 900 μ L 80% acetone with 100 μ L of extract was used to determine the absorbance. The spectrophotometer was blanked at 750 nm, and the absorbances of 1/10 diluted samples were measured at 663, 646, and 470 nm for each sample. For every batch of seedlings, three biological replicates were obtained. The amounts of carotenoid pigments, chlorophyll a, and chlorophyll b were then measured using the Lichtenthaler & Wellburn (1983) formula for 80% acetone.

$$C_a = 12.21 A_{663} - 2.81 A_{646}$$

$$C_b = 20.13 A_{646} - 5.03 A_{663}$$

$$C_{\text{carotenoid}} = (1000 A_{470} - 3.27 C_a - 104 C_b) / 229$$

4.2.7 Bimolecular fluorescence complementation and transient expression assays

Agrobacterium tumefaciens was transformed with binary plant gene expression plasmids, including fusion constructs with either nYFP or cYFP), and cultures of 10 mL of YEB media were cultivated for 12–16 hours at 30°C while being shaken at 200 rpm. Each culture was centrifuged for ten minutes at 2000Xg rpm. The pellets were then resuspended in an infiltration buffer (10 mM MgCl₂, 10 mM MES, 150 μ M acetosyringone (pH = 5.6) Prior to agroinfiltration, the resultant cultures were kept at room temperature for four to six hours. Using 1 mL syringes, filled with *Agrobacterium* in the infiltration buffer, three leaves on the abaxial (lower) sides of each tobacco plant were infiltrated. Depending on the interactions to be tested, one or two distinct *Agrobacterium* cultures were mixed before infiltrated into the leaves. The leaves were infiltrated until the solution infiltration was visible on at least 80% of each leaf. To prevent aggregation of the proteins expressed from the plasmids due to

overexpression, the plants were maintained at growth chamber conditions for 48–60 hours following agroinfiltration. Imaging was then carried out with a Nikon C2/TIRF confocal microscope to visualize the interactions. The microscope was configured to detect the yellow fluorescent protein (YFP) signals at 530 nm.

4.3 Results

4.3.1 Identification of phosphatases that control chloroplast development and biogenesis

Among 23 reported dual specificity MKPs in Arabidopsis, only five are functional. When the phylogenetic analysis of five MKPs with a unique AY [L/I]M motif is done, MKP2 and DsPTP1 appear as the two phosphatases with highest amino acid sequence identity (64%) and sequence similarity (81%) (Sun 2022). Individual T-DNA insertion mutants of *mkp2-2* (SALK_045800) and *dsptp1-1* (SALK_092811) have no effect on the phenotype when compared with the WT at 2 weeks after germination (Tamnanloo *et al.*, 2018). Hence, to investigate the possible functional redundancy of these two MKPs, students from our lab previously generated *mkp2 dsptp1* double mutants by crossing *mkp2-2* (SALK_045800) and *dsptp1-1* (SALK_092811) mutants. Remarkably, the *mkp2 dsptp1* double mutants displayed a pronounced albino phenotype, characterized by tiny-yellowish seedlings, which contrast sharply with the phenotypes observed in the single mutants (Figure 4.3 A). The homozygous *mkp2 dsptp1* plants showed a limited viability, surviving approximately 10 days post-germination showing importance of MKPs in early plant development.

To investigate if the loss of function mutation, i.e., albino phenotype, in *mkp2 dsptp1* seedlings is attributable to the loss-of-function mutations in *MKP2* and *DsPTP1*, I created transgenic Arabidopsis plants that expressed the full-length coding sequences of *DsPTP1* in the *mkp2 dsptp1* double mutant background, utilizing its native promoter for expression. Due to seedling lethality of double mutant *mkp2 dsptp1*, the construct *DsPTP1pro::DsPTP1* was introduced into *mkp2 dsptp1/+* plants. The line, homozygous for *mkp2* and heterozygous for *dsptp1*, *mkp2 dsptp1/+* did not show a phenotype deviating from WT (Figure 4.3 B) but its offspring show a 3:1 segregation of normal to albino with seedling lethality. Subsequently, the offsprings were then examined to check if the transgene introduced rescues the albino phenotype of *mkp2 dsptp1*. The offspring of plants homozygous for the *DsPTP1pro::DsPTP1* transgene in the *mkp2 dsptp1/+* mutant background all showed WT phenotype. This indicated that the expected quarter of these transgenic seedlings segregating as *mkp2 dsptp1* double mutants were rescued by the *DsPTP1* transgene. Both the genotype of the double mutants and the transgene *DsPTP1pro::DsPTP1* were confirmed by PCR. In conclusion, the complementation analysis suggests that the loss of function of *MKP2* and *DsPTP1* is directly responsible for the albino seedling phenotype observed in the *mkp2 dsptp1* double mutants.

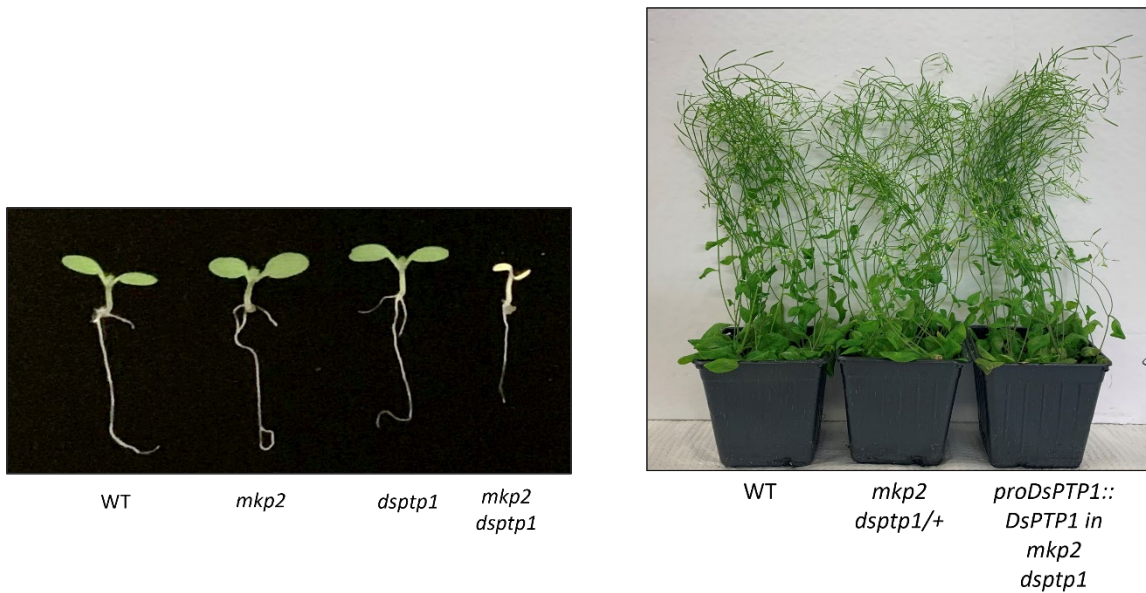


Figure 4.3: Identification and complementation of the *mkp2 dsptp1* mutant. (A) Phenotypes of 5-day-old seedlings of wild-type WT, *mkp2*, *dsptp1*, and *mkp2 dsptp1* mutant. (B) Phenotypes of 34-day-old seedlings of WT, *mkp2 dsptp1/+*, and transgenic *mkp2 dsptp1* expressing a full-length clone of *DsPTP1* driven by its native promoter (*proDsPTP1::DsPTP1*).

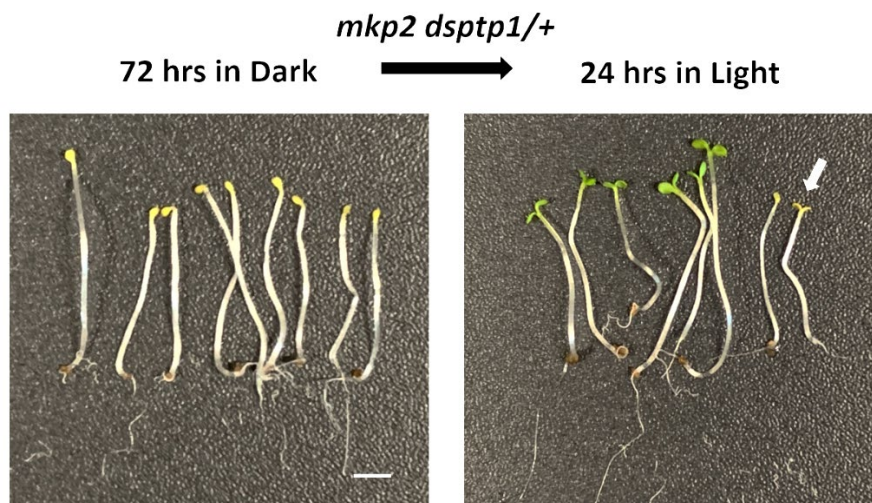


Figure 4.4: Developmental characteristics of the *mkp2 dsptp1/+* mutant. Seventy-two h dark-grown progeny of a *mkp2 dsptp1/+* heterozygote subjected to 24 h of 50 $\mu\text{mol/s}$ white light to trigger photomorphogenesis. White arrowheads indicate a *mkp2 dsptp1* homozygous mutant after subjection to light. The expected segregation of $1/4$ being homozygous for both mutations. The scale bars indicate a length of one millimeter.

4.3.2 Photomorphogenic response in *mkp2 dsptp1* mutants and silique seed segregation assay

To determine if the process of photomorphogenesis is impaired in mutant seedlings, the photomorphogenic response was observed. For this, in a series of experiments, seeds from the *mkp2 dsptp1/+* mutants were subjected to a period of darkness for 72 hours, followed by a subsequent exposure to light for 24 hours. All seedlings grown in dark were etiolated exhibiting elongated hypocotyls and chlorotic cotyledons as a response to the absence of light and heterozygous and homozygous seedlings remained indistinguishable (Figure 4.4). However, subsequent exposure to light for 24 hours caused significant changes in phenotype of all seedlings. Irrespective of the type of seedlings, all had opened cotyledons showing positive response to light exposure. Moreover, all seedlings except *mkp2 dsptp1* had enlarged cotyledonary leaves accompanied by reversal of chlorosis. The *mkp2 dsptp1* seedlings failed to expand cotyledonary leaves and remained yellowish and small (Figure 4.4). These results suggest that chloroplast biogenesis in *mkp2 dsptp1* double mutants is impaired and is independent of photomorphogenesis.

To further examine the albinism found in *mkp2 dsptp1* mutants at the seedling stage and to evaluate its influence at seed development stage, I performed a silique seed segregation assay. For this, *mkp2 dsptp1/+* plants as well as complementation lines carrying *proDsPTP1::DsPTP1* with double mutant background were grown for 6 weeks post germination to observe the seed development in maturing siliques. The use of heterozygous double mutant assisted in revealing the genetic nature of the mutation in seeds via segregation. The resulting seeds in the *mkp2 dsptp1/+* line showed a 3:1 segregation of green to albino. The native promoter-controlled complementation lines showed all normal green seed development (due to greening of the embryo) and established that complementation occurs at the seed stage of development (Figure 4.5).

The siliques from *mkp2 dsptp1/+* mutants had both green and white seeds with a segregation ratio of 3:1 indicating the formation of chloroplasts is already inhibited in homozygous embryos. Observed frequencies were 177 green seeds and 58 albino seeds, with expected frequencies calculated as 176.25 and 58.75, respectively. A chi-square test was performed to assess goodness-of-fit. A 3:1 segregation ratio predicts expected numbers of 176.25 green seeds and 58.75 white seeds. The chi-square value, χ^2 (df=1, N=235) = 0.004, $p \gg 0.5$, indicating no significant deviation from the expected Mendelian ratio, 3:1. (Figure 4.5). Interestingly, the seed development and maturation of these mutants does progress to produce

seeds that are able to germinate. The siliques from WT as well as complementation lines carrying *proDsPTP1::DsPTP1* with double mutant background had siliques with a homogenous distribution of green seeds. This confirmed that the albino seeds are indeed the result of the homozygous double mutant *mkp2 dsptp1*. The fact that the albino seeds developed and that their ability to germinate remained uncompromised indicated that double mutation in these phosphatases may interfere with chloroplast development but not hinder proper embryo development and that seedling lethality is caused by the inability to perform photosynthesis.

4.3.3 Effects of *mkp2 dsptp1* double mutant on chloroplast production, chloroplast volume and photosynthetic pigments in the guard cells

Albinism in plants is often a direct result of compromised chloroplast development and the production of associated photosynthetic pigments. To investigate this, chloroplast assays quantifying the number of chloroplasts and the volume of chloroplasts per 100 stomata were measured by confocal microscopy using Z-stack setting and autofluorescence of chloroplast in guard cells of 5dpg seedlings (Figure 4.6A). Guard cells were used since they are rich in chloroplasts. Unlike other epidermal cells, which often lack chloroplasts, guard cells consistently contain 12-16 functional chloroplasts, making them ideal for chloroplast-related assays.

Confocal images presented in (Figure 4.6A) reveal that the average number of chloroplasts in guard cells of the WT and *proDsPTP1::DsPTP1* lines in the *mkp2 dsptp1* background was approximately 8.01 ± 0.21 . This number significantly decreased to 5.15 ± 0.22 in the *mkp2 dsptp1* lines. On the other hand, the average volume of chloroplasts in double mutant lines was measured at $62 \pm 0.54 \mu\text{m}^3$. In contrast, the average volume observed in WT and complementation lines was approximately two-fold higher, at $125 \pm 0.05 \mu\text{m}^3$.

The levels of total chlorophyll (chl a+b) and carotenoids were quantified to assess overall chloroplast development. For this analysis, in addition to double-mutant and complementation lines, overexpression lines of *MKP2* and *DsPTP1* driven by the *CaMV 35S* promoter were also analyzed. The content of photosynthetic pigments was estimated using the equations provided by Lichtenthaler & Wellburn (1983) (Figure 4.7 A-B).

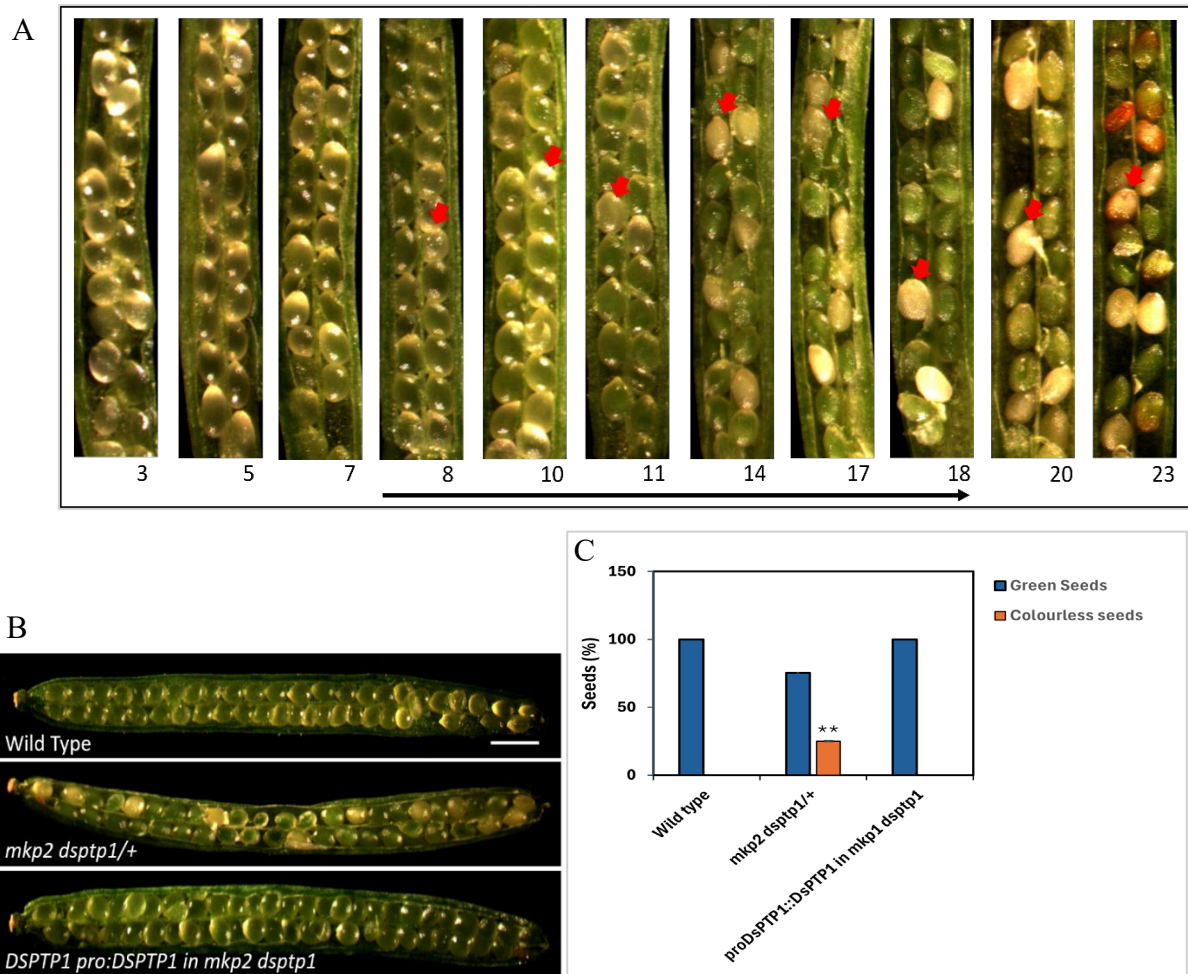


Figure 4.5: Embryo greening and seed silique segregation analysis in 6-Week-Old Arabidopsis. (A) Opened siliques of *mkp2 dsptp1/+* plant of 4 weeks showing the embryo greening. The given number is the position rank of the silique from top to bottom (left to right) of the inflorescence presenting the segregation of homozygous and heterozygous seeds. Red arrows point at albino seeds. Segregation in the younger siliques is not done since embryos are too small for seed to appear green at these stages.

(B) Seeds within the silique of a wild type (WT), *mkp2 dsptp1/+* heterozygous plant and complementation plants expressing the *proDsPTP1::DsPTP1* transgene in a double mutant background. The scale bars indicate a length of one millimeter. Segregation ratios of albinism were recorded in the siliques of each plant genotype (n=6). (C) Segregation ratio of albinism in the siliques of each plant genotype (n=6). One-way ANOVAs were followed by Tukey's HSD tests to evaluate the differences in green and albino seeds among plant lines. Significant differences at $p < 0.001$, are indicated with ** asterisk.

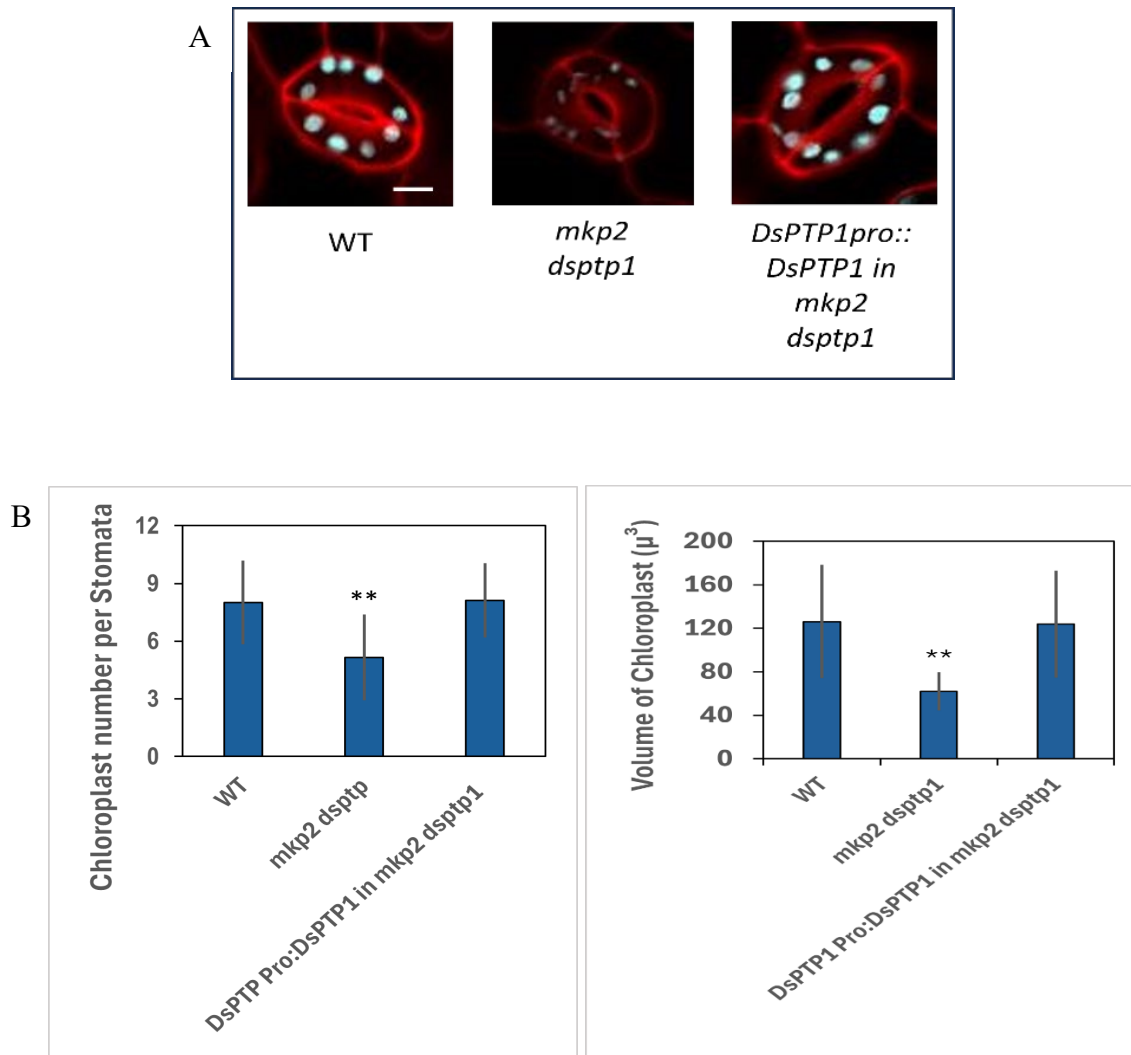


Figure 4.6 Effect of knockout *mkp2 dsptp1* on chloroplast production and chloroplast volume in stomata guard cells: (A) Representative images of seedlings 5 dpg stomata guard cells (scale bar, 10 μm). Chloroplasts are visualized by chlorophyll autofluorescence (cyan) and cell walls by propidium iodide (red). (B) The data represent number of chloroplasts per stomata and volume of chloroplasts. Data are means \pm SD of experiment with single replicates with 100 stomata. Statistical analysis was carried out by ANOVA, and Dunnett's Multiple Comparison test was performed to compare total number and volume of chloroplast in 100 stomata for between *mkp2 dsptp1* and complementation line *proDsPTP1::DsPTP1* in *mkp2 dsptp1* with WT. ** $p < 0.001$ versus WT.

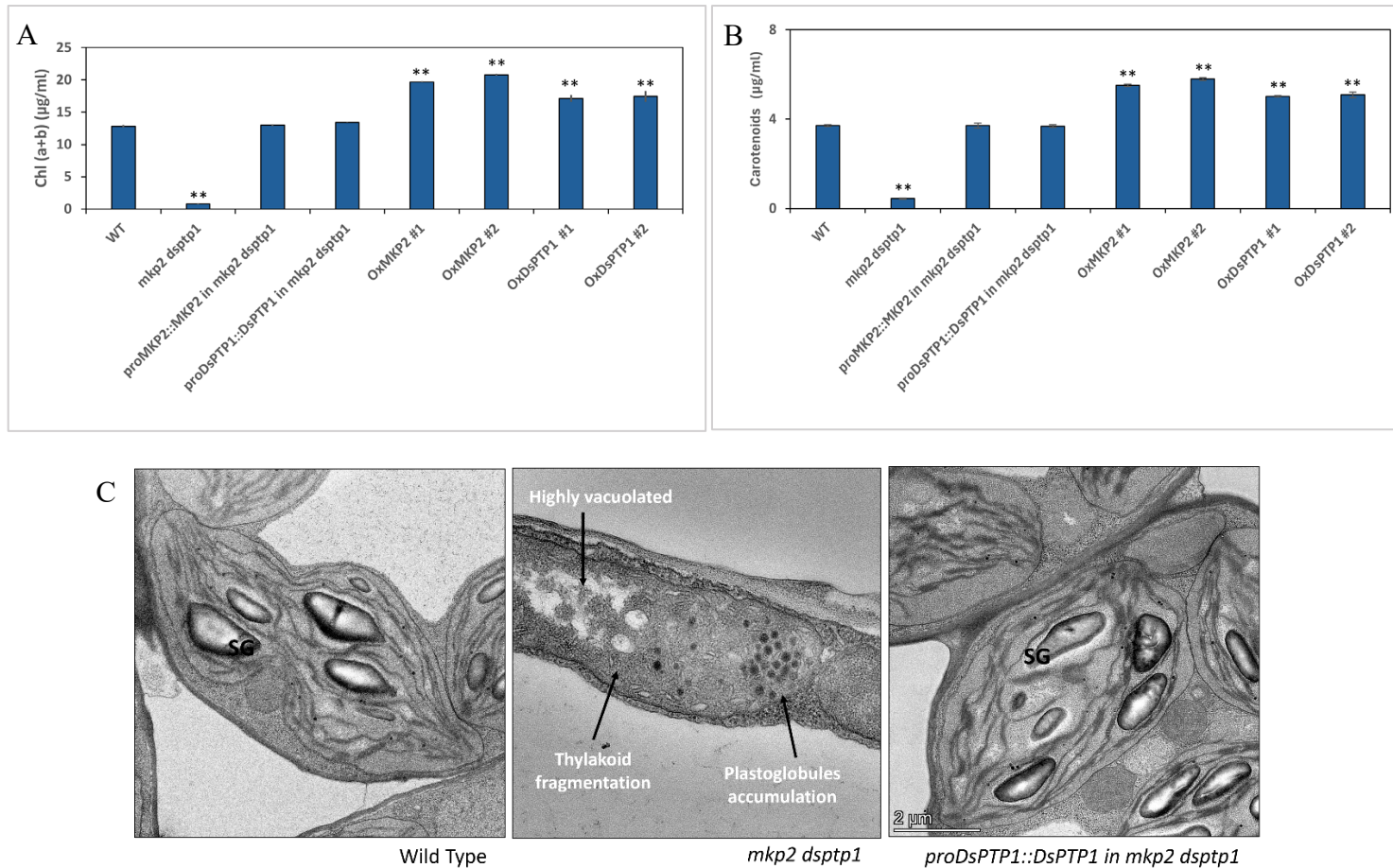


Figure 4.7: Photosynthetic pigment quantification assay and chloroplast ultrastructure: Total chlorophyll (A) and carotenoid (B) pigment concentrations of 5 dpg seedlings measured in WT, *mkp2 dsptp1*, complementation lines with both *proMKP2::MKP2* and *proDsPTP1::DsPTP1 in mkp2 dsptp1*, and two independent overexpression lines of *35S::MKP2* and *35S::DsPTP1*. Data are means \pm standard error of an experiment with three biological replicates. Following one-way ANOVA, Dunnett's Multiple Comparison test was performed comparing means of pigment concentration to that of WT. ** $p < 0.001$ versus WT. (C) Representative TEM images showing ultrastructure of chloroplast (Scale bar 2 μ m) from cotyledons of 5 dpg WT, *mkp2 dsptp1* and *proDsPTP1::DsPTP1 in mkp2 dsptp1* seedlings. SG: Starch Granule.

The chlorophyll quantification assay further confirmed the impaired chloroplast development in double mutant lines. The levels of total chlorophyll and carotenoids were between one eighth and one sixteenth the level in the WT. The levels of these photosynthetic pigments were restored to normal WT levels in either complementation line. The pigment content was reported to be increased in the Ox lines with a 1.3-1.6-fold increase in comparison to WT. To summarize, *mkp2 dsptp1* lines exhibits albinism, indicating that *MKP2* and *DsPTP1* are involved in normal chloroplast development and chlorophyll content.

4.3.4 Analysis of chloroplast ultrastructure

To examine how loss of function phosphatase in *mkp2 dsptp1* double mutants affected the development of chloroplasts, the ultrastructure of chloroplasts of 5 days old seedling from WT, *mkp2 dsptp1* and *DsPTP1pro::DsPTP1* in *mkp2 dsptp1* was analyzed (Figure 4.7C). The TEM imaging from WT and *DsPTP1pro::DsPTP1* revealed that chloroplasts were well-developed and organized with stacked grana and no significant difference was observed in their ultrastructure. In contrast, *mkp2 dsptp1* chloroplasts were much smaller, highly vacuolated with fragmented thylakoids. In addition, increased accumulation of plastoglobuli in *mkp2 dsptp1* showed signs of chloroplast degradation. Together, the evidence suggests that *mkp2 dsptp1* loss of function results in abnormal chloroplast morphology and reduced photosynthetic pigments in *mkp2 dsptp1* plants directly impacting chloroplast biogenesis.

4.4 Downstream MAPKs regulating chloroplast development

4.4.1 Seedling phenotype and Guard Cell chloroplasts of high order mutants

After characterizing the role of *MKP2* and *DsPTP1* in chloroplast biogenesis based on *mkp2 dsptp1* albino double mutant analysis, I tried to identify which MAPKs interact and act downstream of these phosphatases. For this, a series of candidate MAPKs were screened based on existing studies and preliminary data. For interaction studies, MPK3, MPK4, MPK6, MPK8 and MPK15 were chosen based on previous preliminary interaction studies with *MKP2* by lab member, Jain Lei Sun. For epistatic analysis, we created some higher order mutants by crossing *mpk* mutants with existing *mkp2 dsptp1* mutant. In addition, to investigate physical interactions between *MKP2*, *DsPTP1* and their potential substrate MAPKs, bimolecular fluorescence complementation (BiFC) techniques were employed to determine if they have physical interactions.

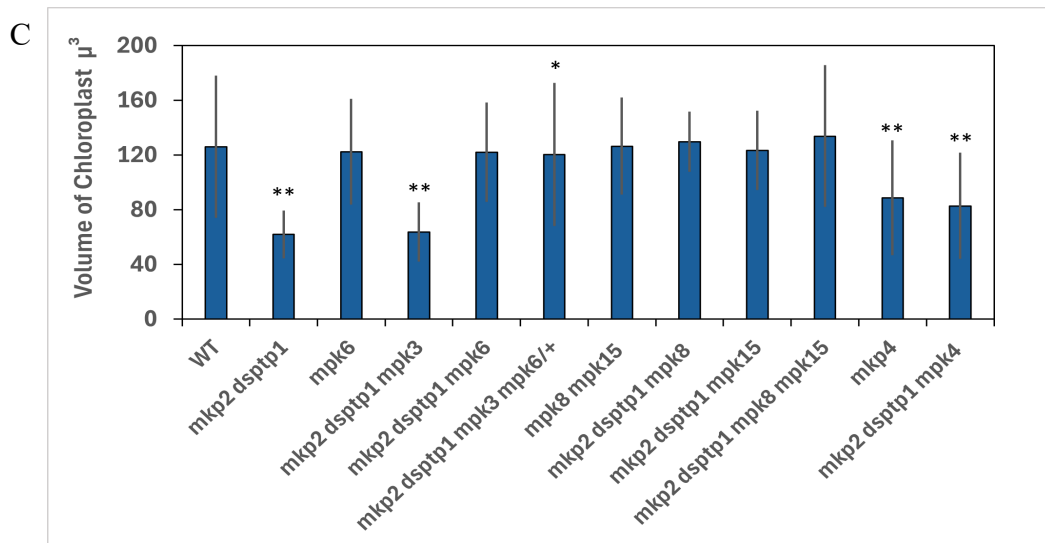
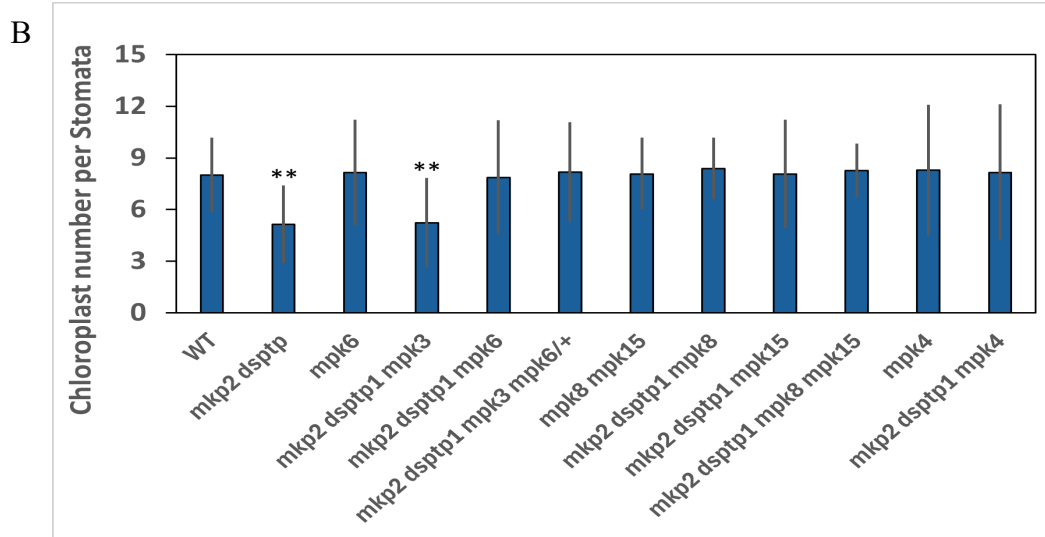
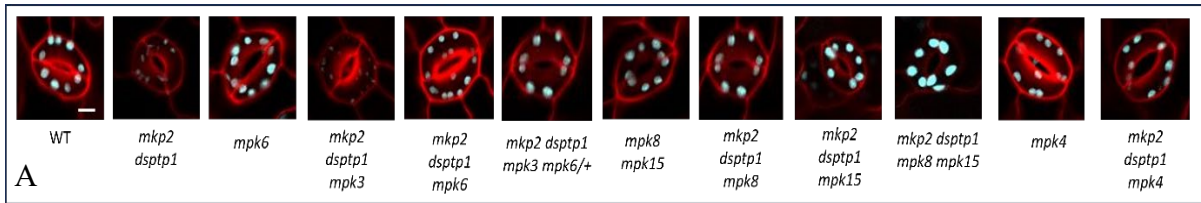


Figure 4.8: Epistatic analysis of high-order mutants using chloroplast production assay:

(A) Representative images of 5 dpg seedling stomata guard cells (scale bar, 10 μm). Chloroplasts are visualized by chlorophyll autofluorescence (cyan) and cell walls by propidium iodide (red). The data represents the number of chloroplasts per stomata (B) and volume of chloroplast (C). Data are means \pm SD of experiment with single replicates with 100 stomata. Following one-way ANOVA, Dunnett's Multiple Comparison test was performed comparing means of chloroplast per 100 stomata and chloroplast number against WT. ** $p < 0.001$, * $p < 0.05$ versus WT.

In the WT, phosphatases function to dephosphorylate and inactivate MPKs. Therefore, in the absence of a specific phosphatase, MPKs remain constitutively active, which can lead to aberrant signaling and associated albino phenotypes. However, in a higher order mutant where both the phosphatase and the corresponding upstream kinase are absent, the MPK is not activated, functionally mimicking the inactivation observed in the WT and hence, showing a green phenotype. In this analysis of the number and volume of chloroplasts in guard cells by confocal imaging (chlorophyll autofluorescence and 3-D imaging) revealed that the absence of MPK4, MPK6, MPK8 or MPK15 alone did not cause albino phenotypes. Moreover, triple mutants *mkp2 dsptp1 mpk6*; *mkp2 dsptp1 mpk8* and *mkp2 dsptp1 mpk15* showed a green phenotype revealing normal chloroplast abundance and volume in comparison with WT. This showed that mutations in each of these MAP kinases reversed the effect of the *mkp2 dsptp1* double mutation and indicated that the kinases were targets of the phosphatases. However, *mkp2 dsptp1 mpk3* mutants were albino and chlorophyll autofluorescence and 3D images of guard cells showed a similar phenotype as that of *mkp2 dsptp1* suggesting that MPK3 might not be a target of these phosphatases. The quadruple mutants, *mkp2 dsptp1 mpk3 mpk6/+* and *mkp2 dsptp1 mpk8 mpk15*, showed similar normal phenotypes as the triple mutants, *mkp2 dsptp1 mpk6*; *mkp2 dsptp1 mpk8* and *mkp2 dsptp1 mpk15* (Figure 4.8).

4.4.2 Bimolecular fluorescence complementation (BiFC) assays in transient tobacco system

To explore the possible physical interactions between MKP2 and DsPTP1 phosphatases and the candidate MAPK substrates *in vivo*, I performed bimolecular fluorescence complementation (BiFC) experiments. For this, I developed gene constructs for MKP2 and DsPTP1 fused to the N-terminus of split yellow fluorescent protein (YFP) as “bait”, along with constructs for the MAP kinases fused to the C-terminus as “prey”. The interaction between these proteins could be confirmed by the restoration of fluorescence, which occurs only when the bait and prey interact and cause the N- and C-terminal halves of the YFP to interact and reconstitute the full YFP molecule.

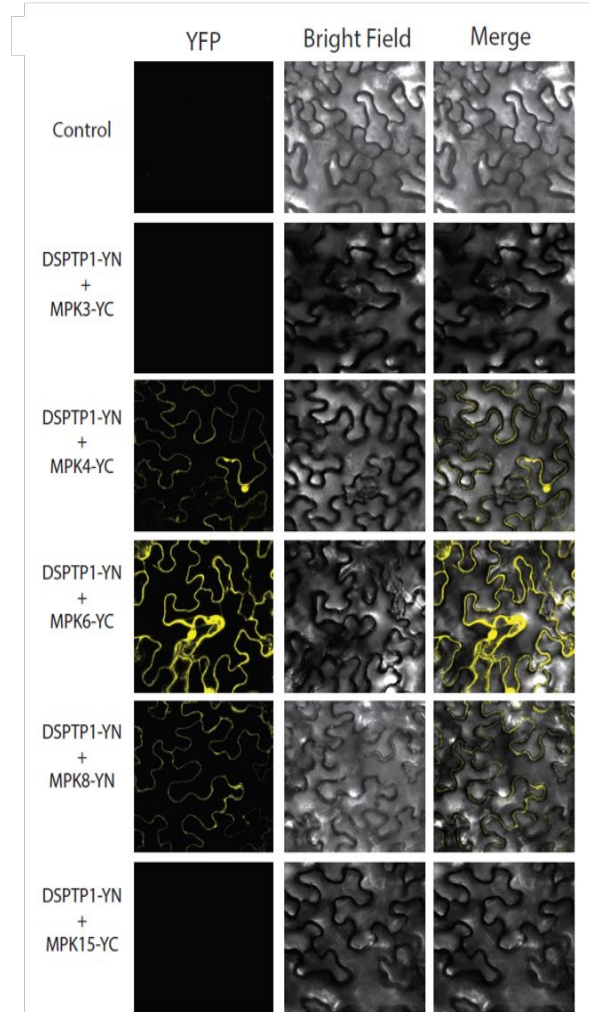
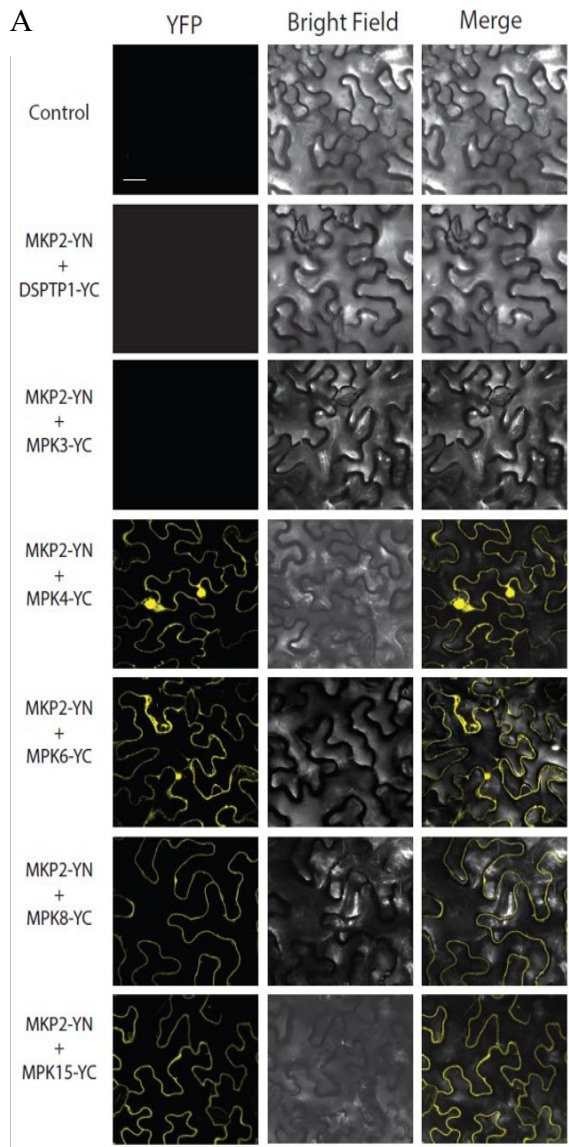
As a negative control, I employed two empty cloning vectors that express the N- or C-terminus (pBaTL-nYFP and pBaTL-cYFP). When they were transformed together, they resulted in no fluorescent signals, confirming the lack of interaction. MKP2-nYFP did not show any fluorescent signals when co-expressed with DsPTP1-cYFP indicating that two phosphatases do not interact with each other (Figure 4.9A).

When we tested MKP2-nYFP interaction with MPK6-cYFP, a strong fluorescent signal was observed. Additionally, co-expression of MPK4-cYFP, MPK8-cYFP or MPK15-cYFP with MKP2-nYFP resulted in a fluorescent signal which showed direct evidence of their *in vivo* interaction which was in accordance with epistatic analysis and chloroplast production data. In addition, the restored fluorescence signal appears strongly in both the plasma membranes and nuclei for with the co-expression of MKP2-nYFP with MPK4-cYFP or MPK6-cYFP. Conversely, the signal is only present in the plasma membranes and is weaker for the MKP2-nYFP co-expressed with MPK8-cYFP or MPK15-cYFP. Unsurprisingly, MKP2-nYFP did not show even traces of fluorescent signals upon co-expression with MPK3-cYFP further supporting the lack of interaction between these proteins that was also indicated by characterization of chloroplast number and volume in the triple mutants which showed normal deficient development (Figure 4.9A).

Furthermore, catalytically inactive (CI) variants of the phosphatases (MKP2C109S and DsPTP1C135S), created by modifying a conserved serine residue at the catalytic active site, were fused with nYFP and cYFP to create CIMKP2-nYFP and CIDsPTP1-nYFP constructs. These were used to test interactions with candidate MAPKs. By utilizing these variants, we could determine if the phosphatase activities of MKP2 and DsPTP1 are required for physical interaction with target kinases *in vivo*. The interaction studies of CIMKP2-nYFP with target MPKs candidates yielded identical results to those observed for the active forms MKP2-nYFP. Co-expression of MPK4-cYFP and MPK6-cYFP with CIMKP2-nYFP yielded strong fluorescent signals in the plasma membrane as well as nucleus and that with MPK8-cYFP and MPK15-cYFP showed the signal being restricted to plasma membrane with no interaction was observed for MPK3-cYFP (Figure 4.9 B). These findings indicate that a functional catalytic domain is not necessary for the MKP2 protein interactions with kinase substrates as the inactive version of the protein shows the same interaction affinity patterns as the active one.

The physical interaction of DsPTP1 with candidate MAPKs was also tested, and the results differed from those with MKP2. Positive interaction signals were seen in the plasma membrane and nuclei when DsPTP1-nYFP was co-expressed with MPK4-cYFP and MPK6-cYFP. For MPK8-cYFP, a weak positive signal was present on the plasma membrane, but MPK15-cYFP did not show a positive interaction signal with DsPTP1-nYFP, indicating that MPK15 is not a target of DsPTP1, unlike MKP2 (Figure 4.9 B). Similar to MKP2, DsPTP1-nYFP did not exhibit fluorescent signals with MPK3-cYFP. These *in vivo* interactions had previously been tested by yeast 2-hybrid analysis and neither MKP2 nor DsPTP1 were found

to interact with any of these kinases in the yeast 2-hybrid system (Brahim 2023 MSc thesis; Lee lab unpublished work).



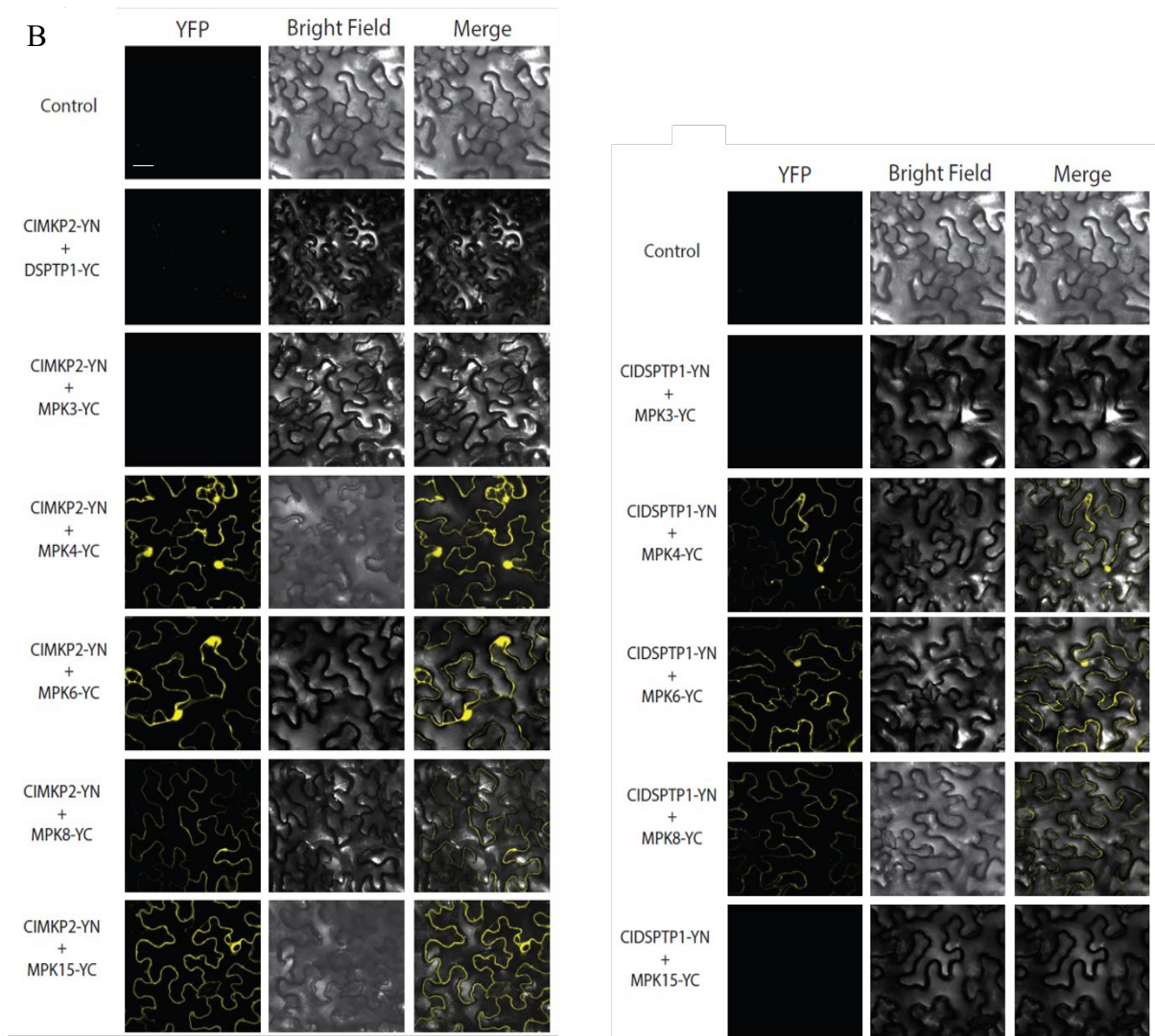


Figure 4.9: Bimolecular fluorescence complementation (BiFC) analysis to test for physical interaction between MKP2/CIMKP2, DsPTP1/CIDSPTP1 and candidate kinases. The YFP, DIC, and compound channels are shown (Scale bars = 50 μ m). Scale bar in the control YFP column is applicable to all images. (A) BiFC testing for interactions between the MKP2-nYFP bait construct and prey constructs for candidate kinase substrates. (B) CIMKP2-nYFP bait construct and kinase constructs. The PBaTL-nYFP + pBaTL-cYFP combination is used as a negative control.

4.5 Discussion

Chloroplast biogenesis is a highly regulated process that involves transformation of proplastids also known as “undifferentiated plastids” into fully functional chloroplasts. However, depending on the environmental cues and developmental signals, these can transform into other types of plastids such as etioplasts and leucoplasts. For chloroplast development, the presence of light is a key trigger that activates the expression of genes in both the nuclear and plastid genomes, including the activation of chlorophyll biosynthesis, which is essential for photosynthesis. Upon light dependent chloroplast morphogenesis, the Chloroplast Calcium sensor triggers the releases Ca^{2+} from chloroplast to cytosol. An increase in cytosolic Ca^{2+} concentration promotes the interaction between the 14-3-3 ω protein and the MAPK cascade (MKK4/5, MPK3/6), which enhances the activation of MPK3/6. Activated MPK3/6 phosphorylates ABI4, allowing it to compete with GBF (G-box-binding factor) and thereby inhibiting the transcription of LHCB (light-harvesting chlorophyll a/b binding protein) in the nucleus (Guo *et al.*, 2016). However, if MAPK is continuously activated the cascade could trigger an excessive inhibition of LHCB transcription in the nucleus subsequently disrupting chloroplast development leading to an albino phenotype. Therefore, cells balance the MAPK pathway by the activation by phosphorylation and the inactivation by dephosphorylation. For this reason, MAPKs (MPK3, MPK4, MPK6, MPK8 and MPK15) were screened as potential targets of phosphatases MKP2 and DSPTP1 to investigate whether their interactions play a regulatory role in facilitating proper chloroplast development.

Previous studies from our group suggest that mutation of *mkp2* or *dsptp1* shows no difference in chloroplast development from that of WT and that MKP2 and DSPTP1 may function redundantly as only homozygous loss of function in the double mutants causes seedling-lethal albino phenotype (Sun, 2022). To establish if the albino phenotype of double mutants is due to inhibition of photomorphogenesis or impaired chloroplast development, the photomorphogenic response of Arabidopsis seedlings was observed. Photomorphogenesis is characterized by the suppression of hypocotyl elongation, the enlargement of cotyledons, the production of photosynthetic pigments and the initiation of light-sensitive gene expression (Chory *et al.*, 1996). In this study, we found that all seedlings including *mkp2 dsptp1* double mutants had expanded cotyledons, showing a positive response to light exposure. Interestingly, only double mutant plants showed an albino phenotype and were seedling lethal. These results confirmed the redundancy of two phosphatases ensuring that if one is compromised, the other can still function to regulate essential processes.

A further embryo greening and seed segregation assay from *mkp2 dsptp1/+* parent lines indicated that albino phenotype is present in an expected Mendelian ratio (3:1; normal to albino) showing that normal chloroplast formation is prevented in double homozygous mutant embryos; however, seed development and maturation is not affected by mutation in only *MKP2* or *DSPTP2* genes. In addition, chloroplast assay and photosynthetic pigments measurements revealed the involvement of phosphatases in chloroplast biogenesis. Unlike single mutants *mkp2* and *dsptp1*, in double mutants, chlorophyll accumulation was severely reduced. However, the incorporation of *DsPTP1pro::DsPTP1* in double mutant lines recovers the albino phenotype showing that the double mutant phenotype was indeed caused by *DSPTP1* and *MKP2* inactivated. In addition, carotenoids were also lowest in *mkp2 dsptp1* mutants. Carotenoids and chlorophyll are known to share common precursors with interconnected biosynthetic pathways. The presence of chlorophyll can influence carotenoid synthesis and vice versa. It is known that carotenoids protect chloroplasts from excessive light maintaining membrane integrity from free radicals generated in stress (Quian-Ulloa and Stange, 2021). Hence, the albino phenotype results from collective impaired synthesis of these pigments necessary for chloroplast biogenesis.

The chloroplast assay also revealed the statistically significant decrease in the number of chloroplasts in the *mkp2 dsptp1* double mutant compared to the WT indicating either degradation of existing chloroplasts or inhibition of proplastids to chloroplasts transformations. The mutant's albinism is probably caused by a complex syndrome that inhibits the development of chloroplasts while leaving the plastids intact (Grübler *et al.*, 2017). Retrograde plastidial signaling involves signals that act during early chloroplast biogenesis i.e. in seed development and germination (Liebers *et al.*, 2022). Complementation lines expressing *DsPTP1* in the double mutant background had not only similar chloroplasts number but also levels of photosynthetic pigments like the WT, further indicating that the developmental defect in chloroplasts originates from *mkp2 dsptp1* double mutants. A significant difference in ultrastructure of *mkp2 dsptp1* chloroplasts compared to WT and complementary lines further provided evidence of degradation of existing chloroplasts. The *mkp2 dsptp1* chloroplasts were significantly smaller with signs of degradation such as lack of intact lamellar structure and plastoglobules accumulation.

Guo *et al.* (2016) demonstrated positive regulation of *ABI4* by MAPK cascade ultimately suppressing the *LHCB* expression during retrograde signaling. Similarly, *ABI4* is also known to bind promoters of chlorophyll synthesis genes in the nucleus (Yuan *et al.*, 2017).

Mutation in MKP2 and DsPTP1 double mutants may lead to increased activity of MPK6, MPK8 and MPK15 which potentially cause the complete repression of LHCB and other chlorophyll synthesis genes due to the action of over-phosphorylated ABI4 protein. Within Photosystem II, LHCB acts as an apoprotein that together with chlorophylls capture light energy (Ruban 2012). This energy is then used to trigger the electron transport chain on the thylakoid membrane during photosynthesis. The absence of the chlorophyll-LHCB complex leads to malfunctioning thylakoids and impaired photosynthesis in plant cells (Vayghan *et al.*, 2022). Without light-dependent photosynthesis, dark reactions cannot produce sugars due to a shortage of ATP and NADPH, resulting in the exhaustion and degradation of chloroplasts.

The albino phenotype of Arabidopsis can arise from various mutations affecting chloroplast development and function. Disruption of the gene coding for phytoene desaturase (*PDS3*) leads to loss of phytoene destruction, an important step in carotenoid biosynthesis resulting in albino and dwarf phenotypes in Arabidopsis (Qin *et al.*, 2007). The albino phenotype observed in the *mkp2 dsptp1* double mutant may stem from significant oxidation by free radicals or from a disruption in the transcriptional pathway necessary for *PDS3* expression. However, further experiments are needed to confirm this hypothesis. It would be interesting to measure the expression of *PDS3* in *mkp2 dsptp1* plants to see if the expression of *PDS3* is compromised in these double mutants then subsequent members of this signaling pathway involving *PDS3*. These phosphatases should be screened to further uncover the pathway regulating chloroplast biogenesis.

In my study, protein-protein interaction analysis via BiFC showed that DSPTP1 interacts with MPK3 but not with MPK6. Lee *et al.* (2007) reported that DsPTP1 does not dephosphorylate MPK3 and MPK6. In contrast, a recent report from Altmann *et al.* (2020) showed a DSPTP1 interaction with MPK3 using yeast two hybrid prey pooling approaches. However, more biochemical studies such as pull-down assay and co-immunoprecipitation assay are required to support these findings.

I also tested potential interactions between DsPTP1 and other candidate MAPKs. BiFC data showed strong physical interaction between DsPTP1 and MPK4 further confirming the previous findings of Gupta *et al.* (1998). DsPTP1 also showed positive results for interaction with MPK6. In a recent study Kim *et al.* (2021) provided direct evidence of MPK6 inactivation by dephosphorylation by DsPTP1 both *in vivo* and *in vitro*. These authors also concluded that DsPTP1 directed dephosphorylation of MPK6 was strongly inhibited by calmodulin. In

addition, the observed inhibition was caused by the association of CaM with the calmodulin binding domain II (CaMBDII) found in DsPTP1. DsPTP1 dephosphorylated the phospho-Tyr residue in the TEY motif of MPK6.

The LHCB1 gene exhibits higher expression levels in *mpk4* plants compared to WT hybrid aspen (*Populus tremula* × *tremuloides*). This increased expression is essential for efficient light energy harvesting and for balancing the excitation of PSII and PSI (Witoń *et al.*, 2021). Consequently, MPK4 serves as a key kinase in regulating developmental and acclimation responses. Witoń *et al.* (2016; 2021) also reported increased levels of chlorophyll and carotenoids, enhanced energy dissipation mechanisms, and elevated expression of heat shock transcription factors and proteins, all of which contribute to protection against oxidative stress. These points collectively suggest that MPK4 is crucial in moderating the distribution of photosynthetic energy, balancing the priorities of growth with acclimation and defense responses. Recently, Rodríguez-Alcocer *et al.* (2023) identified that a loss-of-function mutation in the chloroplast-localized AtHsp90.5 protein, a member of the heat shock protein 90 (HSP90) family, can lead to albinism in Arabidopsis. Witoń *et al.* 2021 reported the induction of HSP90 expression by MPK4, allowing us to speculate that MPK4 activity might be compromised in the *mkp2 dsptp1* double mutant potentially resulting in the albino phenotype due to compromised expression of MPK4 controlled AtHsp90.5. However, experiments measuring AtHsp90.5 expression in these phosphatase double mutants are required to validate this hypothesis.

Our protein-protein interaction analysis also showed positive interactions between DsPTP1 and MPK8 but not with MPK15. MPK8 and MPK15 are both known to act in response to stress. MPK8 is involved in regulating ROS accumulation, but no direct evidence of its direct involvement in chloroplast development has been reported so far. In this study the triple mutant *mkp2 dsptp1 mpk8* and quadruple mutant *mkp2 dsptp1 mpk8 mpk15* were epistatic to the *mkp2 dsptp1* double mutant and had normal chloroplasts showing the potential role of these kinases in chloroplast development. Besides interaction studies of phosphatases with their potential MAP kinase targets, previous research from our research lab found that plants that express catalytically inactive variants of MKP2 and DsPTP1 in the *mkp2 dsptp1* background have phenotypes identical to that of *mkp2 dsptp1*. Current findings reveal that a phosphatase's ability to bind to MAP kinases is independent of their catalytic activity and is facilitated by the

non-catalytic domain. Therefore, it is likely that the catalytically inactive forms of the protein could out compete the endogenous active forms of the proteins.

The potential dual presence of MKP2 and DsPTP1 could offer a more robust regulatory mechanism within MAPK signaling cascades. For instance, if both phosphatases operate simultaneously under stress conditions, they might provide a buffering effect against fluctuations in MAPK activity, thereby ensuring that chloroplast biogenesis remains efficient even when external conditions change. Subsequent studies aimed at identifying the targets of these dual phosphatases will provide deeper insights into the mechanisms of chloroplast development. For example, analyzing the expression of genes associated with albinism, such as phytoene desaturase and AtHSP90.5, in phosphatase double mutants could serve as an initial step in identifying the ultimate targets of these phosphatases.

5. Conclusions

With the increasing global population, escalating water scarcity and climate change, the agriculture sector faces significant challenges in enhancing photosynthetic productivity while mitigating yield losses caused by drought stress. To address these issues, innovative agricultural practices and technologies must be adopted to optimize water use efficiency and improve crop resilience. Achieving this requires a comprehensive analysis of plant growth and development processes, allowing targeted interventions that enhance plant adaptability to changing environmental conditions.

Therefore, this PhD project aimed to address these challenges by 1) analyzing stomatal development, 2) investigating plant responses to drought stress and 3) exploring the mechanisms underlying chloroplast development to improve photosynthesis. The findings from this PhD research contribute to our growing understanding of plant growth and development processes that can help in shaping informed strategies to combat the impacts of water scarcity and climate change, thereby contributing to the promotion of sustainable agriculture.

The first chapter of this PhD explored the roles of Brachypodium epidermal patterning factors (BdEPFs) in stomatal development. By generating transgenic *Arabidopsis* lines with estradiol-inducible constructs for six BdEPFL homologs, I identified distinct phenotypes associated with their overexpression. Notably, overexpression of *BdEPFL1-1*, *BdEPFL2-2*, *BdEPFL6-1*, and *BdEPFL6-2* showed epidermal defects, characterized by asymmetric divisions and reduced stomatal density. Complementation analysis revealed that *BdEPFL2-2* effectively complements *AtEPF1*, while *BdEPFL1-1*, *BdEPFL6-1*, and *BdEPFL6-2* show partial complementation with *AtEPF1* and *AtEPF2*. These findings highlight both shared and species-specific roles of BdEPFs in stomatal development. In Brachypodium, overexpressing BdEPFL1-1 led to reduced stomatal density, stunted growth, and delayed flowering, indicating its negative regulatory role. Overall, this study highlighted the sophisticated regulatory mechanisms of BdEPFs in stomatal development, revealing conserved pathways across distantly related species.

Future studies on Brachypodium EPFs should focus on confirming the regulatory roles of the remaining EPFs through the analysis of overexpression lines. Peptide bioassays could also serve as a powerful tool to validate the roles of these peptides in monocot stomatal development. However, preparing transgenic lines in monocots presents technical challenges and can be time-consuming. Therefore, optimizing transformation protocols could improve our efficiency in studying developmental processes in monocots.

The second chapter of this PhD examines the role of EPF signaling peptides in drought tolerance in Arabidopsis. Previous research from our lab showed that overexpressing *EPFL1-1* enhances drought tolerance, leading to an interest in the drought responses of *EPFL1*, *EPFL2*, and *EPFL3* due to their close evolutionary relationships. ABA, a key regulator of plant growth, influences processes like seed germination and stomatal closure, prompting an investigation of overlaps between EPFLs and ABA signaling. Under drought conditions, overexpression lines of *EPFL1* and *EPFL2* maintained turgor and showed no desiccation, while mutants *epfl1* and *epfl2* displayed sensitivity. Relative water loss assays confirmed that *epfl1* and *epfl2* mutants had higher water loss, while overexpression lines had lower rates.

The expression of drought-responsive genes *RD29A* and *DREB* under ABA treatment in various EPFL lines revealed significantly greater upregulation in O_xEPFL1 and O_xEPFL2, with O_xEPFL2 showing higher expression. Epidermal scoring revealed no significant difference in stomatal density for *epfl1* compared to WT, but *epfl2* and *epfl1/2* showed increases. Thus, confirming the role of *EPFL2* in stomata development. In conclusion, this study shed light on the functions of *EPFL1* and *EPFL2* in stomatal development and responses to ABA, establishing the groundwork for future research on their regulatory mechanisms.

Additionally, investigating the corresponding receptors of these EPFLs through similar experimental approaches utilizing both mutant and overexpression lines, along with high-order mutants, would provide valuable insights into the ligand-receptor interactions that drive various physiological processes.

The third chapter of the thesis examined the role of MPK phosphatases in regulating chloroplast development. Building on early studies of all five Arabidopsis MKPs, our research examined the roles of MKP2 and DsPTP1 in plant growth and development. Single *mkp2* or *dsptp1* mutants showed no visible defects, while double mutants *mkp2 dsptp1* exhibited an albino phenotype, stunted growth, small yellowish seedlings, and abnormal chloroplasts. Introducing a transgenic copy of DsPTP1 into the double mutant background effectively complemented the phenotype, highlighting the functional redundancy of MKP2 and DsPTP1 in early plant development. By subjecting *mkp2 dsptp1/+* seeds to dark conditions followed by light exposure, normal photomorphogenic development was observed; however, chloroplast development was impaired in 25% of the seeds, indicating that the double homozygous mutations were responsible for the albino phenotype. The development of both green and white seeds in siliques of heterozygous *mkp2 dsptp1/+* mutants suggested that chloroplast formation is compromised in early development in homozygous embryos. Moreover, TEM

imaging of chloroplasts revealed that double mutants have highly vacuolated chloroplast, fragmented thylakoids with plastoglobule accumulation, further confirming the role of MKP2 and DsPTP1 in chloroplast biogenesis.

To assess the interaction between these phosphatases and five MAPKs (MPK3, MPK4, MPK6, MPK8, and MPK15), high-order mutants were analyzed. The rescue of the albino phenotype when mutations in MPK4, MPK6, MPK8, or MPK15 were introduced into the *mkp2 dsptp1* background indicated that these MAPKs may be substrates for the phosphatases and play a role in chloroplast development. BiFC analysis demonstrated that MPK4, MPK6, MPK8, and MPK15 interact with MKP2, while MPK4, MPK6, and MPK8 interact with DsPTP1. Notably, MPK3 did not interact with either phosphatase. Thus, the phosphatase activity is not required for the physical interaction of either phosphatase with its target substrates.

The findings presented in this thesis hold potential for engineering agriculturally relevant plants. By targeting reductions in water loss from transpiration and optimizing crop yield, EPFL peptides could play a crucial role in developing improved crop varieties. Building on results from Chapter 1, major cereal crops like wheat and rice could be engineered to have improved growth under extreme climate conditions through altering the EPF peptide signaling. Chapter 2's findings suggest that altering EPFL2 signaling could effectively change stomatal density and regulate stomata closing, providing a way to alter water-use efficiency and generate drought tolerant crops. Additionally, results from Chapter 3 indicate that optimizing crop photosynthetic efficiency may be achieved by modulating the expression of MKP2 and DSPTP1.

To successfully engineer improved crop varieties, integrating biochemical strategies with genetic approaches is essential for a deeper understanding of these mechanisms. Thus, mutations and overexpression lines are valuable tools for investigating the roles of specific genes in important processes like stomatal regulation. By optimizing the expression of relevant genes, it may be possible to enhance stomatal density and regulate stomatal aperture more effectively under water stress conditions. In addition, biochemical approaches such as yeast-two-hybrid and mass spectrometry-based phospho-protein profiling can serve as powerful tools to understand the interaction between signaling peptides and their receptors. Therefore, employing a combination of genetic and biochemical approaches would allow for a detailed analysis of the regulatory pathways involved in cellular responses.

6. References

1. Abe, H., Yamaguchi-Shinozaki, K., Urao, T., Iwasaki, T., Hosokawa, D., & Shinozaki, K. (1997). Role of Arabidopsis MYC and MYB homologs in drought- and abscisic acid-regulated gene expression. *The Plant Cell*, 9(10), 1859–1868. <https://doi.org/10.1105/tpc.9.10.1859>
2. Abrash, E. B., Davies, K. A., & Bergmann, D. C. (2011). Generation of Signaling Specificity in Arabidopsis by Spatially Restricted Buffering of Ligand–Receptor Interactions. *The Plant Cell*, 23(8), 2864–2879. <https://doi.org/10.1105/tpc.111.086637>
3. Alberts B, Johnson A, Lewis J, *et al.* Molecular Biology of the Cell. 4th edition. New York: Garland Science; 2002. Chloroplasts and Photosynthesis. Available from: <https://www.ncbi.nlm.nih.gov/books/NBK26819/>
4. Anami, S., De Block, M., Machuka, J., & Van Lijsebettens, M. (2009). Molecular Improvement of Tropical Maize for Drought Stress Tolerance in Sub-Saharan Africa. *Critical Reviews in Plant Sciences*, 28(1–2), 16–35. <https://doi.org/10.1080/07352680802665305>
5. Andrès, C., Agne, B., & Kessler, F. (2010). The TOC complex: preprotein gateway to the chloroplast. *Biochimica et Biophysica Acta (BBA)-Molecular Cell Research*, 1803(6), 715–723.
6. Aoyama, K., Nagata, M., Oshima, K., Matsuda, T., & Aoki, N. (2001). Molecular Cloning and Characterization of a Novel Dual Specificity Phosphatase, LMW-DSP2, That Lacks the Cdc25 Homology Domain *. *Journal of Biological Chemistry*, 276(29), 27575–27583. <https://doi.org/10.1074/jbc.M100408200>
7. Ashapkin, V. V., Kutueva, L. I., Aleksandrushkina, N. I., & Vanyushin, B. F. (2020). Epigenetic mechanisms of plant adaptation to biotic and abiotic stresses. *International journal of molecular sciences*, 21(20), 7457.
8. Barros-Galvão, T., Dave, A., Gilday, A. D., Harvey, D., Vaistij, F. E., & Graham, I. A. (2020). ABA INSENSITIVE4 promotes rather than represses PHYA-dependent seed germination in Arabidopsis thaliana. *New Phytologist*, 226(4), 953–956. <https://doi.org/https://doi.org/10.1111/nph.16363>
9. Bartels, S., Anderson, J. C., González Besteiro, M. A., Carreri, A., Hirt, H., Buchala, A., Métraux, J.-P., Peck, S. C., & Ulm, R. (2009). MAP KINASE PHOSPHATASE1 and PROTEIN TYROSINE PHOSPHATASE1 Are Repressors of Salicylic Acid Synthesis and SNC1-Mediated Responses in Arabidopsis. *The Plant Cell*, 21(9), 2884–2897. <https://doi.org/10.1105/tpc.109.067678>

10. Bergmann, D. C., Lukowitz, W., & Somerville, C. R. (2004). Stomatal Development and Pattern Controlled by a MAPKK Kinase. (5676), 1494–1497. <https://doi.org/10.1126/science.1096014>
11. Bessho-Uehara, K., Wang, D. R., Furuta, T., Minami, A., Nagai, K., Gamuyao, R., Asano, K., Angeles-Shim, R. B., Shimizu, Y., Ayano, M., Komeda, N., Doi, K., Miura, K., Toda, Y., Kinoshita, T., Okuda, S., Higashiyama, T., Nomoto, M., Tada, Y., ... Ashikari, M. (2016). Loss of function at RAE2, a previously unidentified EPFL, is required for awnlessness in cultivated Asian rice. *Proceedings of the National Academy of Sciences*, 113(32), 8969–8974. <https://doi.org/10.1073/pnas.1604849113>
12. Bhaskara, G. B., Nguyen, T. T., & Verslues, P. E. (2012). Unique Drought Resistance Functions of the Highly ABA-Induced Clade A Protein Phosphatase 2Cs. *Plant Physiology*, 160(1), 379–395. <https://doi.org/10.1104/pp.112.202408>
13. Bhave, N. S., Velez, K. M., Nadeau, J. A., Lucas, J. R., Bhave, S. L., & Sack, F. D. (2009). TOO MANY MOUTHS promotes cell fate progression in stomatal development of Arabidopsis stems. *Planta*, 229(2), 357–367. <https://doi.org/10.1007/s00425-008-0835-9>
14. Bheri, M., Mahiwal, S., Sanyal, S. K., & Pandey, G. K. (2021). Plant protein phosphatases: What do we know about their mechanism of action? *The FEBS Journal*, 288(3), 756–785. <https://doi.org/https://doi.org/10.1111/febs.15454>
15. Bigeard, J., & Hirt, H. (2018). Nuclear Signaling of Plant MAPKs. *Frontiers in Plant Science*, 9. <https://doi.org/10.3389/fpls.2018.00469>
16. Brahim, L. Z. (2023). *Characterization of Two MAPK Phosphatases, MKP2 and DsPTP1, and Their Potential MAPK Substrates* (Masters dissertation, Concordia University).
17. Brandt, B., Munemasa, S., Wang, C., Nguyen, D., Yong, T., Yang, P. G., Poretsky, E., Belknap, T. F., Waadt, R., Alemán, F., & Schroeder, J. I. (2015). Calcium specificity signaling mechanisms in abscisic acid signal transduction in Arabidopsis guard cells. *ELife*, 4, e03599. <https://doi.org/10.7554/eLife.03599>
18. Carles, C., Bies-Etheve, N., Aspart, L., Léon-Kloosterziel, K. M., Koornneef, M., Echeverria, M., & Delseny, M. (2002). Regulation of Arabidopsis thaliana Em genes: role of ABI5. *The Plant Journal*, 30(3), 373–383. <https://doi.org/https://doi.org/10.1046/j.1365-313X.2002.01295.x>

19. Carrera-Castaño, G., Calleja-Cabrera, J., Pernas, M., Gómez, L., & Oñate-Sánchez, L. (2020). An Updated Overview on the Regulation of Seed Germination. In *Plants* (Vol. 9, Issue 6). <https://doi.org/10.3390/plants9060703>
20. Carvalho, D. R. A., Vasconcelos, M. W., Lee, S., Koning-Boucoiran, C. F. S., Vreugdenhil, D., Krens, F. A., Heuvelink, E., & Carvalho, S. M. P. (2016). Gene expression and physiological responses associated to stomatal functioning in *Rosa*×*hybrida* grown at high relative air humidity. *Plant Science*, 253, 154–163. <https://doi.org/https://doi.org/10.1016/j.plantsci.2016.09.018>
21. Chen, Z.-H., Chen, G., Dai, F., Wang, Y., Hills, A., Ruan, Y.-L., Zhang, G., Franks, P. J., Nevo, E., & Blatt, M. R. (2017). Molecular Evolution of Grass Stomata. *Trends in Plant Science*, 22(2), 124–139. <https://doi.org/10.1016/j.tplants.2016.09.005>
22. Chen, K., Li, G. J., Bressan, R. A., Song, C. P., Zhu, J. K., & Zhao, Y. (2020). Abscisic acid dynamics, signaling, and functions in plants. *Journal of Integrative Plant Biology*, 62(1), 25–54. <https://doi.org/10.1111/jipb.12899>
23. Chory, J., Chatterjee, M., Cook, R. K., Elich, T., Fankhauser, C., Li, J., Nagpal, P., Neff, M., Pepper, A., Poole, D., Reed, J., & Vitart, V. (1996). From seed germination to flowering, light controls plant development via the pigment phytochrome. *Proceedings of the National Academy of Sciences*, 93(22), 12066–12071. <https://doi.org/10.1073/pnas.93.22.12066>
24. Clough, S. J., & Bent, A. F. (1998). Floral dip: a simplified method for *Agrobacterium*-mediated transformation of *Arabidopsis thaliana*. *The plant journal*, 16(6), 735-743.
25. Colcombet, J., & Hirt, H. (2008). *Arabidopsis* MAPKs: a complex signalling network involved in multiple biological processes. *Biochemical Journal*, 413(2), 217–226. <https://doi.org/10.1042/BJ20080625>
26. Comas, L. H., Becker, S. R., Cruz, V. M. V., Byrne, P. F., & Dierig, D. A. (2013). Root traits contributing to plant productivity under drought. *Frontiers in plant science*, 4, 442.
27. Conklin, P. A., Strable, J., Li, S., & Scanlon, M. J. (2019). On the mechanisms of development in monocot and eudicot leaves. *New Phytologist*, 221(2), 706–724. <https://doi.org/https://doi.org/10.1111/nph.15371>
28. Cutler, S. R., Rodriguez, P. L., Finkelstein, R. R., & Abrams, S. R. (2010). Abscisic Acid: Emergence of a Core Signaling Network. *Annual Review of Plant Biology*, 61(Volume 61, 2010), 651–679. <https://doi.org/https://doi.org/10.1146/annurev-arplant-042809-112122>

29. Deak, K. I., & Malamy, J. (2005). Osmotic regulation of root system architecture. *The Plant Journal*, 43(1), 17–28. <https://doi.org/10.1111/j.1365-313X.2005.02425.x>
30. Dekkers, B. J. W., He, H., Hanson, J., Willems, L. A. J., Jamar, D. C. L., Cueff, G., Rajjou, L., Hilhorst, H. W. M., & Bentsink, L. (2016). The Arabidopsis 1 gene affects 5 (5) expression and genetically interacts with 3 during Arabidopsis seed development. *The Plant Journal*, 85(4), 451–465. <https://doi.org/10.1111/tpj.13118>
31. Dóczi, R., Brader, G., Pettkó-Szandtner, A., Rajh, I., Djamei, A., Pitzschke, A., Teige, M., & Hirt, H. (2007). The Arabidopsis Mitogen-Activated Protein Kinase Kinase MKK3 Is Upstream of Group C Mitogen-Activated Protein Kinases and Participates in Pathogen Signaling. *The Plant Cell*, 19(10), 3266–3279. <https://doi.org/10.1105/tpc.106.050039>
32. Dunn, J., Hunt, L., Afsharinafar, M., Meselmani, M. A., Mitchell, A., Howells, R., ... & Gray, J. E. (2019). Reduced stomatal density in bread wheat leads to increased water-use efficiency. *Journal of Experimental Botany*, 70(18), 4737–4748.
33. Edwards, K., Johnstone, C., & Thompson, C. (1991). A simple and rapid method for the preparation of plant genomic DNA for PCR analysis. *Nucleic Acids Research*, 19(6), 1349. <https://doi.org/10.1093/nar/19.6.1349>
34. Fang, Y., & Xiong, L. (2015). General mechanisms of drought response and their application in drought resistance improvement in plants. *Cellular and Molecular Life Sciences*, 72(4), 673–689. <https://doi.org/10.1007/s00018-014-1767-0>
35. Ferguson, J. N., Schmuker, P., Dmitrieva, A., Quach, T., Zhang, T., Ge, Z., Nersesian, N., Sato, S. J., Clemente, T. E., & Leakey, A. D. B. (2024). Reducing stomatal density by expression of a synthetic EPF increases leaf intrinsic water use efficiency and reduces plant water use in a C4 crop. *BioRxiv*. <https://doi.org/10.1101/2024.02.01.578512>
36. Finkelstein, R. (2013). Abscisic Acid synthesis and response. *The Arabidopsis Book*, 11, e0166. <https://doi.org/10.1199/tab.0166>
37. Frank, L., & Gray, J. E. (2009). The Signaling Peptide EPF2 Controls Asymmetric Cell Divisions during Stomatal Development. *Current Biology*, 19(10), 864–869. <https://doi.org/10.1016/j.cub.2009.03.069>
38. Freschet, G. T., Roumet, C., Comas, L. H., Weemstra, M., Bengough, A. G., Rewald, B., Bardgett, R. D., De Deyn, G. B., Johnson, D., Klimešová, J., Lukac, M., McCormack, M. L., Meier, I. C., Pagès, L., Poorter, H., Prieto, I., Wurzburger, N.,

- Zadworny, M., Bagniewska-Zadworna, A., Stokes, A. (2021). Root traits as drivers of plant and ecosystem functioning: current understanding, pitfalls and future research needs. *New Phytologist*, 232(3), 1123–1158. <https://doi.org/https://doi.org/10.1111/nph.17072>
39. Gao, H., McCormick, A. J., Roston, R. L., & Lu, Y. (2023). Editorial: Structure and function of chloroplasts, Volume III. *Frontiers in Plant Science*, 14. <https://www.frontiersin.org/journals/plant-science/articles/10.3389/fpls.2023.1145680>
 40. Germon, A., Laclau, J. P., Robin, A., & Jourdan, C. (2020). Tamm Review: Deep fine roots in forest ecosystems: Why dig deeper?. *Forest Ecology and Management*, 466, 118135.
 41. Grübler, B., Merendino, L., Twardziok, S. O., Mininno, M., Alloreant, G., Chevalier, F., Liebers, M., Blanvillain, R., Mayer, K. F. X., Lerbs-Mache, S., Ravanel, S., & Pfanschmidt, T. (2017). Light and Plastid Signals Regulate Different Sets of Genes in the Albino Mutant Pap7-1. *Plant Physiology*, 175(3), 1203–1219. <https://doi.org/10.1104/pp.17.00982>
 42. Gudesblat, G. E., Schneider-Pizoń, J., Betti, C., Mayerhofer, J., Vanhoutte, I., van Dongen, W., Boeren, S., Zhiponova, M., de Vries, S., Jonak, C., & Russinova, E. (2012). SPEECHLESS integrates brassinosteroid and stomata signalling pathways. *Nature Cell Biology*, 14(5), 548–554. <https://doi.org/10.1038/ncb2471>
 43. Guo, H., Feng, P., Chi, W., Sun, X., Xu, X., Li, Y., Ren, D., Lu, C., David Rochaix, J., Leister, D., & Zhang, L. (2016). Plastid-nucleus communication involves calcium-modulated MAPK signalling. *Nature Communications*, 7(1), 12173. <https://doi.org/10.1038/ncomms12173>
 44. Gupta, R., Huang, Y., Kieber, J., & Luan, S. (1998). Identification of a dual-specificity protein phosphatase that inactivates a MAP kinase from. *The Plant Journal*, 16(5), 581–589. <https://doi.org/https://doi.org/10.1046/j.1365-313x.1998.00327.x>
 45. Guseman, J. M., Lee, J. S., Bogenschutz, N. L., Peterson, K. M., Virata, R. E., Xie, B., & Torii, K. U. (2010). Dysregulation of cell-to-cell connectivity and stomatal patterning by loss-of-function mutation in *Arabidopsis thaliana* (glucan synthase-like 8). *Development*, 137(10), 1731–1741.
 46. Gutiérrez-Nava, M. de la L., Gillmor, C. S., Jiménez, L. F., Guevara-García, A., & León, P. (2004). CHLOROPLAST BIOGENESIS Genes Act Cell and Noncell Autonomously in Early Chloroplast Development. *Plant Physiology*, 135(1), 471–482. <https://doi.org/10.1104/pp.103.036996>

47. Han, S.-K., Kwak, J. M., & Qi, X. (2021). Stomatal Lineage Control by Developmental Program and Environmental Cues. *Frontiers in Plant Science*, 12. <https://doi.org/10.3389/fpls.2021.751852>
48. Hara, K., Kajita, R., Torii, K. U., Bergmann, D. C., & Kakimoto, T. (2007). The secretory peptide gene EPF1 enforces the stomatal one-cell-spacing rule. *Genes and Development*, 21(14), 1720–1725. <https://doi.org/10.1101/gad.1550707>
49. Hara, K., Yokoo, T., Kajita, R., Onishi, T., Yahata, S., Peterson, K. M., Torii, K. U., & Kakimoto, T. (2009). Epidermal Cell Density is Autoregulated via a Secretory Peptide, EPIDERMAL PATTERNING FACTOR 2 in Arabidopsis Leaves. *Plant and Cell Physiology*, 50(6), 1019–1031. <https://doi.org/10.1093/pcp/pcp068>
50. Hepworth, C., Caine, R. S., Harrison, E. L., Sloan, J., & Gray, J. E. (2018). Stomatal development: focusing on the grasses. *Current Opinion in Plant Biology*, 41, 1–7. <https://doi.org/https://doi.org/10.1016/j.pbi.2017.07.009>
51. Herrmann, A., & Torii, K. U. (2021). Shouting out loud: signaling modules in the regulation of stomatal development. *Plant Physiology*, 185(3), 765–780. <https://doi.org/10.1093/plphys/kiaa061>
52. Hobe, S., Niemeier, H., Bender, A., & Paulsen, H. (2000). Carotenoid binding sites in LHCIIB: Relative affinities towards major xanthophylls of higher plants. *European journal of biochemistry*, 267(2), 616-624.
53. Huang, Y., Tao, Z., Liu, Q., Wang, X., Yu, J., Liu, G., & Wang, H. (2014). BnEPFL6, an EPIDERMAL PATTERNING FACTOR-LIKE (EPFL) secreted peptide gene, is required for filament elongation in Brassica napus. *Plant Molecular Biology*, 85(4), 505–517. <https://doi.org/10.1007/s11103-014-0200-2>
54. Hunt, L., & Gray, J. E. (2009). The Signaling Peptide EPF2 Controls Asymmetric Cell Divisions during Stomatal Development. *Current Biology*, 19(10), 864–869. <https://doi.org/10.1016/j.cub.2009.03.069>
55. Hussain, H. A., Hussain, S., Khaliq, A., Ashraf, U., Anjum, S. A., Men, S., & Wang, L. (2018). Chilling and Drought Stresses in Crop Plants: Implications, Cross Talk, and Potential Management Opportunities. *Frontiers in Plant Science*, 9. <https://www.frontiersin.org/journals/plant-science/articles/10.3389/fpls.2018.00393>
56. Inoue, S., & Kinoshita, T. (2017). Blue Light Regulation of Stomatal Opening and the Plasma Membrane H⁺-ATPase. *Plant Physiology*, 174(2), 531–538. <https://doi.org/10.1104/pp.17.00166>

57. Jacobsen, J. V., Pearce, D. W., Poole, A. T., Pharis, R. P., & Mander, L. N. (2002). Abscisic acid, phaseic acid and gibberellin contents associated with dormancy and germination in barley. *Physiologia Plantarum*, *115*(3), 428–441. <https://doi.org/https://doi.org/10.1034/j.1399-3054.2002.1150313.x>
58. Jagodzik, P., Tajdel-Zielinska, M., Ciesla, A., Marczak, M., & Ludwikow, A. (2018). Mitogen-Activated Protein Kinase Cascades in Plant Hormone Signaling. *Frontiers in Plant Science*, *9*. <https://www.frontiersin.org/journals/plant-science/articles/10.3389/fpls.2018.01387>
59. Jangra, R., Brunetti, S. C., Wang, X., Kaushik, P., Gulick, P. J., Foroud, N. A., Wang, S., & Lee, J. S. (2021). Duplicated antagonistic EPF peptides optimize grass stomatal initiation. *Development*, *148*(16), dev199780. <https://doi.org/10.1242/dev.199780>
60. Jiao, P., Liang, Y., Chen, S., Yuan, Y., Chen, Y., & Hu, H. (2023). Bna. EPF2 enhances drought tolerance by regulating stomatal development and stomatal size in *Brassica napus*. *International Journal of Molecular Sciences*, *24*(9), 8007.
61. Kalapos, B., Hlavová, M., Nádai, T. V., Galiba, G., Bišová, K., & Dóczi, R. (2019). Early Evolution of the Mitogen-Activated Protein Kinase Family in the Plant Kingdom. *Scientific Reports*, *9*(1), 4094. <https://doi.org/10.1038/s41598-019-40751-y>
62. Kanaoka, M. M., Pillitteri, L. J., Fujii, H., Yoshida, Y., Bogenschutz, N. L., Takabayashi, J., Zhu, J.-K., & Torii, K. U. (2008). SCREAM/ICE1 and SCREAM2 Specify Three Cell-State Transitional Steps Leading to Arabidopsis Stomatal Differentiation. *The Plant Cell*, *20*(7), 1775–1785. <https://doi.org/10.1105/tpc.108.060848>
63. Katsir, L., Davies, K. A., Bergmann, D. C., & Laux, T. (2011). Peptide Signaling in Plant Development. *Current Biology*, *21*(9), R356–R364. <https://doi.org/10.1016/j.cub.2011.03.012>
64. Kawamoto, N., Del Carpio, D. P., Hofmann, A., Mizuta, Y., Kurihara, D., Higashiyama, T., Uchida, N., Torii, K. U., Colombo, L., Groth, G., & Simon, R. (2020). A Peptide Pair Coordinates Regular Ovule Initiation Patterns with Seed Number and Fruit Size. *Current Biology*, *30*(22), 4352–4361.e4. <https://doi.org/10.1016/j.cub.2020.08.050>
65. Kerk, D., Templeton, G., & Moorhead, G. B. G. (2008). Evolutionary radiation pattern of novel protein phosphatases revealed by analysis of protein data from the completely sequenced genomes of humans, green algae, and higher plants. *Plant Physiology*, *146*(2), 351–367. <https://doi.org/10.1104/pp.107.111393>

66. Keyse, S. M. (2008). Dual-specificity MAP kinase phosphatases (MKPs) and cancer. *Cancer and Metastasis Reviews*, 27(2), 253–261. <https://doi.org/10.1007/s10555-008-9123-1>
67. Kim, K. E., Nguyen, N. T., Kim, S. H., Bahk, S., Cheong, M. S., Park, H. C., ... & Chung, W. S. (2021). Ca²⁺/Calmodulin Activates an MAP Kinase Through the Inhibition of a Protein Phosphatase (DsPTP1) in Arabidopsis. *Journal of Plant Biology*, 1-10.
68. Kondo, T., Kajita, R., Miyazaki, A., Hokoyama, M., Nakamura-Miura, T., Mizuno, S., Masuda, Y., Irie, K., Tanaka, Y., Takada, S., Kakimoto, T., & Sakagami, Y. (2010). Stomatal Density is Controlled by a Mesophyll-Derived Signaling Molecule. *Plant and Cell Physiology*, 51(1), 1–8. <https://doi.org/10.1093/pcp/pcp180>
69. Kosentka, P. Z., Overholt, A., Maradiaga, R., Mitoubsi, O., & Shpak, E. D. (2019). EPFL Signals in the Boundary Region of the SAM Restrict Its Size and Promote Leaf Initiation. *Plant Physiology*, 179(1), 265–279. <https://doi.org/10.1104/pp.18.00714>
70. Lampard, G. R., Lukowitz, W., Ellis, B. E., & Bergmann, D. C. (2009). Novel and Expanded Roles for MAPK Signaling in Arabidopsis Stomatal Cell Fate Revealed by Cell Type-Specific Manipulations. *The Plant Cell*, 21(11), 3506–3517. <https://doi.org/10.1105/tpc.109.070110>
71. Lampard, G. R., MacAlister, C. A., & Bergmann, D. C. (2008). Arabidopsis Stomatal Initiation Is Controlled by MAPK-Mediated Regulation of the bHLH SPEECHLESS. *Science*, 322(5904), 1113–1116. <https://doi.org/10.1126/science.1162263>
72. Lampard, G. R., Wengier, D. L., & Bergmann, D. C. (2014). Manipulation of Mitogen-Activated Protein Kinase Kinase Signaling in the Arabidopsis Stomatal Lineage Reveals Motifs That Contribute to Protein Localization and Signaling Specificity. *The Plant Cell*, 26(8), 3358–3371. <https://doi.org/10.1105/tpc.114.127415>
73. Lee, J. S., & Ellis, B. E. (2007). Arabidopsis MAPK Phosphatase 2 (MKP2) Positively Regulates Oxidative Stress Tolerance and Inactivates the MPK3 and MPK6 MAPKs. *Journal of Biological Chemistry*, 282(34), 25020–25029. <https://doi.org/10.1074/jbc.M701888200>
74. Lee, J. S., Wang, S., Sritubtim, S., Chen, J.-G., & Ellis, B. E. (2009). Arabidopsis mitogen-activated protein kinase MPK12 interacts with the MAPK phosphatase IBR5 and regulates auxin signaling. *The Plant Journal*, 57(6), 975–985. <https://doi.org/10.1111/j.1365-313X.2008.03741.x>

75. Lee, J. S., Kuroha, T., Hnilovabrea, M., Khatayevich, D., Kanaoka, M. M., McAbee, J. M., Sarikaya, M., Tamerler, C., & Torii, K. U. (2012). Direct interaction of ligand–receptor pairs specifying stomatal patterning. *Genes & Development*, 26(2), 126–136. <https://genesdev.cshlp.org/content/26/2/126.abstract>
76. Lee, J. S., Hnilova, M., Maes, M., Lin, Y.-C. L., Putarjunan, A., Han, S.-K., Avila, J., & Torii, K. U. (2015). Competitive binding of antagonistic peptides fine-tunes stomatal patterning. *Nature*, 522(7557), 439–443. <https://doi.org/10.1038/nature14561>
77. Lee, K., Lee, H. G., Yoon, S., Kim, H. U., & Seo, P. J. (2015). The Arabidopsis MYB96 Transcription Factor Is a Positive Regulator of ABSCISIC ACID-INSENSITIVE4 in the Control of Seed Germination. *Plant Physiology*, 168(2), 677–689. <https://doi.org/10.1104/pp.15.00162>
78. Lee, S. C., Lan, W., Buchanan, B. B., & Luan, S. (2009). A protein kinase-phosphatase pair interacts with an ion channel to regulate ABA signaling in plant guard cells. *Proceedings of the National Academy of Sciences*, 106(50), 21419–21424. <https://doi.org/10.1073/pnas.0910601106>
79. Leung, J., Merlot, S., & Giraudat, J. (1997). The Arabidopsis ABSCISIC ACID-INSENSITIVE2 (ABI2) and ABI1 genes encode homologous protein phosphatases 2C involved in abscisic acid signal transduction. *The Plant Cell*, 9(5), 759–771. <https://doi.org/10.1105/tpc.9.5.759>
80. Levitt, J. (1980). Responses of plants to environmental stresses. *Vol. II. Academic Press. New York.*
81. Li, M., Lv, M., Wang, X., Cai, Z., Yao, H., Zhang, D., ... & Gou, X. (2023). The EPFL–ERf–SERK signaling controls integument development in Arabidopsis. *New Phytologist*, 238(1), 186–201.
82. Liang, J., Zhang, Q., Liu, Y., Zhang, J., Wang, W., & Zhang, Z. (2022). Chlorosis seedling lethality 1 encoding a MAP3K protein is essential for chloroplast development in rice. *BMC Plant Biology*, 22(1), 20. <https://doi.org/10.1186/s12870-021-03404-9>
83. Lichtenthaler, H. K., & Wellburn, A. R. (1983). Determinations of total carotenoids and chlorophylls *a* and *b* of leaf extracts in different solvents. *Biochemical Society Transactions*, 11(5), 591–592. <https://doi.org/10.1042/bst0110591>
84. Liebers, M., Cozzi, C., Uecker, F., Chambon, L., Blanvillain, R., & Pfannschmidt, T. (2022). Biogenic signals from plastids and their role in chloroplast development. *Journal of Experimental Botany*, 73(21), 7105–7125. <https://doi.org/10.1093/jxb/erac344>

85. Lin, C., & Chen, S. (2018). New functions of an old kinase MPK4 in guard cells. *Plant Signaling & Behavior*, 13(5), e1477908. <https://doi.org/10.1080/15592324.2018.1477908>
86. Liu, R., Xu, Y.-H., Jiang, S.-C., Lu, K., Lu, Y.-F., Feng, X.-J., Wu, Z., Liang, S., Yu, Y.-T., Wang, X.-F., & Zhang, D.-P. (2013). Light-harvesting chlorophyll a/b-binding proteins, positively involved in abscisic acid signalling, require a transcription repressor, WRKY40, to balance their function. *Journal of Experimental Botany*, 64(18), 5443–5456. <https://doi.org/10.1093/jxb/ert307>
87. Liu, R., Liu, Y., Ye, N., Zhu, G., Chen, M., Jia, L., Xia, Y., Shi, L., Jia, W., & Zhang, J. (2015). AtDsPTP1 acts as a negative regulator in osmotic stress signalling during Arabidopsis seed germination and seedling establishment. *Journal of Experimental Botany*, 66(5), 1339–1353. <https://doi.org/10.1093/jxb/eru484>
88. Liu, S., Wang, C., Jia, F., An, Y., Liu, C., Xia, X., & Yin, W. (2016). Secretory peptide PdEPF2 enhances drought tolerance by modulating stomatal density and regulates ABA response in transgenic Arabidopsis thaliana. *Plant Cell, Tissue and Organ Culture*, 125(3), 419–431. <https://doi.org/10.1007/s11240-016-0957-x>
89. Liu, S., Chen, T., Li, X., Cui, J., & Tian, Y. (2024). Genome-wide identification and expression analysis of EPF/EPFL gene family in Populus trichocarpa. *Frontiers in Genetics*, 15. <https://doi.org/10.3389/fgene.2024.1432376>
90. Liu, T., Ohashi-Ito, K., & Bergmann, D. C. (2009). Orthologs of Arabidopsis thaliana stomatal bHLH genes and regulation of stomatal development in grasses. *Development*, 136(13), 2265–2276. <https://doi.org/10.1242/dev.032938>
91. Loudya, N., Barkan, A., & López-Juez, E. (2024). Plastid retrograde signaling: A developmental perspective. *The Plant Cell*, 36(10), 3903–3913. <https://doi.org/10.1093/plcell/koae094>
92. Lu, J., He, J., Zhou, X., Zhong, J., Li, J., & Liang, Y. K. (2019). Homologous genes of epidermal patterning factor regulate stomatal development in rice. *Journal of plant physiology*, 234, 18-27.
93. Lumberras, V., Vilela, B., Irar, S., Solé, M., Capellades, M., Valls, M., Coca, M., & Pagès, M. (2010). MAPK phosphatase MKP2 mediates disease responses in Arabidopsis and functionally interacts with MPK3 and MPK6. *The Plant Journal*, 63(6), 1017–1030. [https://doi.org/https://doi.org/10.1111/j.1365-313X.2010.04297.x](https://doi.org/10.1111/j.1365-313X.2010.04297.x)

94. MacAlister, C. A., Ohashi-Ito, K., & Bergmann, D. C. (2007). Transcription factor control of asymmetric cell divisions that establish the stomatal lineage. *Nature*, 445(7127), 537–540. <https://doi.org/10.1038/nature05491>
95. Matkowski, H., & Daszkowska-Golec, A. (2023). Update on stomata development and action under abiotic stress. *Frontiers in Plant Science*, 14. <https://doi.org/10.3389/fpls.2023.1270180>
96. McCarty, D. R., & J. (2000). Conservation and Innovation in Plant Signaling Pathways. *Cell*, 103(2), 201–209. [https://doi.org/10.1016/S0092-8674\(00\)00113-6](https://doi.org/10.1016/S0092-8674(00)00113-6)
97. McKown, K. H., & Bergmann, D. C. (2020). Stomatal development in the grasses: lessons from models and crops (and crop models). *New Phytologist*, 227(6), 1636–1648.
98. Millar, A. A., Jacobsen, J. V, Ross, J. J., Helliwell, C. A., Poole, A. T., Scofield, G., Reid, J. B., & Gubler, F. (2006). Seed dormancy and ABA metabolism in Arabidopsis and barley: the role of ABA 8'-hydroxylase. *The Plant Journal*, 45(6), 942–954. <https://doi.org/https://doi.org/10.1111/j.1365-313X.2006.02659.x>
99. Mohamed, D., Vonapartis, E., Corcega, D. Y., & Gazzarrini, S. (2023). ABA guides stomatal proliferation and patterning through the EPF-SPCH signaling pathway in Arabidopsis thaliana. *Development*, 150(23), dev201258. <https://doi.org/10.1242/dev.201258>
100. Monroe-Augustus, M., Zolman, B. K., & Bartel, B. (2003). IBR5, a Dual-Specificity Phosphatase-Like Protein Modulating Auxin and Abscisic Acid Responsiveness in Arabidopsis. *The Plant Cell*, 15(12), 2979–2991. <https://doi.org/10.1105/tpc.017046>
101. Mukherjee, A., Dwivedi, S., Bhagavatula, L., & Datta, S. (2023). Integration of light and ABA signaling pathways to combat drought stress in plants. *Plant Cell Reports*, 42(5), 829–841. <https://doi.org/10.1007/s00299-023-02999-7>
102. Nadeau, J. A., & Sack, F. D. (2002). Control of Stomatal Distribution on the Arabidopsis Leaf Surface. *Science*, 296(5573), 1697–1700. <https://doi.org/10.1126/science.1069596>
103. Nardini, A., Salleo, S., & Tyree, M. T. (2002). Ecological aspects of water permeability of roots. In *Plant Roots* (pp. 1069-1093). CRC Press.
104. Nerva, L., Chitarra, W., Fila, G., Lovat, L., & Gaiotti, F. (2023). Variability in Stomatal Adaptation to Drought among Grapevine Cultivars: Genotype-Dependent Responses. *Agriculture*, 13(12), 2186.
105. Nomura, H., & Shiina, T. (2014). Calcium signaling in plant endosymbiotic organelles: mechanism and role in physiology. *Molecular plant*, 7(7), 1094-1104.

106. OECD and FAO, United Nations, A. O. (2023). *Cereals*.
107. Ohashi-Ito, K., & Bergmann, D. C. (2006). Arabidopsis FAMA Controls the Final Proliferation/Differentiation Switch during Stomatal Development. *The Plant Cell*, *18*(10), 2493–2505. <https://doi.org/10.1105/tpc.106.046136>
108. Osmolovskaya, N., Shumilina, J., Kim, A., Didio, A., Grishina, T., Bilova, T., Keltsieva, O. A., Zhukov, V., Tikhonovich, I., Tarakhovskaya, E., Frolov, A., & Wessjohann, L. A. (2018). Methodology of Drought Stress Research: Experimental Setup and Physiological Characterization. In *International Journal of Molecular Sciences* (Vol. 19, Issue 12). <https://doi.org/10.3390/ijms19124089>
109. Pei, D., Hua, D., Deng, J., Wang, Z., Song, C., Wang, Y., Wang, Y., Qi, J., Kollist, H., Yang, S., Guo, Y., & Gong, Z. (2022). Phosphorylation of the plasma membrane H⁺-ATPase AHA2 by BAK1 is required for ABA-induced stomatal closure in Arabidopsis. *The Plant Cell*, *34*(7), 2708–2729. <https://doi.org/10.1093/plcell/koac106>
110. Pillitteri, L. J., Sloan, D. B., Bogenschutz, N. L., & Torii, K. U. (2007). Termination of asymmetric cell division and differentiation of stomata. *Nature*, *445*(7127), 501–505. <https://doi.org/10.1038/nature05467>
111. Pillitteri, L. J., & Torii, K. U. (2012). Mechanisms of Stomatal Development. *Annual Review of Plant Biology*, *63*(Volume 63, 2012), 591–614. <https://doi.org/https://doi.org/10.1146/annurev-arplant-042811-105451>
112. Pillitteri, L. J., & Dong, J. (2013). Stomatal Development in Arabidopsis. *The Arabidopsis Book*, *11*(11), e0162. <https://doi.org/10.1199/tab.0162>
113. Price, A. (2002). *QTLs for Root Growth and Drought Resistance in Rice BT - Molecular Techniques in Crop Improvement* (S. M. Jain, D. S. Brar, & B. S. Ahloowalia (eds.); pp. 563–584). Springer Netherlands. https://doi.org/10.1007/978-94-017-2356-5_21
114. Qin, G., Gu, H., Ma, L., Peng, Y., Deng, X. W., Chen, Z., & Qu, L.-J. (2007). Disruption of phytoene desaturase gene results in albino and dwarf phenotypes in Arabidopsis by impairing chlorophyll, carotenoid, and gibberellin biosynthesis. *Cell Research*, *17*(5), 471–482. <https://doi.org/10.1038/cr.2007.40>
115. Quettier, A.-L., Bertrand, C., Habricot, Y., Miginiac, E., Agnes, C., Jeannette, E., & Maldiney, R. (2006). The *phs1-3* mutation in a putative dual-specificity protein tyrosine phosphatase gene provokes hypersensitive responses to abscisic acid in *Arabidopsis thaliana*: PHS1 gene is involved in abscisic acid signalling. *The Plant Journal*, *47*(5), 711–719. <https://doi.org/10.1111/j.1365-313X.2006.02823.x>

116. Quian-Ulloa, R., & Stange, C. (2021). Carotenoid Biosynthesis and Plastid Development in Plants: The Role of Light. In *International Journal of Molecular Sciences* (Vol. 22, Issue 3). <https://doi.org/10.3390/ijms22031184>
117. Raissig, M. T., Abrash, E., Bettadapur, A., Vogel, J. P., & Bergmann, D. C. (2016). Grasses use an alternatively wired bHLH transcription factor network to establish stomatal identity. *Proceedings of the National Academy of Sciences*, *113*(29), 8326–8331. <https://doi.org/10.1073/pnas.1606728113>
118. Richardson, L. G. L., & Torii, K. U. (2013). Take a deep breath: peptide signalling in stomatal patterning and differentiation. *Journal of Experimental Botany*, *64*(17), 5243–5251. <https://doi.org/10.1093/jxb/ert246>
119. Rodríguez-Alcocer, E., Ruiz-Pérez, E., Parreño, R., Martínez-Guardiola, C., Berna, J. M., Çakmak Pehlivanlı, A., Jover-Gil, S., & Candela, H. (2023). Cloning of an Albino Mutation of *Arabidopsis thaliana* Using Mapping-by-Sequencing. In *International Journal of Molecular Sciences* (Vol. 24, Issue 4). <https://doi.org/10.3390/ijms24044196>
120. Rodríguez, J., Calvo, F., González, J. M., Casar, B., Andrés, V., & Crespo, P. (2010). ERK1/2 MAP kinases promote cell cycle entry by rapid, kinase-independent disruption of retinoblastoma–lamin A complexes. *Journal of Cell Biology*, *191*(5), 967–979. <https://doi.org/10.1083/jcb.201004067>
121. Rodriguez, P. L., Benning, G., & Grill, E. (1998). ABI2, a second protein phosphatase 2C involved in abscisic acid signal transduction in *Arabidopsis*. *FEBS Letters*, *421*(3), 185–190. [https://doi.org/https://doi.org/10.1016/S0014-5793\(97\)01558-5](https://doi.org/https://doi.org/10.1016/S0014-5793(97)01558-5)
122. Rosa, P., Eicke, S., Pfister, B., Glauser, G., Falconet, D., Uwizeye, C., ... & Demarsy, E. (2020). Two distinct phases of chloroplast biogenesis during de-etiolation in *Arabidopsis thaliana*.
123. Roston, R. L., Jouhet, J., Yu, F., & Gao, H. (2018). Editorial: Structure and Function of Chloroplasts. *Frontiers in Plant Science*, *9*. <https://doi.org/10.3389/fpls.2018.01656>
124. Rowe, J. H., Topping, J. F., Liu, J., & Lindsey, K. (2016). Abscisic acid regulates root growth under osmotic stress conditions via an interacting hormonal network with cytokinin, ethylene and auxin. *New Phytologist*, *211*(1), 225–239. <https://doi.org/https://doi.org/10.1111/nph.13882>
125. Ruban, A. V. (2012). *The photosynthetic membrane: molecular mechanisms and biophysics of light harvesting*. John Wiley & Sons.

126. Sakai, K., Citerne, S., Antelme, S., Le Bris, P., Daniel, S., Bouder, A., D'Orlando, A., Cartwright, A., Tellier, F., Pateyron, S., Delannoy, E., Laudencia-Chingcuanco, D., Mouille, G., Palauqui, J. C., Vogel, J., & Sibout, R. (2021). BdERECTA controls vasculature patterning and phloem-xylem organization in *Brachypodium distachyon*. *BMC Plant Biology*, *21*(1), 196. <https://doi.org/10.1186/s12870-021-02970-2>
127. Sakuma, Y., Maruyama, K., Osakabe, Y., Qin, F., Seki, M., Shinozaki, K., & Yamaguchi-Shinozaki, K. (2006). Functional Analysis of an Arabidopsis Transcription Factor, DREB2A, Involved in Drought-Responsive Gene Expression. *The Plant Cell*, *18*(5), 1292–1309. <https://doi.org/10.1105/tpc.105.035881>
128. Sattari Vayghan, H., Nawrocki, W. J., Schiphorst, C., Tolleter, D., Hu, C., Douet, V., Glauser, G., Finazzi, G., Croce, R., Wientjes, E., & Longoni, F. (2022). Photosynthetic Light Harvesting and Thylakoid Organization in a CRISPR/Cas9 Arabidopsis Thaliana LHCB1 Knockout Mutant. *Frontiers in Plant Science*, *13*. <https://doi.org/10.3389/fpls.2022.833032>
129. Schroeder, J. I., Kwak, J. M., & Allen, G. J. (2001). Guard cell abscisic acid signalling and engineering drought hardiness in plants. *Nature*, *410*(6826), 327-330.
130. Sena, G., Wang, X., Liu, H.-Y., Hofhuis, H., & Birnbaum, K. D. (2009). Organ regeneration does not require a functional stem cell niche in plants. *Nature*, *457*(7233), 1150–1153. <https://doi.org/10.1038/nature07597>
131. Shi, H., Li, Q., Luo, M., Yan, H., Xie, B., Li, X., Zhong, G., Chen, D., & Tang, D. (2022). BRASSINOSTEROID-SIGNALING KINASE1 modulates MAP KINASE15 phosphorylation to confer powdery mildew resistance in Arabidopsis. *The Plant Cell*, *34*(5), 1768–1783. <https://doi.org/10.1093/plcell/koac027>
132. Shi, J., An, H.-L., Zhang, L., Gao, Z., & Guo, X.-Q. (2010). GhMPK7, a novel multiple stress-responsive cotton group C MAPK gene, has a role in broad spectrum disease resistance and plant development. *Plant Molecular Biology*, *74*(1), 1–17. <https://doi.org/10.1007/s11103-010-9661-0>
133. Shinozaki, K. (2000). Molecular responses to dehydration and low temperature: differences and cross-talk between two stress signaling pathways. *Current Opinion in Plant Biology*, *3*(3), 217–223. [https://doi.org/https://doi.org/10.1016/S1369-5266\(00\)80068-0](https://doi.org/https://doi.org/10.1016/S1369-5266(00)80068-0)
134. Shinozaki, K., & Yamaguchi-Shinozaki, K. (2007). Functional genomics for gene discovery in abiotic stress response and tolerance. In *Rice Genetics V: Vol. Volume 5*

- (pp. 301–311). World Scientific Publishing Company.
https://doi.org/doi:10.1142/9789812708816_0020
135. Shpak, E. D., McAbee, J. M., Pillitteri, L. J., & Torii, K. U. (2005). Stomatal Patterning and Differentiation by Synergistic Interactions of Receptor Kinases. *Science*, 309(5732), 290–293. <https://doi.org/10.1126/science.1109710>
 136. Shpak, E. D. (2013). Diverse Roles of Family Genes in Plant Development. *Journal of Integrative Plant Biology*, 55(12), 1238–1250. <https://doi.org/https://doi.org/10.1111/jipb.12108>
 137. Silva, L. A. S., Sampaio, V. F., Barbosa, L. C. S., Machado, M., Flores-Borges, D. N. A., Sales, J. F., Oliveira, D. C., Mayer, J. L. S., Kuster, V. C., & Rocha, D. I. (2020). Albinism in plants – far beyond the loss of chlorophyll: Structural and physiological aspects of wild-type and albino royal poinciana (*Delonix regia*) seedlings. *Plant Biology*, 22(5), 761–768. <https://doi.org/10.1111/plb.13146>
 138. Stebbins, G. L., & Jain, S. K. (1960). Developmental studies of cell differentiation in the epidermis of monocotyledons: I. Allium, rhoeo, and commelina. *Developmental Biology*, 2(5), 409–426. [https://doi.org/https://doi.org/10.1016/0012-1606\(60\)90025-7](https://doi.org/https://doi.org/10.1016/0012-1606(60)90025-7)
 139. Stokes, K. D., McAndrew, R. S., Figueroa, R., Vitha, S., & Osteryoung, K. W. (2000). Chloroplast Division and Morphology Are Differentially Affected by Overexpression of FtsZ1 and FtsZ2 Genes in Arabidopsis1,. *Plant Physiology*, 124(4), 1668–1677. <https://doi.org/10.1104/pp.124.4.1668>
 140. Sugano, S. S., Shimada, T., Imai, Y., Okawa, K., Tamai, A., Mori, M., & Hara-Nishimura, I. (2010). Stomagen positively regulates stomatal density in Arabidopsis. *Nature*, 463(7278), 241–244. <https://doi.org/10.1038/nature08682>
 141. Sun, J. (2022). Role of MAPK phosphatase MKP2 and DsPTP1 in plant growth and development (Master’s dissertation, Concordia University).
 142. Takahashi, F., Yoshida, R., Ichimura, K., Mizoguchi, T., Seo, S., Yonezawa, M., Maruyama, K., Yamaguchi-Shinozaki, K., & Shinozaki, K. (2007). The Mitogen-Activated Protein Kinase Cascade MKK3–MPK6 Is an Important Part of the Jasmonate Signal Transduction Pathway in Arabidopsis. *The Plant Cell*, 19(3), 805–818. <https://doi.org/10.1105/tpc.106.046581>
 143. Takahashi, F., Kuromori, T., Urano, K., Yamaguchi-Shinozaki, K., & Shinozaki, K. (2020). Drought Stress Responses and Resistance in Plants: From Cellular Responses to Long-Distance Intercellular Communication. *Frontiers in Plant Science*, 11(September), 1–14. <https://doi.org/10.3389/fpls.2020.556972>

144. Tameshige, T., Okamoto, S., Lee, J. S., Aida, M., Tasaka, M., Torii, K. U., & Uchida, N. (2016). A Secreted Peptide and Its Receptors Shape the Auxin Response Pattern and Leaf Margin Morphogenesis. *Current Biology*, 26(18), 2478–2485. <https://doi.org/10.1016/j.cub.2016.07.014>
145. Tamnanloo, F., Damen, H., Jangra, R., & Lee, J. S. (2018). MAP KINASE PHOSPHATASE1 Controls Cell Fate Transition during Stomatal Development. *Plant Physiology*, 178(1), 247–257. <https://doi.org/10.1104/pp.18.00475>
146. Tanaka, Y., Nose, T., Jikumaru, Y., & Kamiya, Y. (2013). ABA inhibits entry into stomatal-lineage development in Arabidopsis leaves. *The Plant Journal*, 74(3), 448–457. <https://doi.org/https://doi.org/10.1111/tpj.12136>
147. Tang, Q., Guittard-Crilat, E., Maldiney, R., Habricot, Y., Miginiac, E., Bouly, J.-P., & Lebreton, S. (2016). The mitogen-activated protein kinase phosphatase PHS1 regulates flowering in Arabidopsis thaliana. *Planta*, 243(4), 909–923. <https://doi.org/10.1007/s00425-015-2447-5>
148. Töldsepp, K., Zhang, J., Takahashi, Y., Sindarovska, Y., Hörak, H., Ceciliato, P. H. O., Koolmeister, K., Wang, Y.-S., Vaahtera, L., Jakobson, L., Yeh, C.-Y., Park, J., Brosche, M., Kollist, H., & Schroeder, J. I. (2018). Mitogen-activated protein kinases MPK4 and MPK12 are key components mediating CO₂-induced stomatal movements. *The Plant Journal*, 96(5), 1018–1035. <https://doi.org/https://doi.org/10.1111/tpj.14087>
149. Toulouse, A., & Nolan, Y. M. (2015). A role for mitogen-activated protein kinase phosphatase 1 (MKP1) in neural cell development and survival. *Neural Regeneration Research*, 10(11). https://journals.lww.com/nrronline/fulltext/2015/10110/a_role_for_mitogen_activated_protein_kinase.15.aspx
150. Tran, L.-S. P., Nakashima, K., Sakuma, Y., Simpson, S. D., Fujita, Y., Maruyama, K., Fujita, M., Seki, M., Shinozaki, K., & Yamaguchi-Shinozaki, K. (2004). Isolation and Functional Analysis of Arabidopsis Stress-Inducible NAC Transcription Factors That Bind to a Drought-Responsive cis-Element in the early responsive to dehydration stress 1 Promoter[W]. *The Plant Cell*, 16(9), 2481–2498. <https://doi.org/10.1105/tpc.104.022699>
151. Tuzet, A. J. (2011). *Stomatal Conductance, Photosynthesis, and Transpiration, Modeling BT - Encyclopedia of Agrophysics* (J. Gliński, J. Horabik, & J. Lipiec (eds.); pp. 855–858). Springer Netherlands. https://doi.org/10.1007/978-90-481-3585-1_213

152. Umezawa, T., Hirayama, T., Kuromori, T., & Shinozaki, K. (2011). Chapter 6 - The Regulatory Networks of Plant Responses to Abscisic Acid. In I. B. T.-A. in B. R. Turkan (Ed.), *Plant Responses to Drought and Salinity Stress* (Vol. 57, pp. 201–248). Academic Press. <https://doi.org/10.1016/B978-0-12-387692-8.00006-0>
153. United Nations. The world population prospects 2019: highlights. New York: UnitedNations;2019.https://population.un.org/wpp/Publications/Files/WPP2019_Highlights.pdfhttps://population.un.org/wpp/Publications/Files/WPP2019_Highlights.pdf
154. Walia, A., Lee, J. S., Wasteneys, G., & Ellis, B. (2009). Arabidopsis mitogen-activated protein kinase MPK18 mediates cortical microtubule functions in plant cells. *The Plant Journal*, 59(4), 565–575. <https://doi.org/10.1111/j.1365-313X.2009.03895.x>
155. Wang, H., Ngwenyama, N., Liu, Y., Walker, J. C., & Zhang, S. (2007). Stomatal Development and Patterning Are Regulated by Environmentally Responsive Mitogen-Activated Protein Kinases in Arabidopsis. *The Plant Cell*, 19(1), 63–73. <https://doi.org/10.1105/tpc.106.048298>
156. Wang, J., Pan, C., Wang, Y., Ye, L., Wu, J., Chen, L., Zou, T., & Lu, G. (2015). Genome-wide identification of MAPK, MAPKK, and MAPKKK gene families and transcriptional profiling analysis during development and stress response in cucumber. *BMC Genomics*, 16(1), 386. <https://doi.org/10.1186/s12864-015-1621-2>
157. Weblink 1 <https://www.fao.org/land-water/water/drought/droughtandag/en/>
158. Weblink 2 [https://www.medbox.org/document/world-population-prospects-2019-highlights-10-key-findings#:~:text=10%20Key%20Findings,-United%20Nations%20Dept&text=The%20world%27s%20population%20is%20projected,double%20by%202050%20\(99%25\)](https://www.medbox.org/document/world-population-prospects-2019-highlights-10-key-findings#:~:text=10%20Key%20Findings,-United%20Nations%20Dept&text=The%20world%27s%20population%20is%20projected,double%20by%202050%20(99%25))
159. Weblink 3 <https://www.ipcc.ch/srccl/chapter/chapter-3/>
160. Witoń, D., Gawroński, P., Czarnocka, W., Ślesak, I., Rusaczonek, A., Sujkowska-Rybkowska, M., ... & Karpiński, S. (2016). Mitogen activated protein kinase 4 (MPK4) influences growth in *Populus tremula* L. × *tremuloides*. *Environmental and Experimental Botany*, 130, 189-205.
161. Witoń, D., Sujkowska-Rybkowska, M., Dąbrowska-Bronk, J., Czarnocka, W., Bernacki, M., Szechyńska-Hebda, M., & Karpiński, S. (2021). MITOGEN-ACTIVATED PROTEIN KINASE 4 impacts leaf development, temperature, and stomatal movement in hybrid aspen. *Plant Physiology*, 186(4), 2190–2204. <https://doi.org/10.1093/plphys/kiab186>

162. Wu, Q., Zhang, X., Peirats-Llobet, M., Belda-Palazon, B., Wang, X., Cui, S., Yu, X., Rodriguez, P. L., & An, C. (2016). Ubiquitin Ligases RGLG1 and RGLG5 Regulate Abscisic Acid Signaling by Controlling the Turnover of Phosphatase PP2CA. *The Plant Cell*, 28(9), 2178–2196. <https://doi.org/10.1105/tpc.16.00364>
163. Xia, H., Wang, Q., Chen, Z., Sun, X., Zhao, F., Zhang, D., ... & Yin, Y. (2024). Identification and functional analysis of the EPF/EPFL gene family in maize (*Zea mays* L.): Implications for drought stress response. *Agronomy*, 14(8), 1734.
164. Xia, H., Wang, Q., Chen, Z., Sun, X., Zhao, F., Zhang, D., Fei, J., Zhao, R., & Yin, Y. (2024). Identification and Functional Analysis of the EPF/EPFL Gene Family in Maize (*Zea mays* L.): Implications for Drought Stress Response. In *Agronomy* (Vol. 14, Issue 8). <https://doi.org/10.3390/agronomy14081734>
165. Xiong, Z., Dun, Z., Wang, Y., Yang, D., Xiong, D., Cui, K., Peng, S., & Huang, J. (2022). Effect of Stomatal Morphology on Leaf Photosynthetic Induction Under Fluctuating Light in Rice. *Frontiers in Plant Science*, 12. <https://www.frontiersin.org/journals/plant-science/articles/10.3389/fpls.2021.754790>
166. Xu, W., Jia, L., Shi, W., Liang, J., Zhou, F., Li, Q., & Zhang, J. (2013). Abscisic acid accumulation modulates auxin transport in the root tip to enhance proton secretion for maintaining root growth under moderate water stress. *New Phytologist*, 197(1), 139–150. <https://doi.org/https://doi.org/10.1111/nph.12004>
167. Yang, X., Jia, Z., Pu, Q., Tian, Y., Zhu, F., & Liu, Y. (2022). ABA Mediates Plant Development and Abiotic Stress via Alternative Splicing. In *International Journal of Molecular Sciences* (Vol. 23, Issue 7). <https://doi.org/10.3390/ijms23073796>
168. Yoo, J. H., Cheong, M. S., Park, C. Y., Moon, B. C., Kim, M. C., Kang, Y. H., Park, H. C., Choi, M. S., Lee, J. H., Jung, W. Y., Yoon, H. W., Chung, W. S., Lim, C. O., Lee, S. Y., & Cho, M. J. (2004). Regulation of the Dual Specificity Protein Phosphatase, DsPTP1, through Interactions with Calmodulin * . *Journal of Biological Chemistry*, 279(2), 848–858. <https://doi.org/10.1074/jbc.M310709200>
169. Yuan, M., Zhao, Y.-Q., Zhang, Z.-W., Chen, Y.-E., Ding, C.-B., & Yuan, S. (2017). Light Regulates Transcription of Chlorophyll Biosynthetic Genes During Chloroplast Biogenesis. *Critical Reviews in Plant Sciences*, 36(1), 35–54. <https://doi.org/10.1080/07352689.2017.1327764>
170. Zhang, W. (2019). *Involvement of Arabidopsis thaliana MAP kinase 8 in the regulation of seed germination: interplay with TCP transcription factors*. <http://www.theses.fr/2019SORUS440/document>

171. Zhang, W., Cochet, F., Ponnaiah, M., Lebreton, S., Matheron, L., Pionneau, C., Boudsocq, M., Resentini, F., Huguet, S., Blázquez, M. Á., Bailly, C., Puyaubert, J., & Baudouin, E. (2019). The MPK8-TCP14 pathway promotes seed germination in *Arabidopsis*. *The Plant Journal*, *100*(4), 677–692. <https://doi.org/https://doi.org/10.1111/tpj.14461>
172. Zhang, Y., Li, Q., Wang, Y., & Sun, L. (2018). Biological Function of Calcium-Sensing Receptor (CAS) and Its Coupling Calcium Signaling in Plants.
173. Zhiling, L., Wenhua, D., & Fangyuan, Z. (2024). Genome-wide identification and phylogenetic and expression pattern analyses of EPF/EPFL family genes in the Rye (*Secale cereale* L.). *BMC Genomics*, *25*(1), 1–12. <https://doi.org/10.1186/s12864-024-10425-9>
174. Zhou, H., Ren, S., Han, Y., Zhang, Q., al, L., & Xing, Y. (2017). Identification and Analysis of Mitogen-Activated Protein Kinase (MAPK) Cascades in *Fragaria vesca*. In *International Journal of Molecular Sciences* (Vol. 18, Issue 8). <https://doi.org/10.3390/ijms18081766>
175. Zuo, J., Niu, Q. W., & Chua, N. H. (2000). An estrogen receptor-based transactivator XVE mediates highly inducible gene expression in transgenic plants. *The Plant Journal*, *24*(2), 265-273.